5-2017

Antimicrobial Biomaterials and Sustainable Polymers from Renewable Biomass

Mitra Shiran Ganewatta
University of South Carolina

ANTIMICROBIAL BIOMATERIALS AND SUSTAINABLE POLYMERS FROM RENEWABLE BIOMASS

by

Mitra Shiran Ganewatta

Bachelor of Science
University of Colombo, 2011

Submitted in Partial Fulfillment of the Requirements

For the Degree of Doctor of Philosophy in

Chemistry

College of Arts and Sciences

University of South Carolina

2017

Accepted by:

Chuanbing Tang, Major Professor

Qian Wang, Committee Member

F. Wayne Outten, Committee Member

Alan W. Decho, Committee Member

Cheryl L. Addy, Vice Provost and Dean of the Graduate School

DEDICATION

To my parents, for their love and support and guiding me to get the best education possible. I appreciate their life long sacrifices to making the person who I am.

To Nadee, my loving wife, for her immense support and love. None of my accomplishments would be possible without her.

To Cooper, the smartest border collie for always being there with a happy face.

ACKNOWLEDGEMENTS

First and foremost, I would like to express my sincere gratitude to my advisor, Dr. Chuanbing Tang. It has been an honor and a privilege to be mentored by such an enthusiastic and knowledgeable person. His passion for polymer science has inspired me to a great extent. I eagerly appreciate his contributions to make my Ph.D. experience diverse, productive and stimulating. I want to appreciate him for the excellent role model he has provided as a successful professor and a caring person. He has made a positive impact on my life.

Then I would like to thank my graduate committee members Dr. Qian Wang, Dr. Alan W. Decho and Dr. F. Wayne Outten for providing me advice, encouragement, and valuable suggestions on my research during graduate school. I admire my committee chair Dr. Qian Wang for being a warm-hearted person and a great teacher in organic chemistry. I want to thank Dr. Decho and his group members Dr. Yunpin Chen and Dr. Kristen Miller for their collaborations with our group. In addition, I want to mention Dr. Mitzi Nagarkatti and her group members Dr. Jihua Zhou, Dr. Pegah Meherpouya-Bharami and Dr. Marpe Bam for their productive collaborations. Computational studies on my research projects were done in collaboration with Dr. Jerry Ebalunode at the University of Houston and I thank him for the valuable contributions. It was a great pleasure to collaborate with Dr. Megan L. Robertson and her student Wenyue Ding at the University of Houston.

Besides the exciting research work, I feel thankful to get the chance to work with Dr. Brian Benicewicz while I served as the president and secretary of the ACS Poly/PMSE Student Chapter at USC. I want to mention Julia, Andrew and Zach for working with me to conduct many projects and services. Volunteering with Dr. Linda Shimizu for the K12 outreach program was a great experience for me.

I am very appreciative of the experiences shared and friendships formed with other graduate students, post-docs and visiting scholars during my stay at USC. I want to specially mention the members in Tang Polymer Group. I thank Dr. Yi Yan for being a terrific mentor for me during the early stages of my graduate career. Dr. Jifu Wang made a great platform to work on and I thank him. Dr. Zhongkai Wang was very motivating through his work. I closely worked with Dr. Jiuyang Zhang, Dr. Kejian Yao, Dr. Perry Wilbon and it was a pleasant experience for me. Dr. Jeffery Hayat and Nathen Trenor were my awesome office mates. Thank you Md Anisur Rahman, Meghan E. Lamm and Xinzhou Zhang for being nice friends. Parker S. Singleton and Louis Mercado were excellent undergraduate students who worked with me. I also want to mention Dr. Yali Qiao, Dr. Xiaodong Ying, Dr. Yanming Han, Dr. Yuzhi Xu, Dr. Hui Li, Dr. Christopher Hardy, Paras Pageni, Tianyu Zhu and many others. It is a great pleasure to work with all of you and learn from you. Thanks for all your help and suggestions!

Further, I want to give my sincerest gratitude to my mother, my father, my wife and other family members for their unconditional love and support. I thank to all my friends from around the world for their encouragement and help. Finally, I acknowledge all the funding supports from University of South Carolina, National Science Foundation (NSF) and National Institutes of Health (NIH).

ABSTRACT

In this dissertation, development of antimicrobial biomaterials and sustainable polymers from renewable biomass is described. In Chapter 1, an overview and recent development about sustainable polymers from renewable biomass, antimicrobial biomaterials and polymerization methods are given. Afterwards, the major research objectives of this doctoral research work are described.

Innovative cationic polymers containing pine resin sourced abietic acid is discussed in Chapter 2. The preparation of cationic compounds is conversed via a combination of Diels-Alder, catalytic esterification, quaternization and subsequent decoration of polycaprolactone that was prepared via ring-opening polymerization (ROP). Furthermore, the antimicrobial activity against a range of bacteria, biocompatibility with mammalian cells and the antimicrobial mechanistic aspects are provided. Chapter 3 is dedicated for sustainable antimicrobial and antibiofilm coatings. They were developed using cationic compounds and polymers grafted on surfaces via copper-catalyzed 'click' chemistry (CuAAC) and surface-initiated atom transfer radical polymerization (SI-ATRP). Antimicrobial, antibiofilm and biocompatibility properties of these surfaces were examined.

Facially amphiphilic antimicrobial polymers using bile acids as the hydrophobic building block are described in Chapter 4. The self-assembly of those polymers to form antimicrobial nanoparticles was investigated. Next, Chapter 5 is reserved for the discussion

of high molecular weight polymers prepared from resin acids via "living" ring-opening metathesis polymerization (ROMP). The entanglement molecular weight, thermal and mechanical properties were investigated. Thermoplastic elastomers were prepared by making block copolymers from a resin acid monomer and a soybean oil based monomer. Finally, Chapter 6 provides a summary of this dissertation research and future directions involving renewable biomass for sustainable development.

TABLE OF CONTENTS

List of Tables

LIST OF FIGURES

LIST OF SYMBOLS

M_n	Number average molecular weight
$Đ$	Dispersity
M_e	Chain entanglement molecular weight
T_g	Glass transition temperature
T_m	Melting temperature
T_{d5}	Temperature at 5% weight loss
T_{d10}	Temperature at 10% weight loss

LIST OF ABBREVIATIONS

AFM .... Atomic Force Microscopy

AIBN .... Azobisisobutyronitrile

AMP .... Antimicrobial Peptide

ATRP .... Atom Transfer Radical Polymerization

CDC .... Centers for Disease Control

CFU .... Colony Forming Unit

CLSM .... Confocal Laser Scanning Microscopy

CMC .... Critical Micellar Concentration

CuAAC .... Copper(I)-Catalyzed Azide-Alkyne Cycloaddition

DCM .... Dichloromethane

DLS .... Dynamic Light Scattering

DMF .... *N*,*N*-Dimethylformamide

DSC .... Differential Scanning Calorimetry

FTIR .... Fourier Transform Infrared Spectrometry

G3 .... Grubbs' Third Generation Catalyst

GPC .... Gel Permeation Chromatography

HC .... Hemolytic Concentration

HDF .... Human Dermal Fibroblasts

HG2 .... Hoveyda-Grubbs' Second Generation Catalyst

HMW .... High Molecular Weight

MDS ....Molecular Dynamics Simulations

MIC ....Minimum Inhibitory Concentration

MRSA .... Methicillin-resistant *Staphylococcus aureus*

NMR .... Nuclear Magnetic Resonance

PBS .... Phosphate-buffered Saline

PHA...Polyhydroxyalkanoate

QA... Quaternary Ammonium

ROMP ....Ring-Opening Metathesis Polymerization

ROP... Ring-Opening Polymerization

SAXS ....Small-Angle X-ray Scattering

SI-ATRP .... Surface Initiated-Atom Transfer Radical Polymerization

TEM .... Transmission Electron Microscopy

TGA .... Thermogravimetric Analysis

THF .... Tetrahydrofuran

TPE .... Thermoplastic Elastomer

TSB .... Tryptic Soy Broth

XPS .... X-ray Photoelectron Spectroscopy

CHAPTER 1

GENERAL INTRODUCTION[1,2]

---

[1] Ganewatta, M. S.; Ryu, C. Y.; Tang, C., Introduction, in Sustainable Polymers from Biomass, Tang C. and Ryu, C. Y. (Eds). Chapter 1, Wiley-VCH Verlag GmbH & Co. KGaA, 2017. Partially reproduced with permission from Wiley. Copyright © 2017 Wiley Ltd.

[2] Ganewatta, M. S.; Tang, C., Controlling Macromolecular Structures Towards Effective Antimicrobial Polymers. *Polymer* **2015**, *63*, A1-A29. Partially reproduced with permission from Elsevier. Copyright © 2015 Elsevier Ltd.

1.1 Sustainable Polymers from Renewable Biomass

The discovery and development of synthetic polymeric materials in the 20th century can undoubtedly be recognized as one of the best inventions humans made to improve the quality of life. Durability, light weight, diverse properties are just a few reasons why polymeric materials' presence span from simple water bottles to modern space stations. Outstanding properties of polymeric materials have displaced other materials, such as wood, metal, and glass to a considerable extent. Packaging, construction, transportation, aerospace, biomedical, energy and military are few examples where polymeric materials prevail. Global production of plastic has risen from 204 million tonnes in the 2002 to about 299 million tonnes in 2013.[1] Manufacture of non-natural polymers is largely associated with the utilization of essentially non-renewable fossil feed stocks either natural gas or petroleum. Approximately, 5-8% of the world's oil production is used for plastics production.[2] Accompanying environmental problems include but not limited to generation of solid waste that accumulates in landfills and oceans, production pollution and related environmental problems.[3]

A major underlying issue of plastics is the enormous carbon footprint associated with production as portrayed by producing 1 kg of plastics generates about 3-6 kg of CO_2.[2] In addition, their impervious nature to enzymatic breakdown and 'linear' consumption as opposed to natural counterparts' results in relentless generation of solid waste from most commercial polymers. Although, polymers can be recycled to produce new materials or incinerated to recover its calorific value, such endeavor is not clearly understood by most consumers nor required technological advances are available in most parts of the world. Depleting oil reserves as well as these detrimental environmental impacts observed in the

21st century have driven academia, and industry to explore sustainable polymers from renewable biomass as a long-term alternative. In addition, the consumers' preference as well as governmental landscape has changed in favor of sustainable products for a greener environment. Significant advancements have been made to discover sustainable polymers, cost effective to manufacture and compete or out perform traditional materials in mechanical aspects as well as environmental stand points.[4] The valuable contributions to the field by several recent books[5, 6] and reviews[7-11] broadly discuss about sustainable polymeric materials.

Given the influence of polymers as an indispensable resource for modern society it should be taken as a stern concern for sustainable development. There are varied definitions for sustainability. "Development that meets the needs of the present without compromising the ability of future generations to meet their own needs" is the working definition given by the report *Our Common Future*, published in 1987 by the World Commission on Environment and Development.[12] In most cases, the terms 'renewable polymers' and 'sustainable polymers' are used with overlapping meanings and without any distinction. Typically, renewable polymers are made from renewable feedstock chemicals. However, to be ideally sustainable those polymers should be more environmentally friendly to produce - denoting less non-renewable chemical or energy use and less pollution emissions and easy to decompose after service lifetime. Development of such polymers from biomass is expected to solve problems associated with the dependence of fossil oil resources as well as water and land pollution by non-degradable polymer waste from consumer products.[13, 14] A comparison of petrochemical polymers and biobased polymers is given in Figure 1.1.

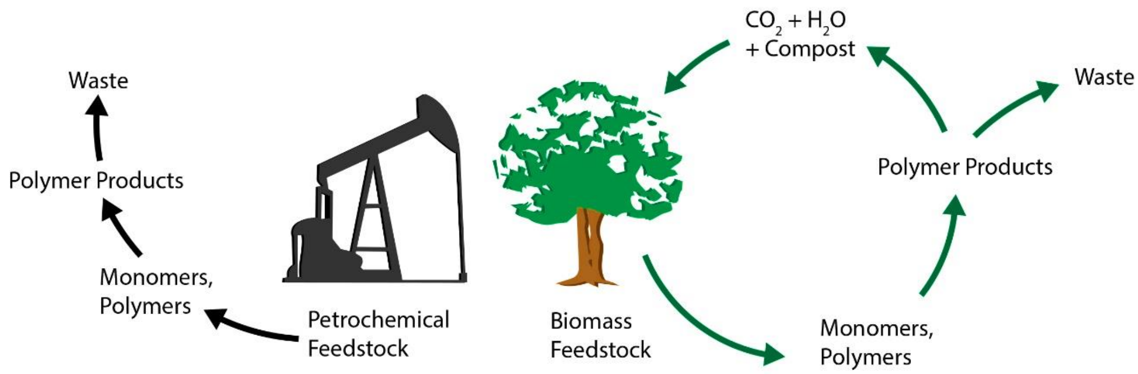

Figure 1.1 A comparison between traditional petrochemical polymers and sustainable polymers.

The prime aspects of the sustainable materials are to utilize renewable biomass resources for raw materials as opposed to petrochemical sources and incorporate degradability to the novel materials such that sustainable polymers inherit a cyclic life cycle considering the time factor.

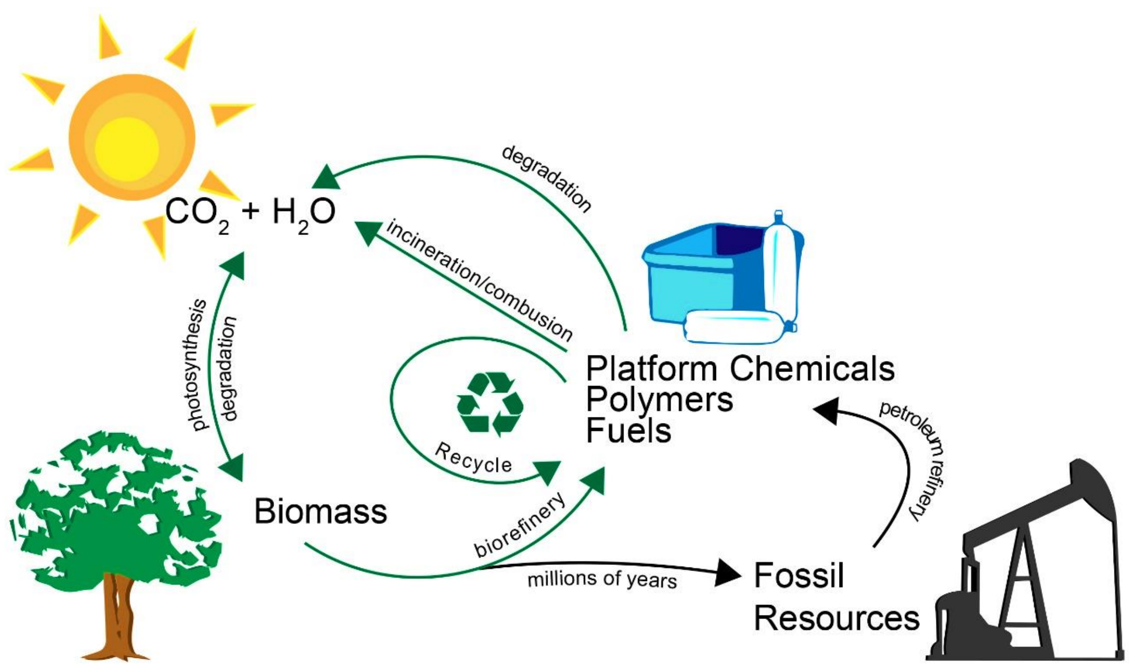

Figure 1.2 Schematic diagram to illustrate the concepts of sustainable polymers from biomass.

As illustrated in Figure 1.2, there is a considerable influence to global carbon cycle by the plastic industry. 'Fossil sourced' carbon dioxide release is overwhelming that natural photosynthesis or other natural sinks cannot equilibrate the global ecosystem. However, a transition from fossil based chemicals to the use of non-petrochemical renewable biomass to produce polymers would diminish the involvement to the greenhouse effects since they are low carbon or carbon neutral as well as promote the sustainable utilization of limited fossil oil resources. Unlike, the unevenly distributed fossil oil, natural biomass is available in many geographic areas throughout the world and can be produced locally or regionally without significant technological intervention. Also, their market price fluctuations would be much favorable compared to crude oil resources and can provide a stable supply over a long period.

Last two decades resulted in a great level of scientific advancements that paves paths towards the initial stages of an era of sustainability, carbon neutrality, and independence from petroleum sources for the generation of polymeric materials. Rapid expansion of this field can be visualized by the exponential increase in the number of scientific reports published on sustainable polymers, appearance of dedicated scientific journals and the steady increase of the market share of renewable bio-based material products for example NatureWorks Ingeo™, DuPont™ Sorona®. Although, market share of bio-based polymers is about 2% in 2013 and it is expected reach more than 4% by 2020 with volume increases faster than that of petroleum based polymers.[15]

Global primary production of the biosphere exceeds 100 billion metric tons of carbon per year which include contributions from both terrestrial and marine communities.[16] It is obvious that this primary produce will mostly end up in food chains or decay and sediment. Valuable raw materials for sustainable polymer production are hidden in the biomass. Unfortunately, deployment of biomass for polymeric material production is lagging largely due to the competitiveness of fossil oil counter parts as well as their well-established technologies for polymer industry. In addition, as the global human population grows rapidly, the demand on biomass for food and energy purposes has perceived an escalating interest. Nevertheless, a modern 'gold rush' is witnessed in recent years to unlock the true potential of biomass chemicals. Generation of sustainable polymers from agricultural feed stock such as sugar cane, corn, potatoes, and other carbohydrates has limitations due to competing food necessities. Therefore, current focus is shifted towards nonfood and feed renewable biomass and waste resources such as lingo-cellulosic resources, paper mill waste, agricultural waste, and food waste.

Renewable biomass derived polymeric materials can be categorized in to three classes. The first class is the naturally occurring biopolymers such as rubber, cotton and starch that were used extensively for years before synthetic polymers were invented. In recent years, reviving of biopolymer research for materials science can be seen. There is enormous growth in biopolymers research such as cellulose, hemicellulose, polysaccharides, chitosan, and lignin (Figure 1.3) to discover novel hybrid materials with improved properties as well as commercialization. Some of the common approaches involve blending or surface modifications of these already-built-in macromolecular structures to manipulate the physical properties. Polymers obtained by the fermentation of sugars or lipids can be considered as the second class of polymers. Examples include polyhydroxyalkanoates (PHAs) such as poly(hydroxybutyric acid).[17, 18] PHAs are a family of biodegradable linear polyesters produced by bacterial fermentation of sugars and lipids.[19] Their structural diversity and analogy to plastics makes them good candidates to replace synthetic thermoplastics. With modern technologies, the PHA research has expanded to produce block copolymers and graft polymers using a variety of bacteria including new isolates and metabolically engineered species.

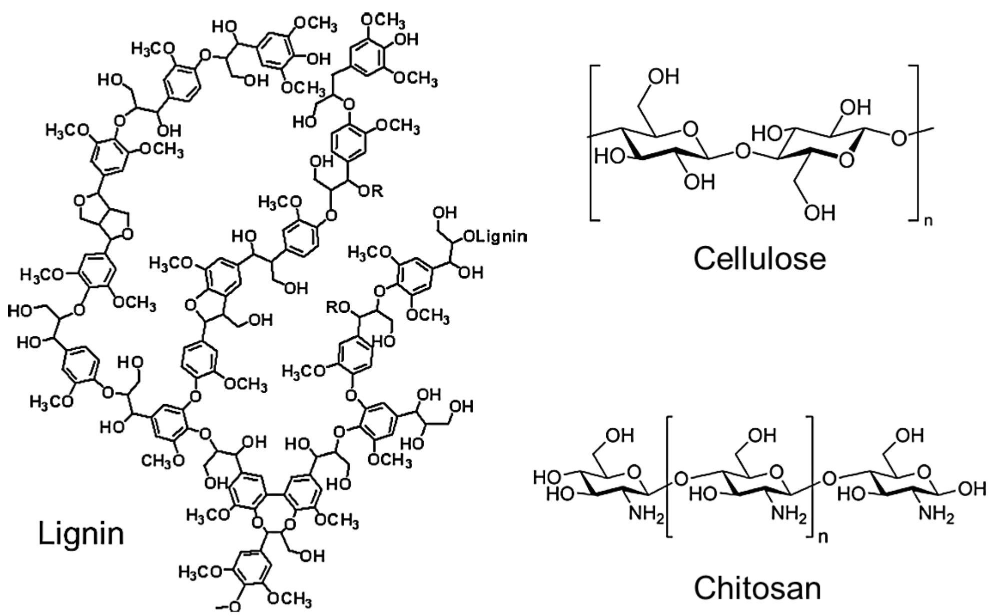

Figure 1.3 Naturally occurring polymers obtained from renewable biomass.

The third class of polymers are obtained by polymerizing small molecular biomass chemicals. The benefit is that these materials can be precisely engineered at a molecular level into polymers with useful properties like some plastics derived from petroleum chemicals. Compared to chemicals from fossil oil refinery, one major drawback in biomass feedstocks is in the direct conversion into high value chemicals that can be used for polymerizations.[20] Technological infancy for such enterprise as well as the operating cost make it far from wide scale feasibility. However, modern chemists and material scientists have cracked down most of these problems and have achieved varying degrees of success. Top biomass platform molecules produced from sugars, which recognized by the US Department of Energy, are shown on Figure 1.4.[21] A recognized approach for transforming raw biomass into market place chemicals is given by the concept of biorefinery.[22] In a biorefinery raw biomass feedstock is processed to generate value added platform chemicals. The products from biorefinery are expected to replace fossil oil based products coming from petrochemical refinery. It is important such method does not compete food based biomass for materials development as the human population keep increasing rapidly.

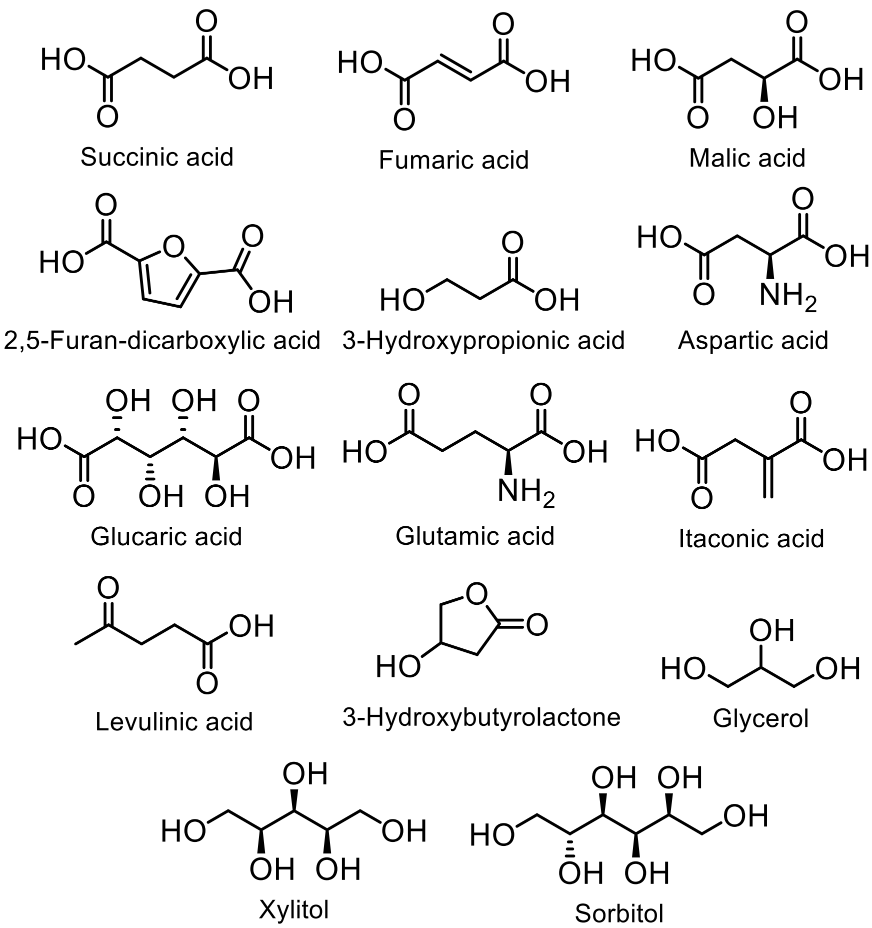

Figure 1.4 Top biomass platform molecules produced from sugars recognized by the US Department of Energy.

Besides these chemicals, hydrocarbon rich biomass such as terpenes including pinene, limonene, resin acids (Figure 1.5), and furans, as well as fatty acids from vegetable oils, cashew nut shell liquid are promising candidates for sustainable polymer preparation.[7, 8, 23-25]

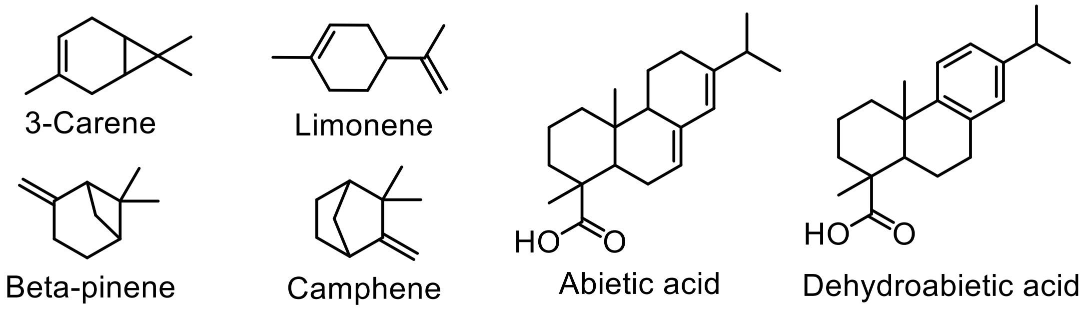

Figure 1.5 Terpene-based compounds used in sustainable polymers.

Terpenes are the largest and most abundant class of natural hydrocarbons in nature. Various olefinic terpenes have been incorporated in to polymeric materials. Resin acids are naturally produced by conifer trees and the production is more than 1 million tons annually. This largely overlooked resource is gaining interest as a source for polymer industry. Triglycerides from natural plant oils are a widely abundant source of biomass to produce sustainable polymers and materials. Various types of thermoset polymers have been developed using plant oils.

The use of biochemical means such as microbial fermentation of various biomass feedstocks to produce bio-based monomers such as lactic acid, succinic acid and itaconic acid have become cost effective with recent advances in biotechnology. These monomers are then polymerized using conventional methods. Example polymers include poly(lactic acid), poly(butylene succinate), poly(ethylene) and poly(itaconic acid) (Figure 1.6). Polylactide or poly (lactic acid) is a type of thermoplastic polyester that is one of the most promising commercialized renewable polymers due to its biodegradability, biocompatibility and sufficient mechanical properties. Long chain branched polylactides (LCB PLAs) have been introduced to overcome shortages of linear versions.

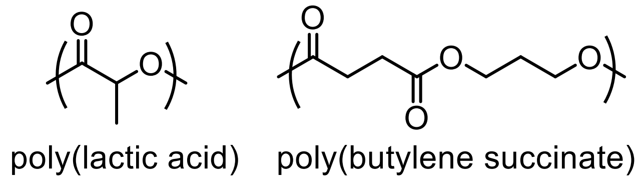

Figure 1.6 Sustainable polymers derived from biotechnologically derived monomers.

Non-hydrocarbon molecular biomass including carbon dioxide (CO_2), carbon disulfide (CS_2) and carbonyl sulfide (COS) is useful in the preparation of copolymers with epoxides that afford C1-based polycarbonate polymers (Figure 1.7). Such polymers could be promising to directly reduce the impact of excessive levels of CO_2 produced by burning of fossil resources. However, the major drawback is the poor activity of the reactants to undergo polymerization. To circumvent that, copolymerization optimization and new catalysts are being investigated.[26]

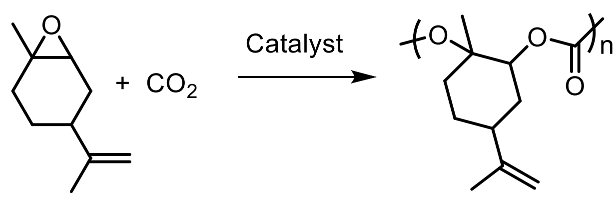

Figure 1.7 Copolymerization of limonene oxide and CO_2.

Renewable biomass chemicals in commodity plastics and advanced applications is ever increasing and highly recognized worldwide. It is unrealistic to envision a future devoid of sustainable polymers. Sustainable polymers from natural biomass will significantly replace the petrochemical derived polymers in the future. But the important question is how long it will take for the transition, because the fossil oil resources will not exist more than few more decades and the heavy burden of environmental problems related to petrochemical sources grow exponentially. More research to improve the performance of sustainable polymers are required to move on the path to transfer from petrochemical based polymer world to bio-based sustainable polymer world.

1.2 Renewable Resin Acids

Rosin is the non-volatile hydrocarbon-rich exudate of pine and other conifer trees produced in large quantities as a chemical and physical defense against herbivore and pathogen attacks.[27] Rosin is considered as an abundant source of high-value diterpene resin acids that is produced in quantities greater than 1.2 million tons annually worldwide. Rosin consists primarily of abietic- and pimaric-type resin acids with characteristic hydrophobic cycloaliphatic or aromatic ring structures generally known as hydrophenanthrene rings. Similar to all terpenoids, oleoresin terpene biosynthesis arises from fundamental precursor isopentenyl diphosphate which undergoes isomerization and condensation to produce geranylgeranyl diphosphate, the precursor of diterpenes. Conversion of the precursor to various tricyclic diterpene olefin structures is catalyzed by diterpene synthases followed by three-step oxidation at C18 to produce corresponding diterpene resin acids (Figure 1.8).[27, 28]

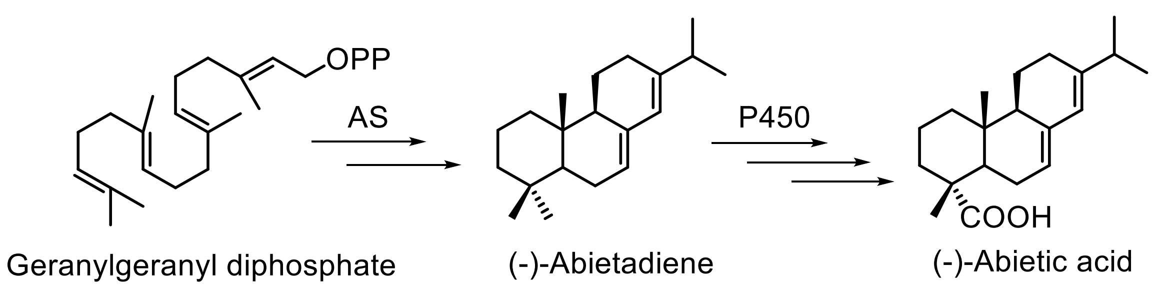

Figure 1.8 Pathway of diterpene resin acid biosynthesis in conifers. AS: abietadiene synthase and P450: multi-substrate P450 oxidase enzymes.

The most abundant resin acid is abietic acid with the empirical formula $C_{20}H_{30}O_2$ meanwhile the other components are different isomers having different unsaturations (Figure 1.9). Resin acids are known to possess a variety of biological activities including antimicrobial,[29] anti-inflammatory[30] and anticonvulsant[31] activities. The presence of carboxyl groups, conjugated double bonds and other functionalities imparts these chemicals a tunable chemical reactivity to obtain derivatives such as salts, esters and maleic anhydride adducts, and hydrogenated or disproportionated resins which are used in a wide range of applications.[7] Rosin is traditionally used as ingredients in fine chemicals such as antifouling caulking agent, in inks, adhesives, cosmetics, vanishes, medicines and chewing gums.[8]

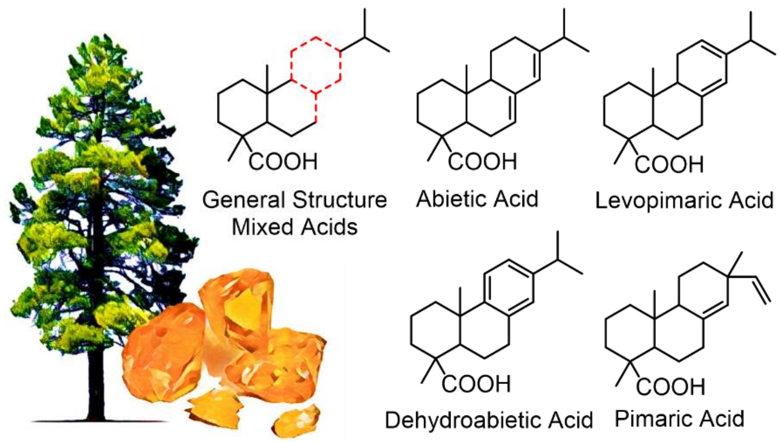

Figure 1.9 Chemical structures of representative resin acids.

Resin acids have similar rigidity and chemical stability to petroleum based cycloaliphatic and aromatic compounds. In addition, compared with other renewable biomass resources, resin acids have several unique properties that make them promising candidates for polymer science.: (1) hydrocarbon-rich chemicals that can increase the hydrophobicity of materials; (2) bulky hydrophenanthrene group improve thermal properties; (3) rosin-derived esters are biocompatible because they are permitted to be used as food additives in chewing gum and beverages, approved by the U.S. Food and Drug Administration; (4) Rosin is a non-food biomass resource that does not have competition for food sources.

Depending on the position of the hydrophenanthrene structure rosin based polymers have been developed as main-chain polymers and side-chain polymers. Main-chain rosin based polymers are prepared via various condensation polymerizations. However, the molecular weights of polymers were low due to many reasons including steric hindrance, monomer impurities, and stoichiometric control.[32-36] However, radical polymerization of side-chain rosin-based polymers have evaded such difficulties to produce polymers with control of molecular weight. Rosin-derived vinyl, acrylic, or allyl ester monomers are utilized to produce side-chain rosin-based polymers.[35] However, the molecular weights were not enough to have chain entanglements. Hence the polymers appeared as powders and it was not possible to make mechanically robust materials. Rosin is an abundant renewable resource that has shown promise in the field of polymer science. To improve the performance of rosin based polymers, more investigations on the polymerization methods of rosin based new monomers is required.

1.3 Bile Acids

Bile of mammals and other vertebrates are rich in bile acids that are amphiphilic steroid acids (Figure 1.10). These are typically stay conjugated with taurine or glycine in the liver forming bile salts that serve as surfactants to solubilize dietary lipids and fats by the formation of micelles allowing digestion of food. Human liver cells produce primary bile acids such as cholic acid and chenodeoxycholic acid via cytochrome P-450 enzyme mediated oxidation of cholesterol in a multi-step pathway.[37] In the intestine, microorganism transform them into secondary bile acids such as deoxycholic acid and lithocholic acid.[38]

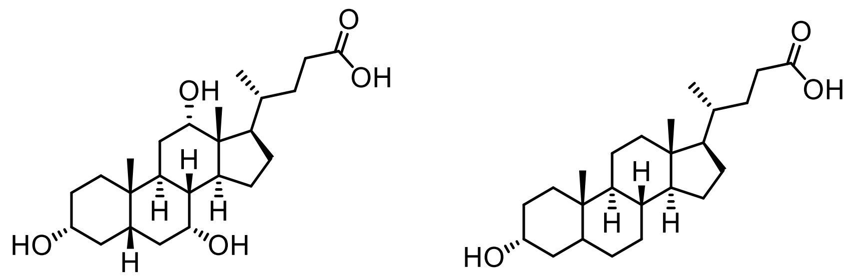

Figure 1.10 Chemical structures of representative bile acids.

Bile acids are abundant in nature and accessible as biomass derived chemicals. Hence, they are desirable for the development of novel building blocks for polymeric materials.[39] The rigid steroidal nucleus of these bile acids provides tough mechanical properties. In addition, biocompatibility of such molecules confers useful biomaterials. Recent advances have investigated a broad variety of structures with bile acids as repeating units in the polymer backbone, as pendant groups along the polymer chain in block or statistical polymer or chain end-functional polymers.[40, 41] Biopolymers containing bile acids in the main chain have been widely prepared using step-growth polymerization via incorporating a variety of linkers, such as esters, amides, triazoles, urethanes, and imines.[42-46] Bile acid containing side-chain polymers have been developed for various applications such as drug delivery, self-healing materials, and sensing.[47, 48] Bile acids are also explored as antimicrobial surfactants.[49] However, bile acids as antimicrobial biomaterials require more attention. Given the amphiphilic nature of the bile acid structure, it is intriguing to see the development of novel biomaterials from these molecules.

1.4 Antimicrobial Polymers

Antimicrobial chemotherapy has revolutionized modern medicine in many aspects and has significantly reduced ailments and death from infectious diseases. Many classes of antibiotics that are clinically used today were discovered during the golden era of antibiotic discovery from 1940s to 1960s.[50, 51] Molecular targets of pathogens, which are absent or significantly different from human cells such as cell wall, 60S ribosomes, cell membranes, genetic materials and biosynthetic pathways, are utilized to design antimicrobial agents (Figure 1.11A). Environmental pressure from the action of antibiotics combined with short life cycles and lateral gene transfer mechanisms have resulted in rapid appearance of resistant pathogenic populations of microorganisms.[52] For example, widespread outbreaks of penicillin-resistant *Staphylococcus aureus* and methicillin-resistant *S. aureus* (MRSA) infections occurred just a few years after the introduction of β-lactam antibiotics, penicillin and methicillin.

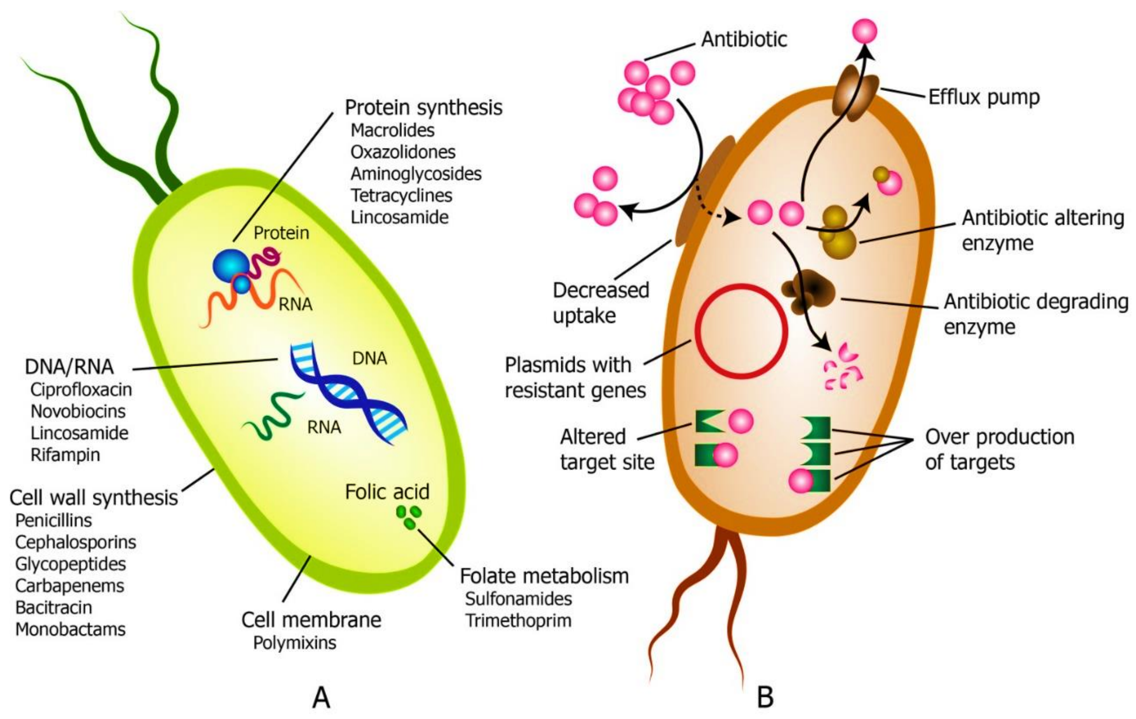

Figure 1.11 An illustration of antibiotic action and microbial resistance. (A) Typical antibiotic target sites present in bacterial cells. (B) Mechanisms of antibiotic resistance.

Resistance mechanisms include efflux pumps, chemical modifications such as phosphorylation, acetylation or hydrolysis, altering target and reprogramming biosynthesis, most of which are against small molecule antimicrobials (Figure 1.11B).[50, 53] The most prominent issue is the expeditious growth of acquired resistance in bacteria that cause major healthcare crisis. For example, since the introduction of the first β-lactam antibiotics, the number of unique β-lactamase enzymes has grown from zero to over 1000.[53] Decades of use and misuse of antibiotics, combined with a forty-year lull in the pipe line of novel antimicrobial agents, have consequences of a global superbug threat that could lead human civilization to a pre-antibiotic era. The devastating nature of the increasing resistance to available antibiotics is a global concern at high priority. Antibiotic resistance seems inevitable. Therefore, it is essential to continuously develop antibiotics with novel modes of action to face the evolving resistance.[54]

Antimicrobial polymers are a class of novel antimicrobial agents that is fueled by the combined knowledge on antimicrobial peptides (AMPs)[55] and polymer disinfectants that have emerged as two distinct fields since the 1980s.[56] There are several books, a variety of reviews and highlights on antimicrobial polymers published over the past few years that give broader and diverse perspectives.[56-73] There has been a rapid expansion of novel antimicrobial polymers and related research in the last decade.

It is increasingly recognized that microbial membranes provide an effective target for the development of de novo designed antimicrobial agents. Recent understanding of the innate immunity mediated by macromolecules highlights the importance of short amphiphilic peptides that modulate host defenses against microbial pathogens.[74] Also known as antimicrobial peptides, these molecules are produced by almost all forms of life.[75] AMPs are potent, broad-spectrum antimicrobials that act as the first line of defense against a wide range of invading pathogens including bacteria, protozoa, yeast, fungi and viruses by rapid and direct killing as well as several other means of modulating host immune systems.[76, 77] Several decades of studies have revealed more than two thousand AMPs with diverse sequences of amino acids and a range of structures. However, all AMPs show a common characteristic: the presence of an amphiphilic structure (in some literature, "amphipathic" is often used). The optimal amphiphilicity, which comes from cationic amino acids (e.g. lysine, arginine) and hydrophobic residues (e.g. isoleucine, valine), enables AMPs to fold into cationic and facially amphiphilic secondary structures. This feature permits AMPs to strongly interact with biological membranes. Interestingly, receptor-mediated antimicrobial activity is generally absent in AMPs. For instance, it was shown that all-D synthetic enantiomer homologous of magainins and cecropins have similar potency to all-L natural peptides.[78] This non-specific property has shown to be a class of promising anti-infective agents that are assumed to defer long-term resistance development compared to small molecule antibiotics.

Essentially, all types of living cells comprise a cytoplasmic membrane made of lipid bilayers that serves as a protective barrier to separate and protect the cell from its surrounding environment. In addition, being a 'semi-permeable membrane,' it acts as a gateway regulating the transport of substances to and from the intracellular space. Therefore, the cytoplasmic membrane has a vital task for the survival of the cell. Most widely accepted mechanism of antimicrobial action of AMPs is direct microbial killing by the disruption, reorganization or pore formation of cell membranes, resulting in the leakage of cellular contents and eventual cell death. Although still under debate, several models such as "barrel stave," "toroidal pore" and "carpet model" have been proposed to explain the membrane damaging interaction of AMPs with lipid bilayers.[79] The fundamental mode of microbicidal activity of synthetic antimicrobial polycationic agents is also found to be similar to that of AMPs [80]. It is interpreted in terms of a sequence of essential processes[81]: (1) It initiates by the adsorption on microbial cell surface. This utmost important step is also the basis of selectivity towards microbes; (2) Then the polycations diffuse through the cell wall and/or (3) interact with the cytoplasmic membrane; (4) This interaction may irreversibly damage the integrity of the cell membrane; (5) subsequently result in the release of cytoplasmic components including K^+ ions, DNA/RNA; and (6) finally lead to cell death. In addition to the membrane disruption by the integration of cationic polymers with lipid membranes, they may also destabilize the membrane surface by displacing divalent cations such as Ca^{2+} associated with the membrane phospholipids.

The basis of the selectivity of AMPs or polymer mimics towards bacterial or fungal cell membranes comes from the fundamental difference in the cell membrane lipid composition and surface components (Figure 1.12).[82] Typically, the cytoplasmic membrane leaflets of mammalian cells are asymmetric in terms of charge. For example, the outer leaflet of human erythrocyte membrane is composed of neutral (zwitterionic) lipids such as phosphatidylcholine, sphingomyelin and phosphatidylethanolamine, while the inner leaflet bears negative charge coming from phosphatidylserine.[71] In contrast, the presence of phosphatidylserine, phosphatidylglycerol or cardiolipin in microbial cell membrane outer leaflets, make the outer surface appealing to cationic molecules such as AMPs. In addition, bacterial and fungal cells have additional cell envelope components essentially, the cell wall that provides sufficient mechanical strength to endure changes in osmotic pressure imposed by the environment. In Gram-positive bacteria, teichoic acids, that are linked to either the peptidoglycan cell wall or to the underlying cell membrane, impart net negative charges because of the presence of phosphate moieties in their structure.

Gram-negative bacteria have an additional outer membrane bearing phospholipids and lipopolysaccharides. The lipopolysaccharides impart a strongly negative charge to cell surface. Fungal cell walls are comprised of glycoproteins and polysaccharides, mainly glucan and chitin that are extensively cross-linked together to form a complex network.[83] The phosphodiester linkages in these glycoproteins result in additional negative charges to the fungal cell surface.[84]

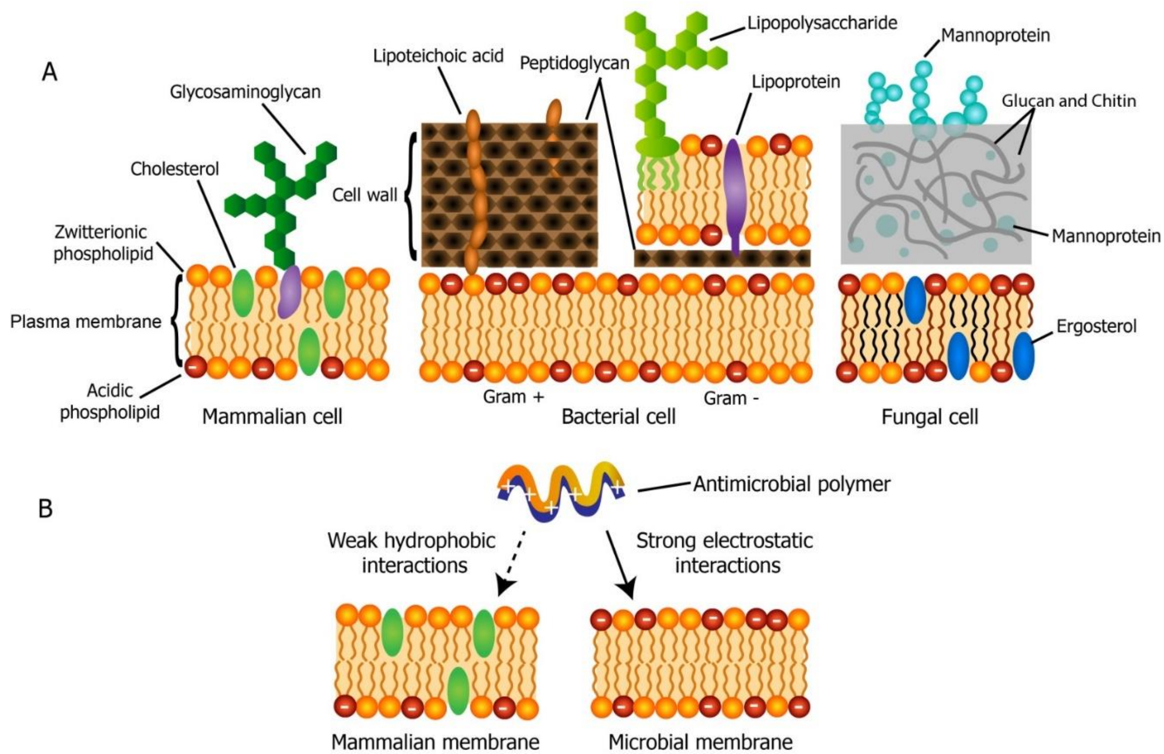

Figure 1.12 Origin of the cell selectivity of cationic antimicrobial macromolecules. (A) Illustration of the cross sections of microbial and mammalian cell envelopes. Mammalian cell membrane surface (left) is largely neutral compared to bacterial (middle) or fungal (right) cell membranes. (B) Selective interactions between cell membranes and cationic polymers.

Typically, the relative chance of microbes to develop resistance to an agent depends on the target specificity of the antimicrobial mechanism of action.[85] This is the obvious fact for the rapid resistance development against antibiotics since they are highly specialized to attack a specific microbial target. In contrast, polycations are mostly nonspecific in their action on microbes. However, it is unrealistic to expect that microbial pathogens are unable to develop resistance against these macromolecules. It should be noted that there are few reports indicating bacterial resistance development against AMPs and synthetic polymers.[86-88] Nevertheless, wide spread and rapid resistance development towards membrane active, cell lysing antimicrobial macromolecules may be unlikely compared to small molecule antimicrobials mediated with specific receptor sites.[89] It has been observed that there is a much greater number of passes required to induce resistance in bacteria against AMPs or synthetic mimics of AMPs under *in vitro* experiments.[90, 91] On the other hand, it is ambiguous how *in vivo* conditions, where a multitude of defense agents and mechanisms are present in the host organism, may define the microbial adaptations against cationic macromolecules.[92] These features may be the reason AMPs have been actively present in biological systems as effective defensive macromolecules in many forms of life for millions of years.

Synthetic mimics of AMPs are rapidly expanding, indicating that AMPs have formed a better platform to develop a class of next generation antimicrobial therapeutics. Several types natural AMPs and mimics of AMPs such as synthetic AMPs,[93] β-peptides,[94, 95] peptoides,[96] and AApeptides[97] have been developed with comparable or even better activities than the natural versions. However, in most situations costly synthetic approaches, fast proteolytic degradation, low bioavailability or toxicity limit their widespread clinical applicability.[98, 99]

The ability to modulate the structural features in to diverse architectures and functionalities, low cost synthesis, potent biological activity and stability make synthetic antimicrobial polymers favorable over other analogs of AMPs. Compared with conventional antibacterial agents of low molecular weight, polymeric antibacterial agents have advantages such as non-volatilization, inability to permeate the skin, longer circulatory time and reduced residual toxicity to the environment. The general term 'antimicrobial polymers' include several classes of materials such as cationic polymers, biocide-releasing polymers and antibiotic-conjugated polymers. Synthetic polymer disinfectants with cationic functionalities that emerged simultaneously with AMPs show strong biocidal activities. These macromolecules usually have cationic functionality such as quaternary ammonium groups, and hydrophobic alkyl moieties and have been mostly derived from poly(styrene)s, poly(vinylpyridine)s, poly(methacrylate)s, etc.[72] However, earlier versions of polycationic biocides showed significant toxicity to human cells. This property could be only in line with their targeted application, which is in the solid state as potent disinfectants or biocidal coatings. Therefore, the improvement of both antimicrobial and biocompatible polymers is essential to enable widespread systemic or topical clinical use of these macromolecules.

1.5 Polymerization Techniques and Modification Chemistries

Ring-Opening Polymerization (ROP). ROP is a very important controlled chain-growth polymerization technique that has been well studied.[100-102] Heteroatom containing rings such as lactones, lactides, carbonates, lactams, ethylene oxide, N-carboxyanhydride, oxazolines and siloxanes, are useful cyclic monomers that can undergo ROP polymerization to afford linear polymers.[103] Several mechanisms in which ROP occurs are anionic, cationic, organo-catalytic and coordination-insertion. Biodegradable polymers poly(lactic acid), polycaprolactone, poly(lactic-*co*-glycolic acid) produced from the ROP of cyclic lactones and lactides are particularly attractive for their environmental friendliness and biomedical applications.[104] Metal based catalysts, such as tin(II) bis(2-ethylhexanoate) ($Sn(Oct)_2$), aluminum alkoxides and zinc salts have been useful for ROP. However, metal free ROP have been gaining much attention recently due to their reduced environmental impact. Metal-free ROP have been developed using organic catalysts such as N-heterocyclic carbenes, 4-dimethylaminopyridine and other organic super bases.[105] Figure 1.13 gives a typical polymerization of ε-caprolactone to get polycaprolactone and several catalysts that have been useful for ROP.

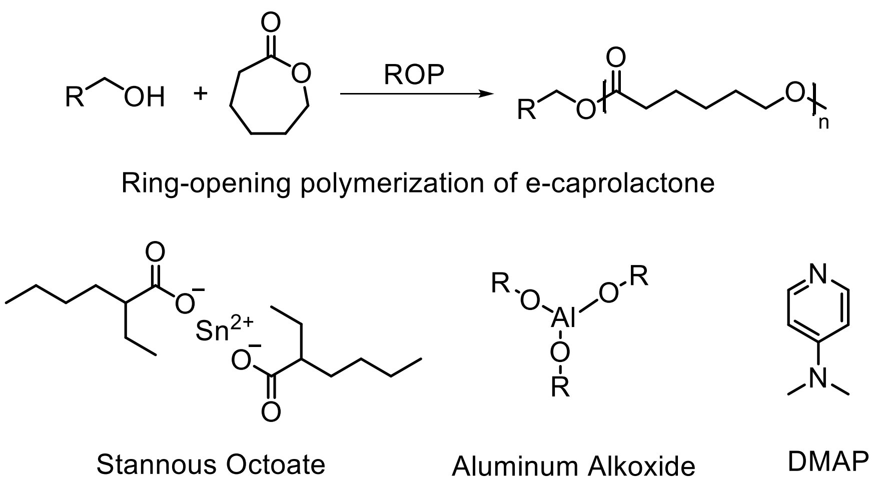

Figure 1.13 ROP of ε-caprolactone and representative ROP catalysts.

Atom Transfer Radical Polymerization (ATRP). Controlled radical polymerization (CRP) of vinyl monomers is important for the synthesis of well-defined polymers with controlled molar mass, narrow molecular weight distribution, and well-defined polymer architectures and control over functionalities.[106-119] ATRP one of the most applicable and widely accepted method for controlled radical polymerization.[112] Figure 1.14 presents a general mechanism for ATRP. The temporal control over the radical species is governed by the rapid and dynamic equilibrium between dormant species (PnX, X=halide) and active radicals (P_n•). The equilibrium is achieved through a reversible redox process of activation with low oxidation transition metal complex (Mt^m/L) and the deactivation with the high oxidation state of the complex ($X\text{-}Mt^{m+1}$/L). Although, Cu^I/L and $X\text{-}Cu^{II}$ has been widely used as the catalytic system, several other redox-active transition metal complexes (Cu, Ru, Fe, Mo, Os, etc.) have been explored. The equilibrium conditions favor a high concentration of dormant species and low concentration of propagating chain ends resulting a significant decrease of chain termination and transfer. Such a behavior provides significant control over radical polymerization.

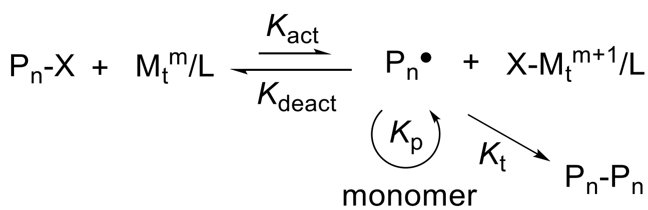

Figure 1.14 Schematic illustration of ATRP mechanism.

The initiating alkyl halides can be in solution or anchored on substrate surfaces (nanoparticles, polymer chain ends or pendent groups, one dimensional surfaces, etc.). This provide the ability to grow free polymers chains in solution or grafted from the substrates which is a significant improvement compared to free radical polymerization.[120, 121] Such grafting from methods is named as surface initiated ATRP (SI-ATRP) which is important in designing hybrid materials for biomedical applications. [122-124] Furthermore, the active polymer chain ends and can be used for chain extension to other monomers via ATRP to produce block copolymers. ATRP has opened the doors to explore polymers with various chain architectures, compositions and diverse functionalities.[125] Recent advances of ATRP polymerization try to lower metal catalyst concentration to extremely low levels, air stable ATRP as well as to explore metal free ATRP.[126-129]

Ring-Opening Metathesis Polymerization (ROMP). Coordination-polymerization methods such as ROMP allow for the synthesis of linear polymers with high molecular weight. ROMP of cyclic olefins undergo chain-growth polymerization with releasing of the ring strain energy as the driving force.[130, 131] A variety of metal alkylidenes are investigated for ROMP. Tungsten and molybdenum catalysts (Schrock catalysts) typically have rapid initiation rates to produce well defined polymers with control. However, Grubbs' ruthenium based catalysts are well-known for their stability, functional group tolerance and ease of use for polymerization under mild conditions. Three different generations of Grubbs' catalysts are given in Figure 1.15.

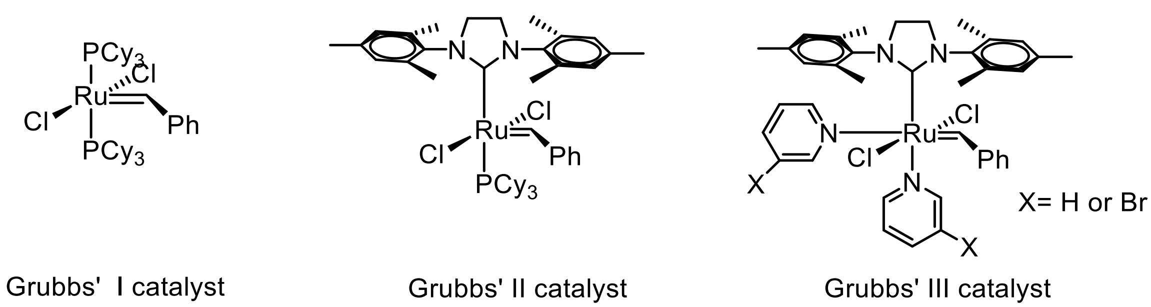

Figure 1.15 Grubbs' catalyst structures.

ROMP undergoes a chain-growth olefin metathesis of the monomers as illustrated in the mechanism (Figure 1.16). The overall mechanism of ROMP is a catalyst-mediated carbon-carbon double bond exchange. The alkylidene catalyst coordinates with the cyclic olefin and a new olefin that is generated coordinates with the catalyst as the polymer chain grows. The metathesize of the unstrained olefinic bonds in the growing polymer chain known as backbiting and chain transfer can increase the dispersity of the polymers.

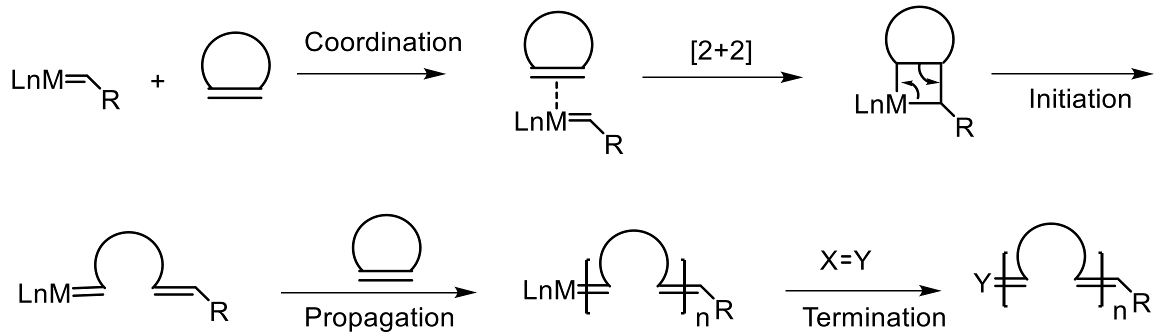

Figure 1.16 Schematic illustration of ROMP mechanism.

Norbornenes, cyclopentenes and cyclooctenes are excellent monomers for ROMP.[132] Although the monomer pool for ROMP is relatively limited, linear polymers with special functionalities can be prepared from substituted cyclic olefins. In addition, sequential monomer additions provide a path for the preparation of block copolymers.[133] ROMP provides an effective platform for synthesizing polymeric materials with diverse functionalities and architectures.

"Click" Chemistry. Click chemistry defined by K. B. Sharpless in 2001 involves many reactions with properties such as high yields, simple to perform, easy to purify and can be conducted in benign solvents.[134] Well-known examples includes copper(I)-catalyzed and strain-promoted azide-alkyne cycloaddition, Diels-Alder cycloaddition, and thiol-ene reaction. Among different click chemistries, copper(I)-catalyzed azide-alkyne cycloaddition (CuAAC) reaction is the most well-studied and widely employed technique to prepare novel polymer materials with various architectures and functional groups.[135, 136] During this reaction, organic azides and terminal alkynes combine to produce 1,4-disubstituted 1,2,3-triazoles (Figure 1.17).

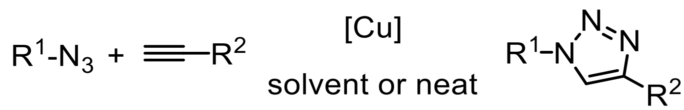

Figure 1.17 Copper catalyzed azide-alkyne cycloaddition.

CuAAC is useful to design functional interfaces through post-polymerization modification such as to make graft to polymers to make side chains as well as to link different types of polymers to obtain block copolymers with various architectures.[137-139]

1.6 Research Objectives

Development of sustainable biomaterials and polymers from natural biomass is widely anticipated to reduce the dependence on fossil oil resources. In addition, the emergence of drug-resistant bacteria necessitates the development of new antimicrobial agents. The objectives of this dissertation are blended on those two areas of research. First, antimicrobial biomaterials were developed using hydrocarbon rich biomass. Abietic acid was converted to cationic compound that contain quaternary ammonium group, and it was grafted to an azide substituted polycaprolactone polymer via CuAAC. These cationic materials demonstrated to be effective antimicrobial agents against bacteria including Methicillin-resistant *Staphylococcus aureus* with low toxicity to mammalian cells. Mechanism of action was determined using molecular dynamics simulations and dye-leakage assays. Sustainable antimicrobial and antibiofilm coatings were developed using the cationic compounds and polymers grafted onto glass surfaces via CuAAC and SI-ATRP. Antimicrobial, antibiofilm and biocompatibility properties of these surfaces were examined. Facially amphiphilic main-chain cationic polymers were developed using bile acids for antimicrobial applications.

Secondly, ROMP was utilized to synthesize high molecular weight resin acid polymers with molecular weights as high as half a million Daltons.[133] Flexible and mechanically robust films from these resin acid polymers were developed. The polymer chain entanglement molecular weight was determined. Furthermore, thermoplastic elastomers were prepared by combining resin acids, and soybean oil derived compounds. Together, these materials show promise for antimicrobial and sustainable polymer development using hydrocarbon rich renewable biomass.

1.7 References

1. Walsh, C., Molecular Mechanisms That Confer Antibacterial Drug Resistance. *Nature* **2000,** *406*, 775-781.

2. Levy, S. B.; Marshall, B., Antibacterial Resistance World-Wide: Causes, Challenges and Responses. *Nat. Med.* **2004,** *10*, S122 - S129

3. Jambeck, J. R.; Geyer, R.; Wilcox, C.; Siegler, T. R.; Perryman, M.; Andrady, A.; Narayan, R.; Law, K. L., Plastic Waste Inputs from Land into the Ocean. *Science* **2015,** *347*, 768-771.

4. Mekonnen, T.; Mussone, P.; Khalil, H.; Bressler, D., Progress in Bio-Based Plastics and Plasticizing Modifications. *J. Mater. Chem. A* **2013,** *1*, 13379-13398.

5. Belgacem, M. N.; Gandini, A., *Monomers, Polymers and Composites from Renewable Resources*. Elsevier: 2011.

6. Azapagic, A.; Emsley, A.; Hamerton, I., *Polymers: The Environment and Sustainable Development*. John Wiley & Sons: 2003.

7. Wilbon, P. A.; Chu, F.; Tang, C., Progress in Renewable Polymers from Natural Terpenes, Terpenoids, and Rosin. *Macromol. Rapid Commun.* **2013,** *34*, 8-37.

8. Yao, K.; Tang, C., Controlled Polymerization of Next-Generation Renewable Monomers and Beyond. *Macromolecules* **2013,** *46*, 1689-1712.

9. Babu, R.; O'Connor, K.; Seeram, R., Current Progress on Bio-Based Polymers and Their Future Trends. *Prog. Biomater.* **2013,** *2*.

10. Gandini, A., The Irruption of Polymers from Renewable Resources on the Scene of Macromolecular Science and Technology. *Green Chem.* **2011,** *13*, 1061-1083.

11. Holmberg, A. L.; Reno, K. H.; Wool, R. P.; Epps III, T. H., Biobased Building Blocks for the Rational Design of Renewable Block Polymers. *Soft Matter* **2014,** *10*, 7405-7424.

12. The Brundtland Commission, Our Common Future, Report of the World Commission

on Environment and Development. *Oxford University Press, Oxford* **1987**.

13. Mecking, S., Nature or Petrochemistry?-Biologically Degradable Materials. *Angew. Chem. Int. Ed.* **2004,** *43*, 1078-1085.

14. Okada, M., Chemical Syntheses of Biodegradable Polymers. *Prog. Polym. Sci.* **2002,** *27*, 87-133.

15. Drawz, S. M.; Bonomo, R. A., Three Decades of B-Lactamase Inhibitors. *Clin. Microbiol. Rev.* **2010,** *23*, 160-201.

16. Field, C. B.; Behrenfeld, M. J.; Randerson, J. T.; Falkowski, P., Primary Production of the Biosphere: Integrating Terrestrial and Oceanic Components. *Science* **1998,** *281*, 237-240.

17. Chen, G.-Q., A Microbial Polyhydroxyalkanoates (Pha) Based Bio- and Materials Industry. *Chem. Soc. Rev.* **2009,** *38*, 2434-2446.

18. Chen, G.-Q.; Patel, M. K., Plastics Derived from Biological Sources: Present and Future: A Technical and Environmental Review. *Chem. Rev.* **2012,** *112*, 2082-2099.

19. Reddy, C. S. K.; Ghai, R.; Rashmi; Kalia, V. C., Polyhydroxyalkanoates: An Overview. *Bioresour. Technol.* **2003,** *87*, 137-146.

20. Bozell, J. J., Feedstocks for the Future – Biorefinery Production of Chemicals from Renewable Carbon. *CLEAN – Soil, Air, Water* **2008,** *36*, 641-647.

21. Werpy, T.; Petersen, G.; Aden, A.; Bozell, J.; Holladay, J.; White, J.; Manheim, A.; Eliot, D.; Lasure, L.; Jones, S. *Top Value Added Chemicals from Biomass. Volume 1-Results of Screening for Potential Candidates from Sugars and Synthesis Gas*; DTIC Document: 2004.

22. Cherubini, F., The Biorefinery Concept: Using Biomass Instead of Oil for Producing Energy and Chemicals. *Energy Convers. Manage.* **2010,** *51*, 1412-1421.

23. Quirino, R. L.; Garrison, T. F.; Kessler, M. R., Matrices from Vegetable Oils, Cashew Nut Shell Liquid, and Other Relevant Systems for Biocomposite Applications. *Green Chem.* **2014,** *16*, 1700-1715.

24. Holmberg, A. L.; Reno, K. H.; Wool, R. P.; Epps, I. I. I. T. H., Biobased Building Blocks for the Rational Design of Renewable Block Polymers. *Soft Matter* **2014,** *10*, 7405-7424.

25. Gandini, A.; Lacerda, T. M.; Carvalho, A. J. F.; Trovatti, E., Progress of Polymers from Renewable Resources: Furans, Vegetable Oils, and Polysaccharides. *Chem. Rev.* **2015**.

26. Coates, G. W.; Moore, D. R., Discrete Metal-Based Catalysts for the Copolymerization of Co2 and Epoxides: Discovery, Reactivity, Optimization, and Mechanism. *Angew.*

Chem. Int. Ed.* **2004,** *43*, 6618-6639.

27. Bohlmann, J.; Keeling, C. I., Terpenoid Biomaterials. *Plant J.* **2008,** *54*, 656-669.

28. Trapp, S.; Croteau, R., Defensive Resin Biosynthesis in Conifers. *Annu. Rev. Plant Biol.* **2001,** *52*, 689-724.

29. Smith, E.; Williamson, E.; Zloh, M.; Gibbons, S., Isopimaric Acid from Pinus Nigra Shows Activity against Multidrug-Resistant and Emrsa Strains of *Staphylococcus aureus*. *Phytother. Res.* **2005,** *19*, 538-542.

30. Fernandez, M. A.; Tornos, M. P.; Garcia, M. D.; de las Heras, B.; Villar, A. M.; Saenz, M. T., Anti-Inflammatory Activity of Abietic Acid, a Diterpene Isolated from *Pimenta Racemosa Var. Grissea*. *J. Pharm. Pharmacol.* **2001,** *53*, 867-872.

31. Talevi, A.; Cravero, M. S.; Castro, E. A.; Bruno-Blanch, L. E., Discovery of Anticonvulsant Activity of Abietic Acid through Application of Linear Discriminant Analysis. *Biorg. Med. Chem. Lett.* **2007,** *17*, 1684-1690.

32. Maiti, S., ; Ray, S.; Kundu, A., Rosin: A Renewable Resource for Polymers and Polymer Chemicals. *Prog. Polym. Sci.* **1989,** *14*, 297-338.

33. Bicu, I., ; Mustata, F., Polymers from a Levopimaric Acid-Acrylic Acid Diels-Alder Adduct: Synthesis and Characterization. *J. Polym. Sci. A Polym. Chem.* **2007,** *45*, 5979-5990.

34. DSilvestre, A., ; Gandini, A., *In Monomers, Polymers and Composites from Renewable Resources*. Elsevier: Amsterdam, 2008; p 67-88.

35. Wang, J.; Yao, K.; Wilbon, P.; Wang, P.; Chu, F.; Tang, C., Rosin-Derived Polymers and Their Progress in Controlled Polymerization. In *Rosin-Based Chemicals and Polymers*, Zhang, J., Ed. ISmithers: Shawbury, UK, 2012; pp 85-127.

36. Wilbon, P.; Gulledge, A.; Benicewicz, B.; Tang, C., Renewable Rosin Fatty Acid Polyesters: The Effect of Backbone Structure on Thermal Properties. *Green Mater.* **2013,** *1*, 96-104.

37. Russell, D. W.; Setchell, K. D. R., Bile Acid Biosynthesis. *Biochemistry* **1992,** *31*, 4737-4749.

38. Björkhem, I., Chapter 9 Mechanism of Bile Acid Biosynthesis in Mammalian Liver. *New Compr. Biochem.* **1985,** *12*, 231-278.

39. Denike, J. K.; Zhu, X. X., Preparation of New Polymers from Bile Acid Derivatives. *Macromol. Rapid Commun.* **1994,** *15*, 459-465.

40. Cunningham, A. J.; Zhu, X. X., Polymers Made of Bile Acids: From Soft to Hard Biomaterials. *Can. J. Chem.* **2016,** *94*, 659-666.

41. Zhu, X.-X.; Nichifor, M., Polymeric Materials Containing Bile Acids. *Acc. Chem. Res.* **2002,** *35*, 539-546.

42. Kumar, A.; Chhatra, R. K.; Pandey, P. S., Synthesis of Click Bile Acid Polymers and Their Application in Stabilization of Silver Nanoparticles Showing Iodide Sensing Property. *Org. Lett.* **2010,** *12*, 24-27.

43. Shaikh, V. A. E.; Ubale, V. P.; Maldar, N. N.; Lonikar, S. V.; Rajan, C. R.; Ponrathnam, S., Main-Chain Liquid Crystalline Poly(Ester-Amide)S Containing Lithocholic Acid Units. *J. Appl. Polym. Sci.* **2006,** *100*, 73-80.

44. Gautrot, J. E.; Zhu, X. X., Main-Chain Bile Acid Based Degradable Elastomers Synthesized by Entropy-Driven Ring-Opening Metathesis Polymerization. *Angew. Chem. Int. Ed.* **2006,** *45*, 6872-6874.

45. Zuluaga, F.; Valderruten, N. E.; Wagener, K. B., The Ambient Temperature Synthesis and Characterization of Bile Acid Polymers. *Polym. Bull.* **1999,** *42*, 41-46.

46. Li, W.; Li, X.; Zhu, W.; Li, C.; Xu, D.; Ju, Y.; Li, G., Topochemical Approach to Efficiently Produce Main-Chain Poly(Bile Acid)S with High Molecular Weights. *Chem. Commun.* **2011,** *47*, 7728-7730.

47. Hao, J.; Li, H.; Zhu, X. X., Preparation of a Comb-Shaped Cholic Acid-Containing Polymer by Atom Transfer Radical Polymerization. *Biomacromolecules* **2006,** *7*, 995-998.

48. Jia, Y.-G.; Zhu, X. X., Self-Healing Supramolecular Hydrogel Made of Polymers Bearing Cholic Acid and Β-Cyclodextrin Pendants. *Chem. Mater.* **2015,** *27*, 387-393.

49. Ye, W.; Li, Y.; Zhou, Z.; Wang, X.; Yao, J.; Liu, J.; Wang, C., Synthesis and Antibacterial Activity of New Long-Chain-Alkyl Bile Acid-Based Amphiphiles. *Bioorg. Chem.* **2013,** *51*, 1-7.

50. Lewis, K., Platforms for Antibiotic Discovery. *Nat. Rev. Drug Discov.* **2013,** *12*, 371-387.

51. von Nussbaum, F.; Brands, M.; Hinzen, B.; Weigand, S.; Habich, D., Antibacterial Natural Products in Medicinal Chemistry-Exodus or Revival? *Angew. Chem. Int. Ed. Engl.* **2006,** *45*, 5072-5129.

52. Gillings, M. R., Evolutionary Consequences of Antibiotic Use for the Resistome, Mobilome and Microbial Pangenome. *Front. Microbiol.* **2013,** *4*, 56-63.

53. Davies, J.; Davies, D., Origins and Evolution of Antibiotic Resistance. *Microbiol. Mol. Biol. Rev.* **2010,** *74*, 417-433.

54. Boucher, H. W.; Talbot, G. H.; Bradley, J. S.; Edwards, J. E.; Gilbert, D.; Rice, L. B.; Scheld, M.; Spellberg, B.; Bartlett, J., Bad Bugs, No Drugs: No ESKAPE! An Update

from the Infectious Diseases Society of America. *Clin. Infect. Dis.* **2009,** *48*, 1-12.

55. Zasloff, M., Antimicrobial Peptides of Multicellular Organisms. *Nature* **2002,** *415*, 389-395.

56. Palermo, E. F.; Kuroda, K., Structural Determinants of Antimicrobial Activity in Polymers Which Mimic Host Defense Peptides. *Appl. Microbiol. Biotechnol.* **2010,** *87*, 1605-1615.

57. Henderson, J. M.; Lee, K. Y. C., Promising Antimicrobial Agents Designed from Natural Peptide Templates. *Curr. Opin. Solid State Mater. Sci.* **2013,** *17*, 175-192.

58. Lienkamp, K.; Madkour, A.; Tew, G., Antibacterial Peptidomimetics: Polymeric Synthetic Mimics of Antimicrobial Peptides. In *Polymer Composites – Polyolefin Fractionation – Polymeric Peptidomimetics – Collagens*, Abe, A.; Kausch, H.-H.; Möller, M.; Pasch, H., Eds. Springer Berlin Heidelberg: 2013; Vol. 251, pp 141-172.

59. Muñoz-Bonilla, A.; Cerrada, M.; Fernández-García, M., *Polymeric Materials with Antimicrobial Activity: From Synthesis to Applications*. Royal Society of Chemistry: 2013; Vol. 10.

60. Sobczak, M.; Dębek, C.; Olędzka, E.; Kozłowski, R., Polymeric Systems of Antimicrobial Peptides—Strategies and Potential Applications. *Molecules* **2013,** *18*, 14122-14137.

61. Takahashi, H.; Palermo, E. F.; Yasuhara, K.; Caputo, G. A.; Kuroda, K., Molecular Design, Structures, and Activity of Antimicrobial Peptide-Mimetic Polymers. *Macromol. Biosci.* **2013,** *13*, 1285-1299.

62. Carmona-Ribeiro, A.; de Melo Carrasco, L., Cationic Antimicrobial Polymers and Their Assemblies. *Int. J. Mol. Sci.* **2013,** *14*, 9906-9946.

63. Kuroda, K.; Caputo, G. A., Antimicrobial Polymers as Synthetic Mimics of Host-Defense Peptides. *Wiley Interdiscip. Rev. Nanomed. Nanobiotechnol.* **2013,** *5*, 49-66.

64. Li, P.; Li, X.; Saravanan, R.; Li, C. M.; Leong, S. S. J., Antimicrobial Macromolecules: Synthesis Methods and Future Applications. *RSC Adv.* **2012,** *2*, 4031-4044.

65. Muñoz-Bonilla, A.; Fernández-García, M., Polymeric Materials with Antimicrobial Activity. *Prog. Polym. Sci.* **2012,** *37*, 281-339.

66. Siedenbiedel, F.; Tiller, J. C., Antimicrobial Polymers in Solution and on Surfaces: Overview and Functional Principles. *Polymers* **2012,** *4*, 46-71.

67. Engler, A. C.; Wiradharma, N.; Ong, Z. Y.; Coady, D. J.; Hedrick, J. L.; Yang, Y.-Y., Emerging Trends in Macromolecular Antimicrobials to Fight Multi-Drug-Resistant Infections. *Nano Today* **2012,** *7*, 201-222.

68. Timofeeva, L.; Kleshcheva, N., Antimicrobial Polymers: Mechanism of Action, Factors of Activity, and Applications. *Appl. Microbiol. Biotechnol.* **2011,** *89*, 475-492.

69. Som, A.; Vemparala, S.; Ivanov, I.; Tew, G. N., Synthetic Mimics of Antimicrobial Peptides. *Biopolymers* **2008,** *90*, 83-93.

70. Giuliani, A.; Pirri, G.; Bozzi, A.; Di Giulio, A.; Aschi, M.; Rinaldi, A. C., Antimicrobial Peptides: Natural Templates for Synthetic Membrane-Active Compounds. *Cell. Mol. Life Sci.* **2008,** *65*, 2450-2460.

71. Gabriel, G. J.; Som, A.; Madkour, A. E.; Eren, T.; Tew, G. N., Infectious Disease: Connecting Innate Immunity to Biocidal Polymers. *Mater. Sci. Eng. R-Rep.* **2007,** *57*, 28-64.

72. Kenawy, E.-R.; Worley, S. D.; Broughton, R., The Chemistry and Applications of Antimicrobial Polymers: A State-of-the-Art Review. *Biomacromolecules* **2007,** *8*, 1359-1384.

73. Tashiro, T., Antibacterial and Bacterium Adsorbing Macromolecules. *Macromol. Mater. Eng.* **2001,** *286*, 63-87.

74. Hancock, R. E.; Diamond, G., The Role of Cationic Antimicrobial Peptides in Innate Host Defences. *Trends Microbiol.* **2000,** *8*, 402-410.

75. Nakatsuji, T.; Gallo, R. L., Antimicrobial Peptides: Old Molecules with New Ideas. *J. Invest. Dermatol.* **2012,** *132*, 887-895.

76. Reddy, K. V. R.; Yedery, R. D.; Aranha, C., Antimicrobial Peptides: Premises and Promises. *Int. J. Antimicrob. Agents* **2004,** *24*, 536-547.

77. Hancock, R. E.; Sahl, H. G., Antimicrobial and Host-Defense Peptides as New Anti-Infective Therapeutic Strategies. *Nat. Biotechnol.* **2006,** *24*, 1551-1557.

78. Wade, D.; Boman, A.; Wåhlin, B.; Drain, C. M.; Andreu, D.; Boman, H. G.; Merrifield, R. B., All-D Amino Acid-Containing Channel-Forming Antibiotic Peptides. *Proc. Natl. Acad. Sci. USA* **1990,** *87*, 4761-4765.

79. Brogden, K. A., Antimicrobial Peptides: Pore Formers or Metabolic Inhibitors in Bacteria? *Nat. Rev. Micro.* **2005,** *3*, 238-250.

80. Gilbert, P.; Moore, L. E., Cationic Antiseptics: Diversity of Action under a Common Epithet. *J. Appl. Microbiol.* **2005,** *99*, 703-715.

81. Kenawy, E.-R.; Abdel-Hay, F. I.; El-Shanshoury, A. E.-R. R.; El-Newehy, M. H., Biologically Active Polymers. V. Synthesis and Antimicrobial Activity of Modified Poly(Glycidyl Methacrylate-Co-2-Hydroxyethyl Methacrylate) Derivatives with Quaternary Ammonium and Phosphonium Salts. *J. Polym. Sci., Part A: Polym. Chem.* **2002,** *40*, 2384-2393.

82. Matsuzaki, K., Control of Cell Selectivity of Antimicrobial Peptides. *Biochim. Biophys. Acta* **2009,** *1788*, 1687-1692.

83. Bowman, S. M.; Free, S. J., The Structure and Synthesis of the Fungal Cell Wall. *Bioessays* **2006,** *28*, 799-808.

84. Ruiz-Herrera, J.; Elorza, M. V.; Valentin, E.; Sentandreu, R., Molecular Organization of the Cell Wall of Candida Albicans and Its Relation to Pathogenicity. *FEMS Yeast Res.* **2006,** *6*, 14-29.

85. Poole, K., Mechanisms of Bacterial Biocide and Antibiotic Resistance. *J. Appl. Microbiol.* **2002,** *92*, 55S-64S.

86. Yeaman, M. R.; Yount, N. Y., Mechanisms of Antimicrobial Peptide Action and Resistance. *Pharmacol. Rev.* **2003,** *55*, 27-55.

87. Nizet, V., Antimicrobial Peptide Resistance Mechanisms of Human Bacterial Pathogens. *Curr. Issues Mol. Biol.* **2006,** *8*, 11-26.

88. Thoma, L. M.; Boles, B. R.; Kuroda, K., Cationic Methacrylate Polymers as Topical Antimicrobial Agents against *Staphylococcus aureus* Nasal Colonization. *Biomacromolecules* **2014,** *15*, 2933-2943.

89. Marr, A. K.; Gooderham, W. J.; Hancock, R. E. W., Antibacterial Peptides for Therapeutic Use: Obstacles and Realistic Outlook. *Curr. Opin. Pharm.* **2006,** *6*, 468-472.

90. Pollard, J. E.; Snarr, J.; Chaudhary, V.; Jennings, J. D.; Shaw, H.; Christiansen, B.; Wright, J.; Jia, W.; Bishop, R. E.; Savage, P. B., In Vitro Evaluation of the Potential for Resistance Development to Ceragenin Csa-13. *J. Antimicrob. Chemother.* **2012,** *67*, 2665-2672.

91. Sovadinova, I.; Palermo, E. F.; Urban, M.; Mpiga, P.; Caputo, G. A.; Kuroda, K., Activity and Mechanism of Antimicrobial Peptide-Mimetic Amphiphilic Polymethacrylate Derivatives. *Polymers* **2011,** *3*, 1512-1532.

92. Peschel, A.; Sahl, H.-G., The Co-Evolution of Host Cationic Antimicrobial Peptides and Microbial Resistance. *Nat. Rev. Micro.* **2006,** *4*, 529-536.

93. Fjell, C. D.; Hiss, J. A.; Hancock, R. E. W.; Schneider, G., Designing Antimicrobial Peptides: Form Follows Function. *Nat. Rev. Drug Discov.* **2012,** *11*, 37-51.

94. Porter, E. A.; Wang, X.; Lee, H.-S.; Weisblum, B.; Gellman, S. H., Antibiotics: Non-Haemolytic *β*-Amino-Acid Oligomers. *Nature* **2000,** *404*, 565-565.

95. Godballe, T.; Nilsson, L. L.; Petersen, P. D.; Jenssen, H., Antimicrobial Β-Peptides and Α-Peptoids. *Chem. Biol. Drug Des.* **2011,** *77*, 107-116.

96. Chongsiriwatana, N. P.; Patch, J. A.; Czyzewski, A. M.; Dohm, M. T.; Ivankin, A.; Gidalevitz, D.; Zuckermann, R. N.; Barron, A. E., Peptoids That Mimic the Structure, Function, and Mechanism of Helical Antimicrobial Peptides. *Proc. Natl. Acad. Sci. U.S.A.* **2008,** *105*, 2794-2799.

97. Niu, Y.; Wu, H.; Li, Y.; Hu, Y.; Padhee, S.; Li, Q.; Cao, C.; Cai, J., Aapeptides as a New Class of Antimicrobial Agents. *Org. Biomol. Chem.* **2013,** *11*, 4283-4290.

98. Yeung, A. Y.; Gellatly, S.; Hancock, R. W., Multifunctional Cationic Host Defence Peptides and Their Clinical Applications. *Cell. Mol. Life Sci.* **2011,** *68*, 2161-2176.

99. Ong, Z. Y.; Wiradharma, N.; Yang, Y. Y., Strategies Employed in the Design and Optimization of Synthetic Antimicrobial Peptide Amphiphiles with Enhanced Therapeutic Potentials. *Adv. Drug Del. Rev.* **2014,** *78*, 28-45.

100. Nuyken, O.; Pask, S., Ring-Opening Polymerization-an Introductory Review. *Polymers* **2013,** *5*, 361.

101. Sutar, A. K.; Maharana, T.; Dutta, S.; Chen, C.-T.; Lin, C.-C., Ring-Opening Polymerization by Lithium Catalysts: An Overview. *Chem. Soc. Rev.* **2010,** *39*, 1724-1746.

102. Albertsson, A.-C.; Varma, I. K., Recent Developments in Ring Opening Polymerization of Lactones for Biomedical Applications. *Biomacromolecules* **2003,** *4*, 1466-1486.

103. Odian, G., Ring-Opening Polymerization. In *Principles of Polymerization,* John Wiley & Sons, Inc, New Jersey, 2004, 544-618.

104. Stridsberg, K. M.; Ryner, M.; Albertsson, A.-C., Controlled Ring-Opening Polymerization: Polymers with Designed Macromolecular Architecture. In *Degradable Aliphatic Polyesters*, Springer: 2002; pp 41-65.

105. Kamber, N. E.; Jeong, W.; Waymouth, R. M.; Pratt, R. C.; Lohmeijer, B. G. G.; Hedrick, J. L., Organocatalytic Ring-Opening Polymerization. *Chem. Rev.* **2007,** *107*, 5813-5840.

106. Matyjaszewski, K.; Davis, T. P., *Handbook of Radical Polymerization*. John Wiley & Sons: Hoboken, 2002.

107. Matyjaszewski, K., *Controlled/Living Radical Polymerization. From Synthesis to Materials*. American Chemical Society: Washington, DC, 2006; Vol. 944.

108. Matyjaszewski, K., *Advances in Controlled/Living Radical Polymerization, ACS Symp. Ser.* American Chemistry Society: Washington, D.C., 2003; Vol. 854.

109. Matyjaszewski, K., *Controlled/Living Radical Polymerization. Progress in Atrp, Nmp, and Raft, ACS Symp. Ser.* American Chemistry Society: San Francisco, 2000; Vol. 768.

110. Benoit, D.; Chaplinski, V.; Braslau, R.; Hawker, C. J., Development of a Universal Alkoxyamine for "Living" Free Radical Polymerizations. *J. Am. Chem. Soc.* **1999,** *121*, 3904-3920.

111. Hawker, C. J.; Bosman, A. W.; Harth, E., New Polymer Synthesis by Nitroxide Mediated Living Radical Polymerizations. *Chem. Rev.* **2001,** *101*, 3661-3688.

112. Matyjaszewski, K., Atom Transfer Radical Polymerization (Atrp): Current Status and Future Perspectives. *Macromolecules* **2012,** *45*, 4015-4039.

113. Kamigaito, M.; Ando, T.; Sawamoto, M., Metal-Catalyzed Living Radical Polymerization. *Chem. Rev.* **2001,** *101*, 3689-3745.

114. Moad, G.; Rizzardo, E.; Thang, S. H., Living Radical Polymerization by the Raft Process. *Aust. J. Chem.* **2005,** *58*, 379-410.

115. Tsarevsky, N. V.; Matyjaszewski, K., “Green” Atom Transfer Radical Polymerization: From Process Design to Preparation of Well-Defined Environmentally Friendly Polymeric Materials. *Chem. Rev.* **2007,** *107*, 2270-2299.

116. Hawker, C. J.; Wooley, K. L., The Convergence of Synthetic Organic and Polymer Chemistries. *Science* **2005,** *309*, 1200-1205.

117. Matyjaszewski, K.; Tsarevsky, N. V., Nanostructured Functional Materials Prepared by Atom Transfer Radical Polymerization. *Nat. Chem.* **2009,** *1*, 276-288.

118. Ouchi, M.; Terashima, T.; Sawamoto, M., Transition Metal-Catalyzed Living Radical Polymerization: Toward Perfection in Catalysis and Precision Polymer Synthesis. *Chem. Rev.* **2009,** *109*, 4963-5050.

119. Moad, G.; Rizzardo, E.; Thang, S. H., Living Radical Polymerization by the Raft Process Â€“ a Third Update. *Aust. J. Chem.* **2012,** *65*, 985-1076.

120. Liu, J.; Lian, X.; Zhao, F.; Zhao, H., Intramolecular Atom Transfer Radical Coupling of Macromolecular Brushes. *J. Polym. Sci., Part A: Polym. Chem.* **2013,** *51*, 3567-3571.

121. Wright, R. A.; Wang, K.; Qu, J.; Zhao, B., Oil-Soluble Polymer Brush-Grafted Nanoparticles as Effective Lubricant Additives for Friction and Wear Reduction. *Angew. Chem. Int. Ed.* **2016**.

122. Siegwart, D. J.; Oh, J. K.; Matyjaszewski, K., Atrp in the Design of Functional Materials for Biomedical Applications. *Prog. Polym. Sci.* **2012,** *37*, 18-37.

123. Hui, C. M.; Pietrasik, J.; Schmitt, M.; Mahoney, C.; Choi, J.; Bockstaller, M. R.; Matyjaszewski, K., Surface-Initiated Polymerization as an Enabling Tool for Multifunctional (Nano-)Engineered Hybrid Materials. *Chem. Mater.* **2014,** *26*, 745-762.

124. Edmondson, S.; Osborne, V. L.; Huck, W. T. S., Polymer Brushes Via Surface-Initiated Polymerizations. *Chem. Soc. Rev.* **2004,** *33*, 14-22.

125. Coessens, V.; Pintauer, T.; Matyjaszewski, K., Functional Polymers by Atom Transfer Radical Polymerization. *Prog. Polym. Sci.* **2001,** *26*, 337-377.

126. Treat, N. J.; Sprafke, H.; Kramer, J. W.; Clark, P. G.; Barton, B. E.; Read de Alaniz, J.; Fors, B. P.; Hawker, C. J., Metal-Free Atom Transfer Radical Polymerization. *J. Am. Chem. Soc.* **2014,** *136*, 16096-16101.

127. Magenau, A. J. D.; Strandwitz, N. C.; Gennaro, A.; Matyjaszewski, K., Electrochemically Mediated Atom Transfer Radical Polymerization. *Science* **2011,** *332*, 81-84.

128. Konkolewicz, D.; Schröder, K.; Buback, J.; Bernhard, S.; Matyjaszewski, K., Visible Light and Sunlight Photoinduced Atrp with Ppm of Cu Catalyst. *ACS Macro Lett.* **2012,** *1*, 1219-1223.

129. Pan, X.; Fang, C.; Fantin, M.; Malhotra, N.; So, W. Y.; Peteanu, L. A.; Isse, A. A.; Gennaro, A.; Liu, P.; Matyjaszewski, K., Mechanism of Photoinduced Metal-Free Atom Transfer Radical Polymerization: Experimental and Computational Studies. *J. Am. Chem. Soc.* **2016,** *138*, 2411-2425.

130. Bielawski, C. W.; Grubbs, R. H., Highly Efficient Ring-Opening Metathesis Polymerization (Romp) Using New Ruthenium Catalysts Containing N-Heterocyclic Carbene Ligands. *Angew. Chem. Int. Ed.* **2000,** *39*, 2903-2906.

131. Bielawski, C. W.; Grubbs, R. H., Living Ring-Opening Metathesis Polymerization. *Prog. Polym. Sci.* **2007,** *32*, 1-29.

132. Sutthasupa, S.; Shiotsuki, M.; Sanda, F., Recent Advances in Ring-Opening Metathesis Polymerization, and Application to Synthesis of Functional Materials. *Polym. J.* **2010,** *42*, 905-915.

133. Ganewatta, M. S.; Ding, W.; Rahman, M. A.; Yuan, L.; Wang, Z.; Hamidi, N.; Robertson, M. L.; Tang, C., Biobased Plastics and Elastomers from Renewable Rosin Via "Living" Ring-Opening Metathesis Polymerization. *Macromolecules* **2016**.

134. Rostovtsev, V. V.; Green, L. G.; Fokin, V. V.; Sharpless, K. B., A Stepwise Huisgen Cycloaddition Process: Copper(I)-Catalyzed Regioselective "Ligation" of Azides and Terminal Alkynes. *Angew. Chem. Int. Ed.* **2002,** *41*, 2596-2599.

135. Sumerlin, B. S.; Vogt, A. P., Macromolecular Engineering through Click Chemistry and Other Efficient Transformations. *Macromolecules* **2009,** *43*, 1-13.

136. Hein, J. E.; Fokin, V. V., Copper-Catalyzed Azide-Alkyne Cycloaddition (Cuaac) and Beyond: New Reactivity of Copper(I) Acetylides. *Chem. Soc. Rev.* **2010,** *39*, 1302-1315.

137. Arnold, R. M.; Huddleston, N. E.; Locklin, J., Utilizing Click Chemistry to Design Functional Interfaces through Post-Polymerization Modification. *J. Mater. Chem.* **2012,** *22*, 19357-19365.

138. Golas, P. L.; Matyjaszewski, K., Marrying Click Chemistry with Polymerization: Expanding the Scope of Polymeric Materials. *Chem. Soc. Rev.* **2010,** *39*, 1338-1354.

139. Binder, W. H.; Sachsenhofer, R., 'Click' Chemistry in Polymer and Materials Science. *Macromol. Rapid Commun.* **2007,** *28*, 15-54.

CHAPTER 2

BIO-INSPIRED RESIN ACID-DERIVED MATERIALS AS ANTIBACTERIAL AGENTS WITH UNEXPECTED ACTIVITIES[3]

[3] Ganewatta, M. S.; Chen, Y. P.; Wang, J.; Zhou, J.; Ebalunode, J.; Nagarkatti, M.; Decho, A. W.; Tang, C., Bio-Inspired Resin Acid-Derived Materials as Anti-Bacterial Resistance Agents with Unexpected Activities. *Chem. Sci.* **2014**, *5*, 2011-2016. Reproduced with permission from The Royal Society of Chemistry.

2.1 Abstract

Methicillin-resistant *Staphylococcus aureus* (MRSA), a complex of multidrug-resistant Gram-positive bacterial strains, has proven especially problematic in both hospital and community-settings, resulting in increased mortality rates and hospitalization costs. Emergence of resistance even to vancomycin, the standard reference for MRSA treatment, builds up pressure for the search of novel alternatives. We report potent natural resin acid-based cationic antimicrobial compounds and polymers that exhibit surprising antimicrobial activity against a range of MRSA strains, yet are largely non-toxic against mammalian cells. Molecular dynamics simulations and dye-leakage assays with anionic phospholipid membrane mimics of bacteria demonstrate a membrane-lysing effect induced by unique fused ring structures of resin acids that may constitute the principal mechanism of action for selective lysis of bacterial cells over mammalian cells. Our antimicrobial materials are derived from an unlikely yet abundant natural source, and offer a novel alternative to currently-used approaches.

2.2 Introduction

Concerns over antibiotic resistance have now evolved into a vexing healthcare crisis.[1, 2] Previously-staple antibiotics, such as penicillin and methicillin, have been rendered relatively ineffective due to the emergence of resistance among many bacteria.[3-6] Methicillin-resistant *Staphylococcus aureus* (MRSA) is responsible for many difficulty-to-treat infections and has become a type of superbugs that lead to serious public health concerns.[7-9] MRSA is associated with, and a major cause of, a wide range of conditions and nosocomial infections such as tissue carbuncles and food poisoning, implant-device and wound-related infections, bacteremia, necrotizing pneumonia and endocarditis, many of which are life-threatening.[10] Currently, vancomycin is the gold-standard approach to treat MRSA infections due to a lower drug acquisition cost and better clinical outcomes even though newer agents with proven efficacy (e.g., linezolid, quinupristin-dalfopristin, daptomycin, and tigecycline) are available.[11-13] However, cytotoxicity must be carefully observed during administration, and many MRSA strains are now having reduced susceptibility to vancomycin.[14, 15] Utilization of higher doses of vancomycin to treat infections by MRSA strains with high minimum inhibitory concentrations [9] show increased rates of nephrotoxicity and failures.[16] These challenges highlight the need for alternative treatment options having novel mechanisms of action and greater selectivity towards MRSA.[17]

Herein we show promising anti-MRSA properties of cationic compounds and polymers derived from an unlikely source, the extract of pine-tree resin with a global production of more than one million metric tons annually.[18, 19] Pine resin consists of diterpene (C_{20}) resin acids that are largely produced by pine and conifer trees as a part of their chemical and physical defense against herbivore or pathogen attacks.[20, 21] The abietane resin, abietic acid, is known to possess a variety of biological activities including antimicrobial[22], anti-inflammatory[23] and anticonvulsant[24] activities. As a part of our research to develop antimicrobial agents in large quantities (at the scale of kilogram in the laboratory) and low cost using natural products that are particularly appealing for developing countries,[25] we identified abietic acid as a potential candidate.

2.3 Experimental section

Materials

Maleic anhydride, furan, ethyl acetate, ethanol, toluene, *N*,*N*-dimethylaminoethylamine (DAEA), abietic acid (85%), propargyl alcohol, triethylamine, p-toluene sulfonic acid (PTS), bromoethane, 2-chlorocyclohexanone, m-chloroperoxybenzoic acid (mCPBA), Sn(II)2-ethylhexanoate($Sn(Oct)_2$), sodium azide, copper iodide and 1,8-diazabicyclo[5.4.0] undec-7-ene (DBU) were purchased from Sigma Aldrich. Acetic acid, dichloromethane (DCM), ethyl acetate, ethanol, hexane, methanol, toluene, tetrahydrofuran (THF), *N*,*N*-dimethylformamide (DMF) were obtained as ACS grade solvents. Triethylamine was distilled after drying over K_2CO_3. Propargyl alcohol was distilled from CaH_2 under reduced pressure. Triton™ X-100, Calcein (97%), Sephadex® G-25 Medium and Peptidoglycan extract from *Staphylococcus aureus* were obtained from Sigma Aldrich and used as received. The phospholipids 1,2-dioleoyl-sn-glycero-3-phospho-(1'-rac-glycerol)(sodium salt) (DOPG) and 1,2-dioleoyl-sn-glycero-3-phosphocholine (DOPC) were obtained as chloroform solutions from Avanti Polar Lipids, Inc. and used as received.

Characterization

^{1}H NMR (300 MHz) and ^{13}C NMR (75 MHz) spectra were recorded on a Varian Mercury spectrometer with tetramethylsilane (TMS) as an internal reference. Fourier transform infrared (FTIR) analysis was performed using a Perkin-Elmer spectrum with Attenuated Total Reflectance (ATR) mode. Gel permeation chromatography (GPC) was performed in DMF at a flow rate of 0.8 mL/min at 50 ºC on a Varian system equipped with a ProStar 210 pump and a Varian 356-LC RI detector and three 5 µm phenogel columns

(Phenomenex Co.) with narrow dispersed polystyrene as standards. Mass spectrometry was conducted on a Waters Micromass Q-Tof mass spectrometer, and the ionization source was positive ion electrospray. Transmission electron microscopy (TEM) images were obtained on a Hitachi 8000 transmission electron microscope at an operating voltage of 150 kV. The TEM samples were prepared by placing a drop of sample on carbon-coated copper grids, dried and stained (with RuO_4) before observation. Fluorescence kinetic measurements were performed on a Varian Cary Eclipse fluorescence spectrophotometer with temperature controlled cells. A Zeiss LSM 410 confocal laser scan microscope (CLSM) was used for fluorescent imaging. Zetasizer Nano ZSP, Malvern Instruments Corporate was used for the determination of liposome size and surface charge. Wallac 1420 VICTOR^{2TM} Multilabel Counter (PerkinElmer, Shelton, CT) was used for absorbance measurements.

Synthesis of Resin Acid Derived Antimicrobial Compounds

Compound 1 was prepared using a modified synthetic strategy from our previous report.[26] The synthetic strategy illustrated in Figure 2.1 allowed us to prepare the compound 1 at large scale without any chromatography purification.

Synthesis of Maleopimaric Acid

Maleopimaric acid was prepared according to our previous report.[26] Abietic acid (100.0 g, 0.28 mol) was heated to 180 °C under a nitrogen atmosphere and maintained for 3h. After adjusting the reaction temperature to 120 °C, maleic anhydride (27.5 g, 0.28 mol) and PTS (0.5 g, 0.0028 mol) dissolved in acetic acid (300.0 mL) were added. The reaction was refluxed at 120 °C for 12 h. The resultant yellow crystals were recrystallized from acetic acid thrice. Then washed with 5 % $NaHCO_3$ the final product was obtained as white crystals. (83 g, yield 73%) ^{1}H NMR (300 MHz, $CDCl_3$) δ (ppm): 5.54 (s, 1H, C*H*=C); 3.10 (d, 1H, C*H*C=O); 2.73 (d, 1H, C*H*C=O); 2.50 (d, 1H, C*H*C=CH); 2.27 (m, 1H, CC*H*(CH_3)$_2$); 2.10 (m, 2H, CC$H_2$$CH_2$); 1.16 (s, 3H, CC$H_3$); 0.98 (m, 6H, CCH(C$H_3$)$_2$); 0.59 (s, 3H, CC$H_3$). ^{13}C NMR (75 MHz, $CDCl_3$) δ: 185.4(*C*OOH); 172.7-170.9 (O=*C*O*C*=O); 148.1 (*C*=CH); 125.1 (C=*C*H); 49.1 (C=OCH*C*HC=O); 46.8(*C*C=O). ES-MS: m/z 400 (theoretical m/z: 399+H^+)

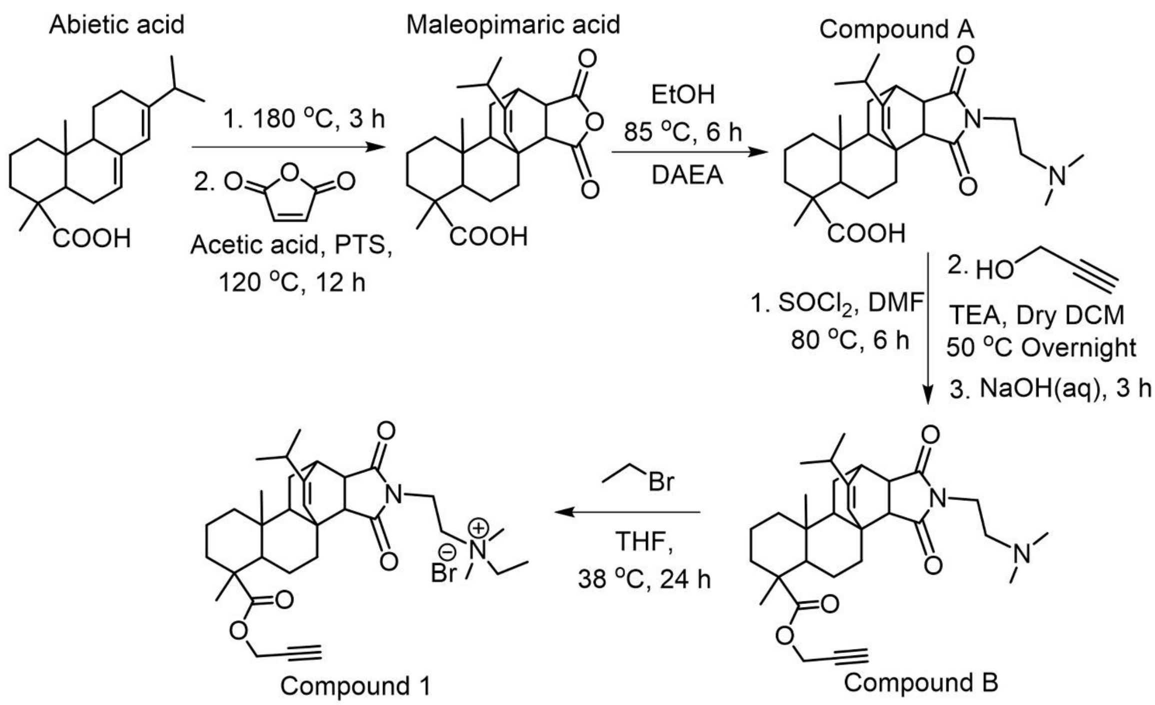

Figure 2.1 Synthesis of resin acid-derived compound 1.

Synthesis of Compound A

Maleopimaric acid (50.0 g, 0.125 mol) was dissolved in ethanol (200.0 mL) followed by adding *N*,*N*-dimethylaminoethylamine (14.0 mL, 0.125 mol) and refluxed at 85 °C for 6 h. The product started to precipitate after about an hour. After 6 h the reaction was cooled using an ice bath to complete the precipitation, then filtrated and washed with cold ethanol and dried. The compound A appeared as a white powder (41.5 g, yield: 71%).

^{1}H NMR (Figure S2) (300 MHz, $CDCl_3$) δ (ppm): 5.52 (s, 1H, C*H*=C); 3.70 (t, 2H, NC$H_2$$CH_2$); 3.43 (d, 1H, C*H*C=O); 3.18 (d, 1H, C*H*C=O); 2.92 (t, 2H, CH_2N$(CH_3)_2$); 2.63 (d, 1H, CH_2C*H*C=CH); 2.35 (s, 6H, CH_2N(CH_3)$_2$); 2.21 (m, 1H, CH_2=CC*H*$(CH_3)_2$). ES-MS: m/z 471 (theoretical m/z: 470+H^+).

Synthesis of Compound B

Compound A (35.0 g, 0.074 mol) was mixed with 50 mL of distilled thionyl chloride in a dry two neck round bottom flask under nitrogen at 0 °C. After adding two drops of dry DMF, it was refluxed for 2 h followed by vacuum distillation to remove unreacted thionyl chloride. Then the yellow colored viscous liquid containing the acid chloride was dissolved in minimum amount of dry DCM. Another dry round bottom flask was charged with dry propargyl alcohol (30 mL) and dry triethylamine (21 mL, 0.15 mol). Then the crude acid chloride was transferred slowly to the second flask and kept stirring for 24 h at 50 °C. The crude mixture was dissolved in THF/DCM mixture and stirred with 3 M NaOH solution for 3 h and extracted into DCM. The ester can be further purified by using a silica column and ethyl acetate as the mobile phase. But this purification is not required. ^{1}H NMR (300 MHz, $CDCl_3$) δ (ppm): δ: 5.37 (s, 1H, C*H*=C); 4.65 (m, 2H, CH_2C≡CH); 3.44 (t, 2H, NC$H_2$$CH_2$); 3.00 (d, 1H, C*H*C=O); 2.77 (s, 1H, CH_2C≡C*H*); 2.49 (d, 1H,C*H*C=O); 2.44 (t, 2H, CH_2N$(CH_3)_2$); 2.00 (s, 6H, N(CH_3)$_2$); 1.16 (s, 3H, CCH_3); 0.98 (m, 6H, CCH(CH_3)$_2$); 0.59 (s, 3H, CCH_3).

Synthesis of Compound 1

The crude product from the previous step was used without chromatography purification. It was dissolved in dry THF and bromoethane (40 mL, 0.37 mol) was added. The mixture was heated at 38 °C for 48 h. The product precipitated in THF in the process of reaction. Then it was filtrated and then washed with THF. Pure product appeared as an off-white powder. The crystals were prepared by dissolving 500 mg of compound 1 in 1 mL of DCM, adding 3 mL of THF and evaporating slowly over night. (41.7 g, yield: 91%) ^{1}H NMR (Figure 2.2) (300 MHz, $CDCl_3$) δ (ppm): 5.39 (s, 1H, C*H*=C); 4.65 (m, 2H, CH_2C≡CH); 3.76 (t, 2H, NCH_2CH_2); 3.73 (m, 2H, NCH_2CH_2); 3.67 (m, 2H, N+CH_2CH_3); 3.39 (s, 6H, N+(CH_3)$_2$); 3.00 (m, 1H, C*H*C=O); 2.96 (s, 1H, CH_2C≡C*H*); 2.64 (d, 1H, C*H*C=O); 2.49 (d, 1H, CH_2C*H*C=CH); 2.16 (m, 1H, CH=CC*H*(CH_3)$_2$); 1.16 (s, 3H, CCH_3); 0.92 (m, 6H, CCH(CH_3)$_2$); 0.58 (s, 3H, CCH_3). ^{13}C NMR (75 MHz, methanol-d4) δ (ppm): 178.5 (C*C*=OO); 177.8-177.0 (O=*C*N*C*=O); 147.2 (*C*=CH); 124.5 (C=*C*H); 77.5 (CH_2*C*≡CH); 74.6 (CH_2C≡*C*H); 59.5-60.0 (CH_2*C*H_2N+ and CH_3*C*H_2N+). ES-MS (Figure S5): m/z 537 (theoretical m/z: 537+81(Br)).

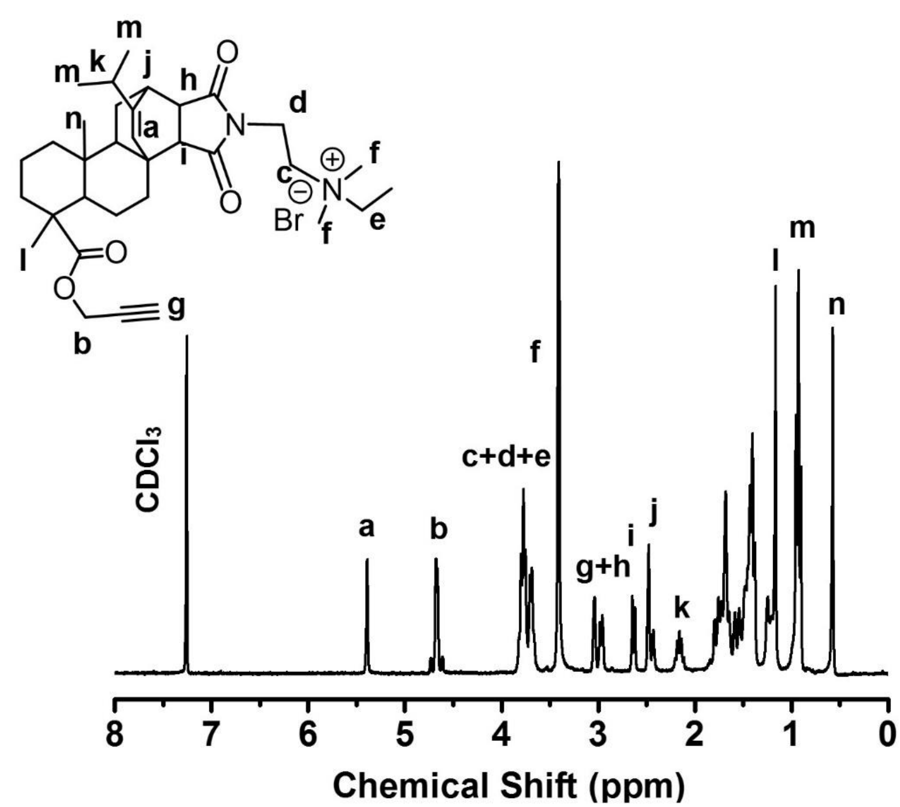

Figure 2.2 ^{1}H NMR spectrum of compound 1 in $CDCl_3$.

Synthesis of Resin Acid Containing Polymers

The polymers were prepared following our previous work as shown in Figure 2.3.[26] ROP was used to polymerize α-Chloro-ε-caprolactone and the chlorine groups was subsequently replaced by azide groups. Characterization was done using GPC (Figure 2.4), ^{1}H NMR (Figure 2.5) and FT-IR. The characteristic azide IR peak at 2100 cm^{-1} disappeared after the click reaction confirming a quantitative completion of the reaction.

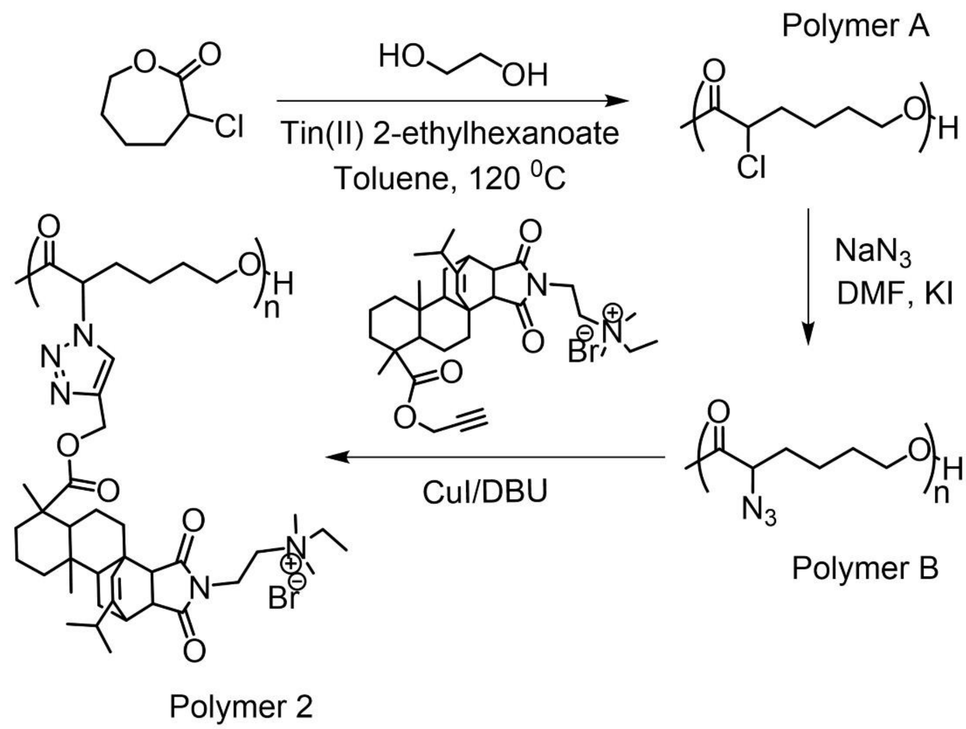

Figure 2.3 Synthesis of resin acid containing polymers.

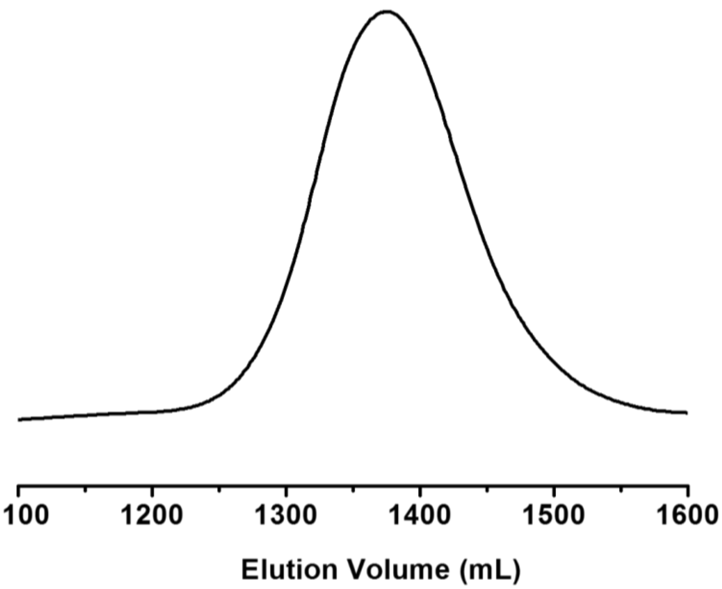

Figure 2.4 GPC trace of polymer A (M_n (GPC) = 27,900 g/mol, $Đ$ = 1.59).

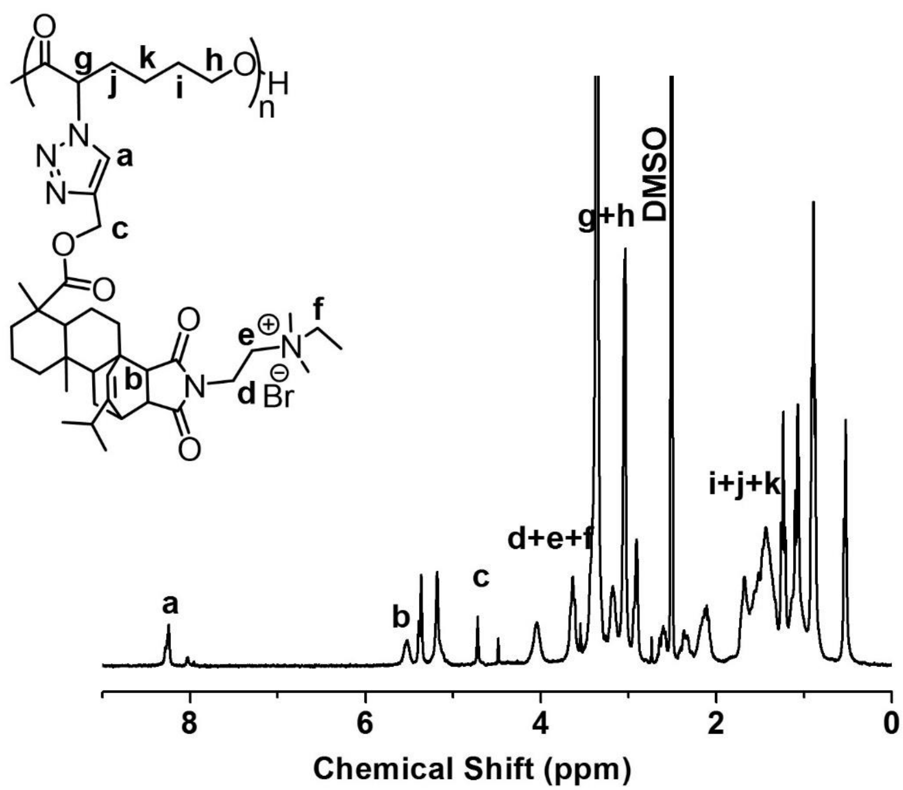

Figure 2.5 ^1H NMR spectrum of polymer 2 in DMSO-d_6.

Agar Disk-diffusion Assays

To conduct the assays, actively-growing cultures of each bacterial strain on Mannitol salt agar (MSA) were inoculated on Tryptic Soy Broth (TSB) agar plates. The bacterial growth culture (cell concentrations were 1.0 x 10^6 CFU/mL) 10 μL was diluted to 1 mL in TSB and 100 μL of that was spread on TSB agar plates to form a bacterial lawn covering the plate surface. Then 6 mm (diameter) filter discs were added to the plate surface, then each compound at different concentrations in DMSO was added to disks, and the plates were incubated at 28 ^oC for 18 h. The development of a clear zone around the disk was indicative of the ability of materials to kill bacteria. By quantifying the area (knowing its diameter and the depth of the agar) of inhibition, a minimum inhibitory concentration was calculated for each material/bacterial combination using established protocols.[27]

Hemolysis Assay

Fresh mouse red blood cells (RBC) were washed with PBS for three times. Next a suspension of $10x10^6$ red blood cells in 50 μL PBS (4% in volume) was placed in each well of 96-well round bottom plates. Compound 1 and polymer 2 were dissolved in PBS added in individual wells at concentrations of 0, 100, 200, 300, 400, 500 μg/ml. PBS, 1% DMSO and 5% Triton solutions were accompanied in separate wells as negative or positive controls. Then all wells were adjusted with PBS to make the final volumes up to 200 μL. A humidified 5% CO_2 incubator was used to incubate the plates at 37 ^oC for 1 h. After incubation, the plates were centrifuged at 1000 g for 10 min. Then 100 μL of supernatants from each well were transferred to wells in a 96-well flat bottom plate. The absorbance at 576 nm for hemoglobin release from RBC was measured. Absorbance of supernatants from RBC lysed with 5% Triton was taken as 100% hemolysis. Percentage hemolysis was calculated using the following formula: Hemolysis (%) = [(O.D.$_{576\ nm}$ in the resin acid material solution − O.D.$_{576\ nm}$ in PBS)/(O.D.$_{576\ nm}$ in 0.5% Triton X-100 − O.D.$_{576\ nm}$ in PBS)] × 100.

Cytotoxicity Assays

In vitro cytotoxicity carried out using mouse splenocytes isolated from C57BL/6 mice and cultured in the presence of QA. Culture medium 200 μL was supplemented with 2 μL of DMSO containing different concentrations, up to 100 μg/mL of compound 1 or polymer 2. DMSO 1% was used as the control. Fluorescence activated cell sorting (FACS) analysis of cell populations in mouse splenocytes after co-culture *in vitro* for two days was employed after staining with fluorochrome conjugated specific Abs to determine the cytotoxicity of compound 1 or polymer 2. For *in vivo* tests the mice received intravenous injections of 10 mg/kg body weight of compound 1 or polymer 2.

Dye-Leakage Studies

Recent literature procedures were followed to prepare the dye-filled liposomes.[28, 29] Chloroform solutions of the lipids (Figure 2.6) (total 15mg) were mixed in a 10 mL round bottom flask and chloroform was removed by a gentle nitrogen stream to form a uniform film. The flask was placed under vacuum for an additional 3 h at room temperature. The dried film was hydrated by addition of 1 mL of 40 mM calcein in phosphate buffer (10 mM) at pH 7.0. The suspension was stirred for 1 h. The suspension was sonicated briefly (5 min) in a bath-type sonicator at room temperature and freeze-thawed (liquid nitrogen/water at 35 ^{o}C temperature) after each sonication. This was repeated 4 times until the suspension changed from milky to nearly clear (i.e., only slightly hazy) in appearance. The non-trapped calcein was removed by eluting through a size exclusion Sephadex G-25-

150 column (15 cm × 1 cm), using phosphate saline buffer (phosphate 10 mM, NaCl 90 mM) at pH 7.0 as the eluent. The vesicle solutions were stored in a vial at 4 °C up to 4 days, and diluted with the PBS buffer as needed. TEM, dynamic light scattering, zeta potential and fluorescence imaging was used to characterize the liposomes (Figure S12).

The dye-leakage from the calcein trapped vesicles was monitored by recording the increase of calcein fluorescence intensity at 515 nm (excit. = 490 nm, slit width 2.5) (Figure S13). The 5-fold diluted vesicles 30 μL was added to 2940 μL PBS buffer in a cuvette. To normalize data, a baseline of calcein fluorescence without compound addition was observed for each sample for 60 sec. Phospholipid vesicles that were suspended in PBS buffer (pH 7.0) were stable, and no increase of fluorescence was observed. Then 30 μL of compound 1 in DMSO was added at t = 60 sec and the solution was mixed using the pipette tip. Lysis was quantified by measuring the increase in fluorescence from solutions after the addition of the compound. Complete vesicle disruption was achieved by addition of 30 μL Triton X-100 (20% in DMSO) at t = 480 sec from the addition of the compound, into the 3 mL of vesicle suspension. The final fluorescence intensity was used as 100% leakage. Lysis caused by the compound was reported as a percentage, calculated as $100 \times [(F-F_o)/(F_t-F_o)]$, where F is the fluorescence intensity after addition of the compound 1 and F_0 and F_t are fluorescence intensities without compound 1 and with Triton X-100, respectively. For the bacterial cell wall mimic, peptidoglycan extract from *S. aureus* was dissolved in DMSO at varying concentrations and compound 1 at a constant concentration, stirred for 12 h at 25 °C before addition to the solution containing dye-filled liposomes.

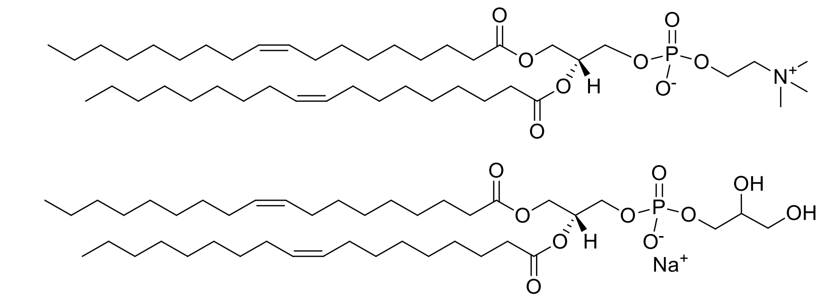

Figure 2.6 Lipids used for dye-leakage assays and molecular dynamics simulations. (A) 1,2-dioleoyl-sn-glycero-3-phosphocholine (DOPC); (B) 1,2-dioleoyl-sn-glycero-3-phospho-(1'-rac-glycerol) (sodium salt) (DOPG).

Molecular Dynamics Simulations

The anionic bacterial membrane was modeled using a 7:3 ratio mixture of dioleoylphosphatidylcholine (DOPC) and anionic dioleoylphosphatidylglycerol bilayer (DOPG)[30], while a quaternary ammonium-containing resin acid-derived agent (QAC) was used for modeling the natural resin acid-derived cationic compound. The system was constructed by placing QAC about 0.8 nm away from the surface of the upper leaflet of a pre-equilibrated DOPC-DOPG membrane. Overall, the equilibrated lipid bilayer contained 304 lipids. The CHARMM36 force field[31-33] parameter set was adopted for modeling DOPC and DOPG lipids. For modeling the cationic compounds, parameters were taken from the CHARMM General Force Field[34] or were derived from ab inito calculations, using the Gaussian09 software[35] performed at the MP2/6-31G* level of theory. All MDS were performed with the GROMACS program suite[36] version 4.6. The solvated bilayer-QAC system was subjected to stepwise energy minimization, equilibration followed by 600 ns of production MDS. A separate control experimental system was prepared by placing a long linear cationic alkyl chain near a similar DOPG-DOPC lipid bilayer under similar conditions. The MDS protocol used for the bilayer-QAC system was also repeated for the control-bilayer system.

The use of unconstrained MD to study the spontaneous insertion of a small compound into a bilayer is generally a difficult problem due to limited sampling. To improve the odds of capturing this event in our studies, we added 5 copies of either precursor of compound 1 or the control compound (alkyl ammonium) to the bulk solution. Using this procedure, two systems were setup. (A) QA-lipid system, consisting of five copies QAC, placed about 0.8 nanometers away from the surface of the upper leaflet of the pre-equilibrated DOPC-DOPG membrane. (B) AA-lipid system, consisting of five molecules of a long linear alkyl ammonium, randomly placed 0.8 nm near the charged surface of another copy of the lipid bilayer. The two complexes were then ionized with 0.1 M NaCl for electro neutrality, and stepwise energy minimization were performed using the GROMACS program.

MD simulations were performed with GROMACS. Bond lengths were constrained with P-LINCS[37] allowing for a 2 fs time step. Long-range electrostatic interactions were calculated using the particle-mesh Ewald method. Lennard-Jones potential and forces were truncated at 1.2 nm. The systems were slowly heated to 300 K. The two heterogeneous lipid systems were equilibrated in three phases. The first phase used an isochoric-isothermal (NVT) ensemble, with temperature controlled using the Berendsen weak coupling algorithm.[38] The NVT ensemble was applied for 500 ps, during which the temperature of the system was maintained at 300 K with a coupling constant of 0.1 ps. Heavy atoms of both the lipid and QAC molecules restrained. Next the systems were equilibrated with respect to pressure under the isobaric-isothermal (NPT) ensemble for 5 ns, using Nose-Hoover thermostat and Parrinello–Rahman barostat. Coupling constants for temperature and pressure were 0.1 and 2.0 ps, respectively. Following this, all atomic restraints were removed, and the systems were further equilibrated for 10 ns under the NPT ensemble. Unconstrained production simulations were performed for 600 nanoseconds under similar conditions.

2.4 Results and Discussion

There are two structural requirements for the antimicrobial activity of diterpenoids: a bulky hydrophobic moiety with a substituted hydrophenanthrene skeleton, and a hydrophilic region.[39] It is well known that quaternary ammonium-containing amphiphilic molecules possess biocidal properties, and hence have been widely used as surfactants to control microbes in clinical and industrial environments for several decades.[40, 41] Furthermore, antimicrobial peptides, an emerging class of novel antimicrobial agents with optimal amphipathicity and desirable size, have shown to selectively kill bacteria over mammalian cells though they have several limitations.[42-44] Based on these previous observations, we hypothesized that a balanced hydrophilicity/hydrophobicity could enhance the selectivity and antimicrobial properties of abietic acid.

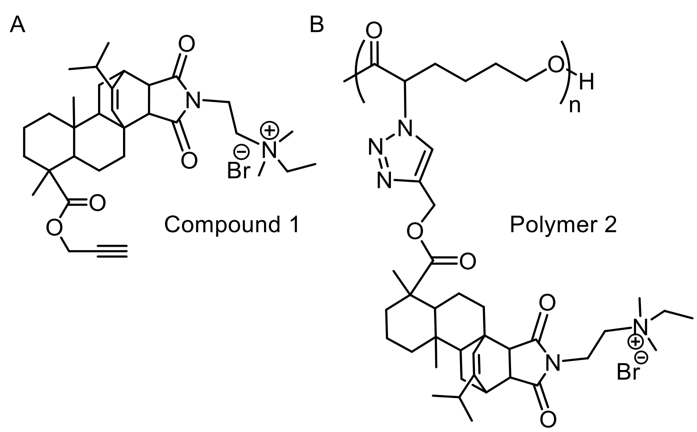

Figure 2.7 Structures of resin acid derived cationic antimicrobial agents. (A) compound 1. (B) polymer 2.

Hence, we chemically modified the fused tricyclic ring structure of abietic acid by decorating it with a quaternary ammonium containing alkyl moiety and a propargyl ester moiety to obtain compound 1 (Figure 2.7A). A new, economical synthetic approach was developed to enable us to prepare compound 1 at a large scale (up to kilograms at our laboratory facilities) without any chromatography purification. The propargyl end, by replacing the carboxylic end group, provides enhanced hydrophobicity to the hydrophenanthrene moiety of abietic acid, while the QA end acts in a hydrophilic manner. In addition, the alkyne functionality of compound 1 provides a platform for further modifications such as to covalently bind to a polymer chain and to produce a resin acid containing antimicrobial polycation, polymer 2 (Figure 2.7B).[26, 45] Though not explored in this study, antimicrobial polymers provide additional attributes such as enhanced stability and efficacy, lower residual toxicity[46-48], and applications as carriers of other antimicrobial agents,[49] antimicrobial surface coatings[50] and antimicrobial micells[51-53].

To examine the anti-MRSA potential we tested compound 1 and polymer 2 against several strains of MRSA including community-associated MRSA (CA-MRSA), traditional hospital-associated MRSA (HA-MRSA) and MRSA-252. Community-associated methicillin-susceptible *S. aureus* (CA-MSSA) was also tested as a positive control to further examine the anti-MRSA potential of the materials. Generally, CA-MRSA is more susceptible to antimicrobial agents compared to HA-MRSA, which is under high selection pressure in hospital environments.[54] MRSA strain 252 is resistant to a wide range of antibiotics such as penicillin, ciprofloxacin, erythromycin, and methicillin.[55, 56] Furthermore, MRSA-252 belongs to the clinically important EMRSA-16 clone that has been responsible for approximately half of all MRSA infections in the U.K.,[55] and the recent detection of EMRSA-16 isolates in several other countries has highlighted the pandemic potential of this clone.[57, 58]

Though our earlier study revealed the antimicrobial efficacy of compound 1 and polymer 2 against a variety of commonly used bacterial strains with promising results,[26] experiments in this report shows surprising anti-MRSA potential of compound 1 and polymer 2. Antimicrobial susceptibility was determined by the conventional agar disk-diffusion assays. Inhibition zone measurements indicated that our materials have remarkable effects against CA-MRSA, HA-MRSA and CA-MSSA (Figure 2.8). Minimum inhibitory concentrations were calculated for each material/bacterial combination using established protocols.[27] Compound 1 resulted in very significant growth inhibition zones even at relatively low concentrations (e.g. 4 μg/disk). In comparison, MRSA-252 is slightly less sensitive to compound 1. Nevertheless, all MICs of compound 1 against MRSA are surprisingly low, in the range of 4.8-7.3 μg/ml (Table 2.1). The MICs for the polymer 2 is also promising with the lowest of 9.9 μg/ml against CA-MRSA. Compared with some of most important cationic quaternary ammonium-containing polymers recently reported,[59-63] our materials have significantly higher efficacy against both *S. aureus* and MRSA. It is worth mentioning that most of these polymeric systems adopt advanced structures. Our system, in contrast, is a compound and a simple homopolymer, which would have high potential to be developed into advanced antimicrobial materials, which we are currently working on.

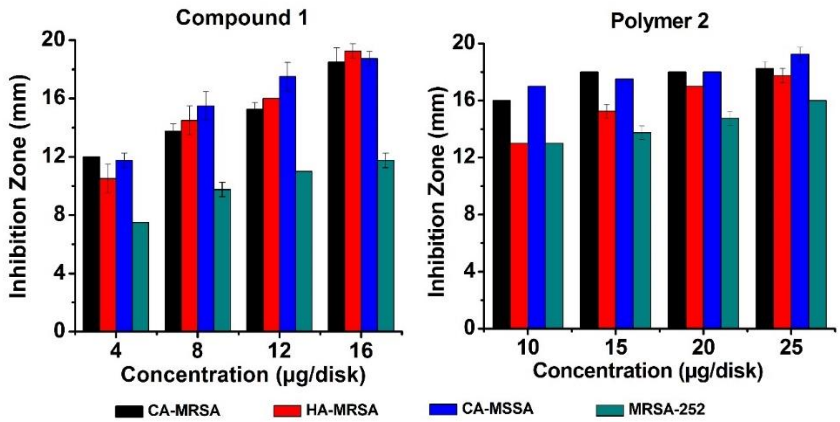

Figure 2.8 Antimicrobial activities of compound 1 and polymer 2. Inhibition zone measurements vs concentration (μg/disk) of the compound 1 and polymer 2 against CA-MRSA, HA-MRSA CA-MSSA and MRSA-252 depicts the potential anti-MRSA properties of these materials.

A crucial step in assessing the feasibility of an antibiotic or an antimicrobial agent that may be later tested for human or animal applications is its cytotoxicity toward mammalian cell lines. To explore this further, we carried out hemolysis and cytotoxicity assays of our compound and polymer, and calculated selectivity indices. Mouse red blood cells were incubated with the antimicrobial materials under different concentrations and evaluated their hemolysis activity. The high selectivity and low cytotoxicity of compound 1 and polymer 2 were indicated by the high selectivity indices (ratios of HC_{50} to MIC, Table 2.1). The highest ratios were greater than 68 and 26 for compound 1 and polymer 2, respectively, which indicated that our antimicrobial agents are capable of selectively lysing microbial cells, but not mammalian cells. When the molar concentration is considered, the cationic polymers show strong activity. For example, the MIC of compound 1 and polymer 2 against CA-MRSA was 8.1 μM and 0.13 μM respectively. However, such low MIC for polymer results from the presence of multiple active units in the polymer chain that can interact with bacterial membranes effectively and in a localized manner.

Table 2.1 Minimum inhibitory concentrations against several bacterial strains, HC_{50} and selectivity index of compound 1 and polymer 2. (Original cell concentration is 1.0 x 10^6 CFU/mL)

	S. aureus strain	Compound 1	Polymer 2
MIC (µg/mL)	CA-MRSA ATCC BAA-1717	5.0	9.9
	HA-MRSA ATCC BAA-29213	6.0	14.0
	CA-MSSA ATCC BAA-1718	7.3	8.8
	MRSA-252 ATCC BAA-1720	4.8	19.0
HC_{50} (µg/mL)		> 500	> 492
Selectivity index (HC_{50}/MIC)		> 68	> 26

As a more useful parameter, *in vitro* and *in vivo* cytotoxicity assays were carried out using immune cells from C57BL/6 mice to rule out nonspecific activity on nucleated mammalian cells. Mouse splenocytes consist of a variety of cell populations. T lymphocytes and B lymphocytes are two major types of immune cells in splenocytes. Based on functions and surface markers, T lymphocytes can be divided into cytotoxic CD8+ T cells and helper CD4+ T cells.[64] Concentrations of both compound 1 and polymer 2 were tested up to 100 µg/mL, *in vitro*. For *in-vivo* tests C57BL/6 mice received intravenous injection of 10 mg/kg body weight of compound 1 or polymer 2. Fluorescence activated cell sorting (FACS) analyses of cell populations in mouse splenocytes after *in vitro* co-culturing with the antimicrobials are illustrated in Figure 2.9A-C. The X-axis represents staining with anti-CD4 Abs directed against CD4+ cells, whereas the Y-axis represents staining with anti-CD3 Abs for T lymphocytes. Anti-CD4 Ab detects the expression of CD4 antigen on CD4+ T cells, whereas anti-CD3 Ab detects the expression of CD3 antigen on all of T lymphocytes including CD4+ and CD8+ T cells. The portion localized in the second quadrant (B2) represents the percentage of CD4+ T cell population in splenocytes. By looking at the summarized data for *in vitro* and *in vivo* cytotoxicity assays shown in Figure 2.9D, it is apparent that both compound 1 and polymer 2 did not significantly change the populations of T and B lymphocytes. This suggests that both antimicrobials resulted in minimal toxicity to nucleated mammalian cells.

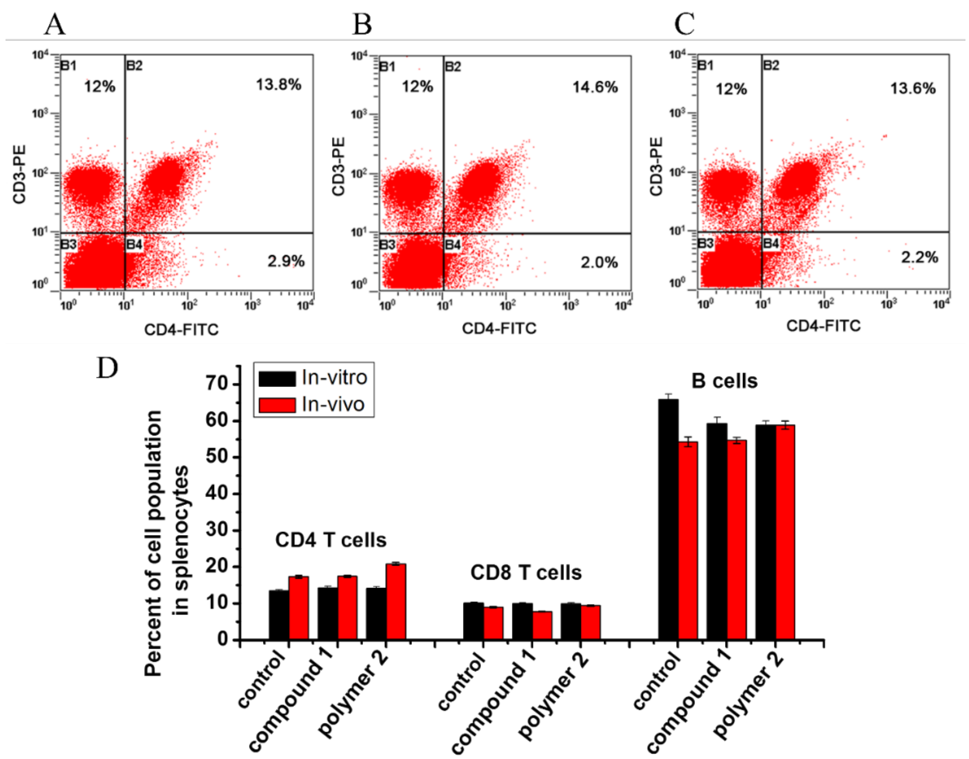

Figure 2.9 Cytotoxicity of compound 1 and polymer 2 against mouse splenocytes. (A, B, C) In vitro cytotoxicity FACS analysis of the effect of antimicrobials on CD4+ T lymphocytes in mouse splenocytes. (A) control (DMSO). (B) incubated with compound 1. (C) incubated with polymer 2. (D) Summary of effect of antimicrobials on CD4+, CD8+ T and B cell populations in splenocytes after culture from in vivo and in vitro incubations with compound 1 and polymer 2, respectively.

Quaternary ammonium containing compounds (QACs) and polymers, in general, have the ability to perturb the lipid membranes of microbes through electrostatic and hydrophobic interactions with the membrane phospholipids.[40, 43, 65, 66] This facilitates membrane permeability alterations, which lead to progressive leakage of cytoplasmic material and consequential lysis of the cells. To investigate such effects, we utilized molecular dynamics simulations and dye-leakage experiments using model anionic lipid membranes. The results provide strong evidence for the membrane destabilizing activity of compound 1.

The interactions between cationic compound and a model anionic membrane were probed by employing all-atom molecular dynamics simulations (MDS). The anionic bacterial membrane bilayer was modeled using a 7:3 ratio mixture of zwittorionic and electrically neutral dioleoylphosphatidylcholine (DOPC), and anionic dioleoylphosphatidylglycerol (DOPG) respectively (Figure 2.6). This lipid mixture is well known to form stable anionic liposomes and suitable to mimic the lipid composition of bacterial plasma membranes.[67, 68] As a simplified model the precursor carboxylic acid containing QAC of compound 1 was utilized (Figure 2.10E).

The bilayer-QAC trajectory indicated that the QAC interacts very strongly with the lipid bilayer via electrostatically attractive forces between the ammonium group of the cationic resin and the nearby phosphate group in the lipid head region. Free energy estimates of the interaction energy between QAC and DOPC-DOPG membrane was 27 kcal/mol with about 5 kcal/mol attributed to Columbic interaction. The binding event of QAC to the lipid bilayer could be summarized in four stages (Figure 2.10A-D): (A) the QA group is pulled towards the phosphate head groups of a cluster of DOPC and DOPG lipid molecules due to electrostatic attraction; (B) QAC is horizontally aligned to lipid bilayer; (C) QAC localizes in the membrane by burying its hydrophenanthrene group close to the lipid alkyl chain; and (D) the hydrophenanthrene moiety of QAC aligns with the alkyl chain of the DOPG and DOPC molecules of the lipid bilayer.

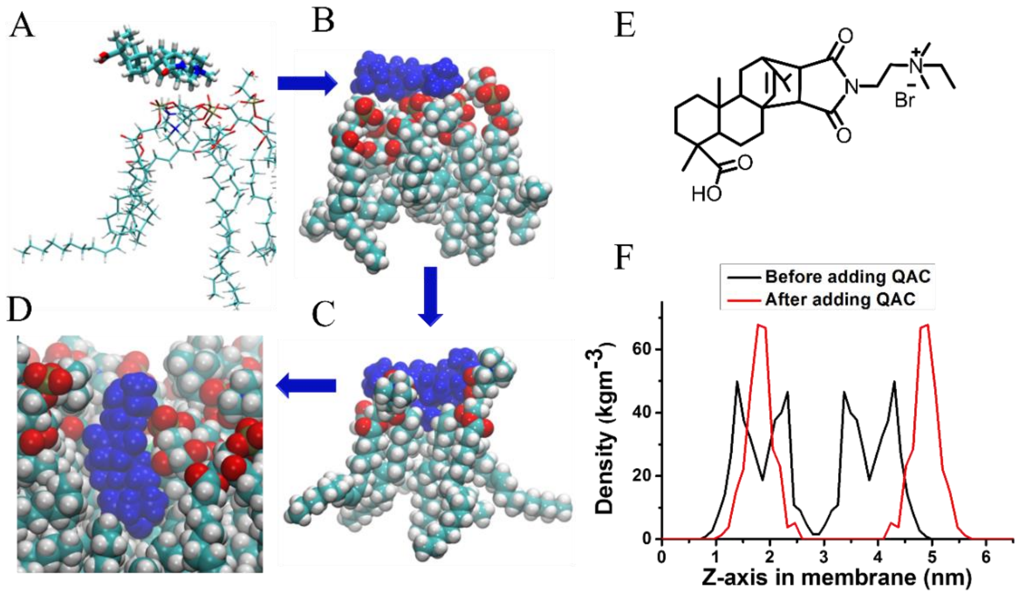

Figure 2.10 Molecular dynamics simulations of the acid format of compound 1 and model lipid bilayer. (A, B, C, D) Simulations snapshots (only neighboring lipid molecules and carboxylic acid containing the QA precursor of compound 1 are shown for clarity). The four stages depict QAC binding to lipid molecules in the model anionic membrane. (E) QAC used for the MDS (F) Plot of partial densities of lipid phosphate head groups along the Z-axis, before- and after- addition of QAC to the system.

The MDS studies also showed that the adsorption of QAC on the external membrane surface leads to horizontal stretching of the lipid alkyl chain group. This causes an unbalanced pressure on the membrane and leads to observed thinning of the membrane in the simulation. The lipid bilayer thickness, estimated from the distance between the head group peaks in the density profile (Figure 2.10F), shows that the lipid bilayer thickness is reduced upon introduction of the QAC, illustrating the impact of structural reorganization of the lipid alkyl chain due to its interaction with the hydrophobic component the model QAC. This observation is strikingly similar to the membrane thinning caused by well-known antimicrobial peptides such as Magainin 2.[42, 67] It is possible to have even stronger hydrophobic interactions with the lipid bilayer when the carboxylic acid of our compound is converted to a more hydrophobic propargyl ester group as in compound 1.[39]

A control experimental simulation involving a long cationic linear alkyl chain (*N*-ethyl-*N*, *N*-dimethyldocosan-1-aminium bromide) was also carried out. The simulation data revealed that even though the alkyl ammonium compound was initially placed near the head group of the lipid membrane, the compound diffused away from the surface of the lipid bilayer during the course of the simulation. The control compound was neither able to specifically interact nor penetrate the lipid bilayer in the manner that was observed during the resin-lipid simulation. The linear alkyl chain compound failed to penetrate the lipid bilayer, despite the presence of both an ammonium head group and alkyl chain. This reinforces hydrophenanthrene moiety as the primary hydrophobic structural determinant necessary for binding and penetrating the lipid membrane.

Dye-leakage assays of dye-filled synthetic lipid vesicles are commonly carried out to determine the membrane disrupting activity of various antimicrobial compounds and polymers.[69-71] Lipid vesicles or liposomes can be prepared from phospholipids with compositions chosen to mimic the properties of bacterial cell membranes in terms of the lipid content and surface charge. We hypothesized that our QAC selectivity towards bacterial cells was facilitated by the net negative charge of the bacterial membranes. Along with MDS studies, we prepared negatively-charged, large unilamellar vesicles having a 7:3 ratio of DOPC and DOPG lipids and loaded with 40 mM calcein solution.[28, 71] The liposomes had a Z-Average diameter of 142.5 nm and Zeta potential of -33.4 mV. At high concentration, the fluorescence of calcein is self-quenched. If the liposome membrane is broken, the calcein will be released into the aqueous environment and increase the fluorescence intensity (Figure 2.11A). The vesicles were stable in pH 7.0 phosphate buffered saline (PBS) and DMSO. The leakage activity of compound 1 was monitored over a range of concentrations. The resulting dye-leakage curve was plotted as percentage leakage (normalized to the standard Triton X-100 by taking initial fluorescence as 0% leakage and fluorescence after the addition of Triton X-100 as 100%) versus the concentration (Figure 2.11B). It can be seen that compound 1 induces dye-leakage starting at 30 μg/mL concentration. But a significant increase in dye-leakage resulted at 120 μg/mL and 100% lysis of phospholipid vesicles was observed above 300 μg/mL concentration. In addition to the concentration dependence, our data suggest that lipid vesicle lysis was also time-dependent. The leakage increased with time for concentrations above 30 μg/mL. For example 100% lysis was achieved for 600 μg/mL of compound 1 after 100 s while it took 470 s for 300 μg/mL concentration to obtain the same result.

Gram-positive bacteria have a relatively thick cell wall, which can prevent the diffusion of the compound toward the inner cell (i.e. plasma) membrane via QAC–peptidoglycan binding or a sieving effect.[29] Although one could not expect a significant sieving effect for a small molecule such as compound 1, there exists the possibility for positively-charged QAC to bind with the negatively-charged cell wall. To rule out any such effect, a dye leakage experiment was carried out with peptidoglycan extract from *S. aureus* bacteria as a model of bacterial cell wall mimic. The compound 1 at a constant concentration was incubated for 12 h with varying concentrations of peptidoglycan, before addition to dye-filled liposomes. The presence of peptidoglycan did not induce significant changes in the percent leakage revealing minimal QAC binding to the peptidoglycan layer

(Figure 2.11C). It is obvious that this characteristic contributes strongly to the observed low MIC values of compound 1 against MRSA.

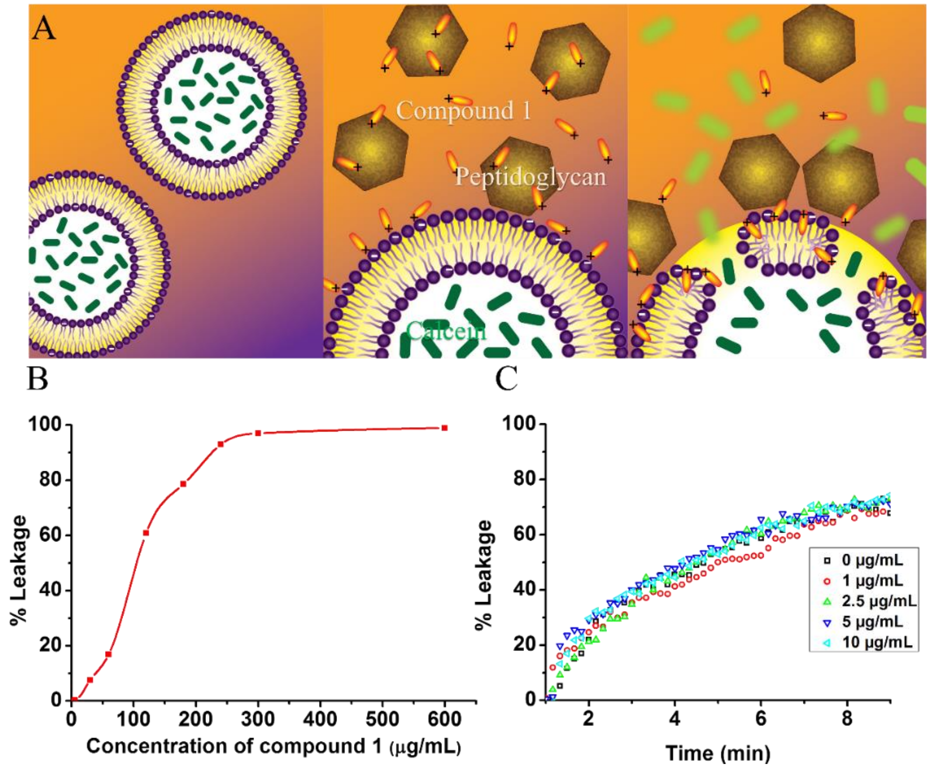

Figure 2.11 Dye-leakage experiment to evaluate the membrane activity of the cationic compound 1. (A) Illustration of the key steps in the dye-leakage assay. (B) Concentration-dependent dye-leakage from anionic lipid vesicles in the presence of different concentrations of compound 1 after 8 minutes of incubation. (C) Dye-leakage in the presence of peptidoglycan with different concentrations and compound 1 at 120 μg/mL.

2.5 Conclusions

In summary, we have discovered that a simple modification of a natural resin acid, surprisingly and dramatically enhances its antimicrobial effects. Both small molecule and polymer have a strong potential to be used as high efficiency anti-MRSA medicines with minimal side effects. Both MDS and dye-leakage experiments have demonstrated that these bio-inspired materials can selectively kill bacteria by permeabilizing the lipid membranes. Our approach will be an effective avenue to developing antimicrobial agents in large quantities, low cost and with a promising mechanism of action to kill multidrug resistant bacteria.

2.6 References

1. Arias, C. A.; Murray, B. E., Antibiotic-Resistant Bugs in the 21st Century - a Clinical Super-Challenge. *N. Engl. J. Med.* **2009,** *360*, 439-443.

2. Walsh, C., Molecular Mechanisms That Confer Antibacterial Drug Resistance. *Nature* **2000,** *406*, 775-781.

3. Levy, S. B.; Marshall, B., Antibacterial Resistance World-Wide: Causes, Challenges and Responses. *Nat. Med.* **2004,** *10*, S122 - S129

4. Davies, J.; Davies, D., Origins and Evolution of Antibiotic Resistance. *Microbiol. Mol. Biol. Rev.* **2010,** *74*, 417-433.

5. Drawz, S. M.; Bonomo, R. A., Three Decades of B-Lactamase Inhibitors. *Clin. Microbiol. Rev.* **2010,** *23*, 160-201.

6. O'Connell, K. M. G.; Hodgkinson, J. T.; Sore, H. F.; Welch, M.; Salmond, G. P. C.; Spring, D. R., Combating Multidrug-Resistant Bacteria: Current Strategies for the Discovery of Novel Antibacterials. *Angew. Chem. Int. Ed.* **2013,** *52*, 10706-10733.

7. Grundmann, H.; Aires-de-Sousa, M.; Boyce, J.; Tiemersma, E., Emergence and Resurgence of Meticillin-Resistant *Staphylococcus aureus* as a Public-Health Threat. *Lancet* **2006,** *368*, 874-885.

8. Calfee, D. P., Methicillin-Resistant *Staphylococcus aureus* and Vancomycin-Resistant *Enterococci*, and Other Gram-Positives in Healthcare. *Curr. Opin. Infect. Dis.* **2012,** *25*, 385-394

9. Watkins, R. R.; David, M. Z.; Salata, R. A., Current Concepts on the Virulence Mechanisms of Meticillin-Resistant *Staphylococcus aureus*. *J. Med. Microbiol.* **2012,** *61*, 1179-1193.

10. Boucher, H.; Miller, L. G.; Razonable, R. R., Serious Infections Caused by Methicillin-Resistant *Staphylococcus aureus*. *Clin. Infect. Dis.* **2010,** *51*, S183-S197.

11. Hidayat, L. K.; Hsu, D. I.; Quist, R.; Shriner, K. A.; Wong-Beringer, A., High-Dose Vancomycin Therapy for Methicillin-Resistant *Staphylococcus aureus* Infections: Efficacy and Toxicity. *Arch. Intern. Med.* **2006,** *166*, 2138-2144.

12. Garau, J.; Bouza, E.; Chastre, J.; Gudiol, F.; Harbarth, S., Management of Methicillin-Resistant *Staphylococcus aureus* Infections. *Clin. Microbiol. Infect.* **2009,** *15*, 125-136.

13. Culos, K. A.; Cannon, J. P.; Grim, S. A., Alternative Agents to Vancomycin for the Treatment of Methicillin-Resistant *Staphylococcus aureus* Infections. *Am. J. Ther.* **2013,** *20*, 200-212.

14. Hiramatsu, K., Vancomycin-Resistant *Staphylococcus aureus*: A New Model of Antibiotic Resistance. *Lancet Infect. Dis.* **2001,** *1*, 147-155.

15. Howden, B. P.; Davies, J. K.; Johnson, P. D. R.; Stinear, T. P.; Grayson, M. L., Reduced Vancomycin Susceptibility in *Staphylococcus aureus*, Including Vancomycin-Intermediate and Heterogeneous Vancomycin-Intermediate Strains: Resistance Mechanisms, Laboratory Detection, and Clinical Implications. *Clin. Microbiol. Rev.* **2010,** *23*, 99-139.

16. Hazlewood, K. A.; Brouse, S. D.; Pitcher, W. D.; Hall, R. G., Vancomycin-Associated Nephrotoxicity: Grave Concern or Death by Character Assassination? *Am. J. Med.* **2010,** *123*, 182.e181-187.

17. Scheffler, R. J.; Colmer, S.; Tynan, H.; Demain, A. L.; Gullo, V. P., Antimicrobials, Drug Discovery, and Genome Mining. *Appl. Microbiol. Biotechnol.* **2013,** *97*, 969-978.

18. Wilbon, P. A.; Chu, F.; Tang, C., Progress in Renewable Polymers from Natural Terpenes, Terpenoids, and Rosin. *Macromol. Rapid Commun.* **2013,** *34*, 8-37.

19. Yao, K.; Tang, C., Controlled Polymerization of Next-Generation Renewable Monomers and Beyond. *Macromolecules* **2013,** *46*, 1689-1712.

20. Savluchinske-Feio, S.; Curto, M.; Gigante, B.; Roseiro, J. C., Antimicrobial Activity of Resin Acid Derivatives. *Appl. Microbiol. Biotechnol.* **2006,** *72*, 430-436.

21. Trapp, S.; Croteau, R., Defensive Resin Biosynthesis in Conifers. *Annu. Rev. Plant Physiol. Plant Mol. Biol.* **2001,** *52*, 689-724.

22. Smith, E.; Williamson, E.; Zloh, M.; Gibbons, S., Isopimaric Acid from Pinus Nigra Shows Activity against Multidrug-Resistant and EMESA Strains of *Staphylococcus aureus*. *Phytother. Res.* **2005,** *19*, 538-542.

23. Fernandez, M. A.; Tornos, M. P.; Garcia, M. D.; de las Heras, B.; Villar, A. M.; Saenz, M. T., Anti-Inflammatory Activity of Abietic Acid, a Diterpene Isolated from *Pimenta Racemosa Var. Grissea*. *J. Pharm. Pharmacol.* **2001,** *53*, 867-872.

24. Talevi, A.; Cravero, M. S.; Castro, E. A.; Bruno-Blanch, L. E., Discovery of Anticonvulsant Activity of Abietic Acid through Application of Linear Discriminant Analysis. *Biorg. Med. Chem. Lett.* **2007,** *17*, 1684-1690.

25. Okeke, I. N.; Laxminarayan, R.; Bhutta, Z. A.; Duse, A. G.; Jenkins, P.; O'Brien, T. F.; Pablos-Mendez, A.; Klugman, K. P., Antimicrobial Resistance in Developing Countries. Part I: Recent Trends and Current Status. *Lancet Infect. Dis.* **2005,** *5*, 481-

493.

26. Wang, J.; Chen, Y. P.; Yao, K.; Wilbon, P. A.; Zhang, W.; Ren, L.; Zhou, J.; Nagarkatti, M.; Wang, C.; Chu, F.; He, X.; Decho, A. W.; Tang, C., Robust Antimicrobial Compounds and Polymers Derived from Natural Resin Acids. *Chem. Commun.* **2012,** *48*, 916-918.

27. Bauer, A.; Kirby, W.; Sherris, J. C.; turck; Turck, M., Antibiotic Susceptibility Testing by a Standardized Single Disk Method. *Am. J. Clin. Pathol.* **1966,** *45*, 493.

28. Ilker, M. F.; Schule, H.; Coughlin, E. B., Modular Norbornene Derivatives for the Preparation of Well-Defined Amphiphilic Polymers: Study of the Lipid Membrane Disruption Activities. *Macromolecules* **2004,** *37*, 694-700.

29. Lienkamp, K.; Kumar, K. N.; Som, A.; Nüsslein, K.; Tew, G. N., "Doubly Selective" Antimicrobial Polymers: How Do They Differentiate between Bacteria? *Chem. Eur. J.* **2009,** *15*, 11710-11714.

30. Balali-Mood, K.; Harroun, T. A.; Bradshaw, J. P., Molecular Dynamics Simulations of a Mixed Dopc/Dopg Bilayer. *Eur. Phys. J. E Soft Matter* **2003,** *12*, 135-140.

31. Klauda, J. B.; Venable, R. M.; Freites, J. A.; O'Connor, J. W.; Tobias, D. J.; Mondragon-Ramirez, C.; Vorobyov, I.; MacKerell, A. D., Jr.; Pastor, R. W., Update of the Charmm All-Atom Additive Force Field for Lipids: Validation on Six Lipid Types. *J. Phys. Chem. B* **2010,** *114*, 7830-7843.

32. Feller, S. E.; Yin, D.; Pastor, R. W.; MacKerell, A. D., Jr., Molecular Dynamics Simulation of Unsaturated Lipid Bilayers at Low Hydration: Parameterization and Comparison with Diffraction Studies. *Biophys. J.* **1997,** *73*, 2269-2279.

33. Mackerell, A. D., Jr.; Feig, M.; Brooks, C. L., 3rd, Extending the Treatment of Backbone Energetics in Protein Force Fields: Limitations of Gas-Phase Quantum Mechanics in Reproducing Protein Conformational Distributions in Molecular Dynamics Simulations. *J. Comput. Chem.* **2004,** *25*, 1400-1415.

34. Vanommeslaeghe, K.; Hatcher, E.; Acharya, C.; Kundu, S.; Zhong, S.; Shim, J.; Darian, E.; Guvench, O.; Lopes, P.; Vorobyov, I.; Mackerell, A. D., Jr., Charmm General Force Field: A Force Field for Drug-Like Molecules Compatible with the Charmm All-Atom Additive Biological Force Fields. *J. Comput. Chem.* **2010,** *31*, 671-690.

35. Frisch, M. J.; Trucks, G. W.; Schlegel, H. B.; Scuseria, G. E.; Robb, M. A.; Cheeseman, J. R.; Scalmani, G.; Barone, V.; Mennucci, B.; Petersson, G. A. *Gaussian 09*, Gaussian, Inc: Wallingford, CT, 2009.

36. Hess, B.; Kutzner, C.; Van Der Spoel, D.; Lindahl, E., Gromacs 4: Algorithms for Highly Efficient, Load-Balanced, and Scalable Molecular Simulation. *J. Chem. Theory Comput.* **2008,** *4*, 435-447.

37. Hess, B., P-Lincs: A Parallel Linear Constraint Solver for Molecular Simulation. *J. Chem. Theory Comput.* **2008,** *4*, 116-122.

38. Berendsen, H. J. C.; Postma, J. P. M.; Vangunsteren, W. F.; Dinola, A.; Haak, J. R., Molecular-Dynamics with Coupling to an External Bath. *J. Chem. Phys.* **1984,** *81*, 3684-3690.

39. Urzúa, A.; Rezende, M.; Mascayano, C.; Vásquez, L., A Structure-Activity Study of Antibacterial Diterpenoids. *Molecules* **2008,** *13*, 882-891.

40. McBain, A. J.; Ledder, R. G.; Moore, L. E.; Catrenich, C. E.; Gilbert, P., Effects of Quaternary-Qmmonium-Based Formulations on Bacterial Community Dynamics and Antimicrobial Susceptibility. *Appl. Environ. Microbiol.* **2004,** *70*, 3449-3456.

41. Gilbert, P.; Moore, L. E., Cationic Antiseptics: Diversity of Action under a Common Epithet. *J. Appl. Microbiol.* **2005,** *99*, 703-715.

42. Brogden, K. A., Antimicrobial Peptides: Pore Formers or Metabolic Inhibitors in Bacteria? *Nat. Rev. Microbiol.* **2005,** *3*, 238-250.

43. Zasloff, M., Antimicrobial Peptides of Multicellular Organisms. *Nature* **2002,** *415*, 389-395.

44. Findlay, B.; Zhanel, G. G.; Schweizer, F., Cationic Amphiphiles, a New Generation of Antimicrobials Inspired by the Natural Antimicrobial Peptide Scaffold. *Antimicrob. Agents Chemother.* **2010,** *54*, 4049-4058.

45. Chen, Y.; Wilbon, P. A.; Chen, Y. P.; Zhou, J.; Nagarkatti, M.; Wang, C.; Chu, F.; Decho, A. W.; Tang, C., Amphipathic Antibacterial Agents Using Cationic Methacrylic Polymers with Natural Rosin as Pendant Group. *RSC Adv.* **2012,** *2*, 10275-10282.

46. Kenawy, E.-R.; Worley, S.; Broughton, R., The Chemistry and Applications of Antimicrobial Polymers: A State-of-the-Art Review. *Biomacromolecules* **2007,** *8*, 1359-1384.

47. Gabriel, G. J.; Som, A.; Madkour, A. E.; Eren, T.; Tew, G. N., Infectious Disease: Connecting Innate Immunity to Biocidal Polymers. *Mater. Sci. Eng. R-Rep.* **2007,** *57*, 28-64.

48. Lienkamp, K.; Madkour, A. E.; Musante, A.; Nelson, C. F.; Tew, G. N., Antimicrobial Polymers Prepared by Romp with Unprecedented Selectivity: A Molecular Construction Kit Approach. *J. Am. Chem. Soc.* **2008,** *130*, 9836-9843.

49. Ng, V. W. L.; Ke, X.; Lee, A. L. Z.; Hedrick, J. L.; Yang, Y. Y., Synergistic Co-Delivery of Membrane-Disrupting Polymers with Commercial Antibiotics against Highly Opportunistic Bacteria. *Adv. Mater.* **2013,** *10*, 6730–6736.

50. Lee, S. B.; Koepsel, R. R.; Morley, S. W.; Matyjaszewski, K.; Sun, Y.; Russell, A. J., Permanent, Nonleaching Antibacterial Surfaces. 1. Synthesis by Atom Transfer Radical Polymerization. *Biomacromolecules* **2004,** *5*, 877-882.

51. Powell, K. T.; Cheng, C.; Wooley, K. L., Complex Amphiphilic Hyperbranched Fluoropolymers by Atom Transfer Radical Self-Condensing Vinyl (Co)Polymerization. *Macromolecules* **2007,** *40*, 4509-4515.

52. Elsabahy, M.; Zhang, S.; Zhang, F.; Deng, Z. J.; Lim, Y. H.; Wang, H.; Parsamian, P.; Hammond, P. T.; Wooley, K. L., Surface Charges and Shell Crosslinks Each Play Significant Roles in Mediating Degradation, Biofouling, Cytotoxicity and Immunotoxicity for Polyphosphoester-Based Nanoparticles. *Sci. Rep.* **2013,** *3*, 3313.

53. Shah, P. N.; Lin, L. Y.; Smolen, J. A.; Tagaev, J. A.; Gunsten, S. P.; Han, D. S.; Heo, G. S.; Li, Y.; Zhang, F.; Zhang, S.; Wright, B. D.; Panzner, M. J.; Youngs, W. J.; Brody, S. L.; Wooley, K. L.; Cannon, C. L., Synthesis, Characterization, and in Vivo Efficacy of Shell Cross-Linked Nanoparticle Formulations Carrying Silver Antimicrobials as Aerosolized Therapeutics. *ACS Nano* **2013,** *7*, 4977-4987.

54. Chen, S.-Y.; Liao, C.-H.; Wang, J.-L.; Chiang, W.-C.; Lai, M.-S.; Chie, W.-C.; Chen, W.-J.; Chang, S.-C.; Hsueh, P.-R., Methicillin-Resistant *Staphylococcus aureus* (MRSA) Staphylococcal Cassette Chromosome Mec Genotype Effects Outcomes of Patients with Healthcare-Associated Mrsa Bacteremia Independently of Vancomycin Minimum Inhibitory Concentration. *Clin. Infect. Dis.* **2012,** *55*, 1329-1337.

55. Johnson, A. P.; Aucken, H. M.; Cavendish, S.; Ganner, M.; Wale, M. C.; Warner, M.; Livermore, D. M.; Cookson, B. D., Dominance of Emrsa-15 and-16 among MRSA Causing Nosocomial Bacteraemia in the Uk: Analysis of Isolates from the European Antimicrobial Resistance Surveillance System (Earss). *J. Antimicrob. Chemother.* **2001,** *48*, 143-144.

56. Enright, M. C.; Day, N. P. J.; Davies, C. E.; Peacock, S. J.; Spratt, B. G., Multilocus Sequence Typing for Characterization of Methicillin-Resistant and Methicillin-Susceptible Clones of *Staphylococcus aureus*. *J. Clin. Microbiol.* **2000,** *38*, 1008-1015.

57. McDougal, L. K.; Steward, C. D.; Killgore, G. E.; Chaitram, J. M.; McAllister, S. K.; Tenover, F. C., Pulsed-Field Gel Electrophoresis Typing of Oxacillin-Resistant *Staphylococcus aureus* Isolates from the United States: Establishing a National Database. *J. Clin. Microbiol.* **2003,** *41*, 5113-5120.

58. Chung, M.; Dickinson, G.; de Lencastre, H.; Tomasz, A., International Clones of Methicillin-Resistant *Staphylococcus aureus* in Two Hospitals in Miami, Florida. *J. Clin. Microbiol.* **2004,** *42*, 542-547.

59. Li, P.; Poon, Y. F.; Li, W.; Zhu, H.-Y.; Yeap, S. H.; Cao, Y.; Qi, X.; Zhou, C.; Lamrani, M.; Beuerman, R. W.; Kang, E.-T.; Mu, Y.; Li, C. M.; Chang, M. W.; Jan Leong, S. S.; Chan-Park, M. B., A Polycationic Antimicrobial and Biocompatible Hydrogel with Microbe Membrane Suctioning ability. *Nat. Mater.* **2011,** *10*, 149-156.

60. Nederberg, F.; Zhang, Y.; Tan, J. P. K.; Xu, K.; Wang, H.; Yang, C.; Gao, S.; Guo, X. D.; Fukushima, K.; Li, L.; Hedrick, J. L.; Yang, Y.-Y., Biodegradable Nanostructures with Selective Lysis of Microbial Membranes. *Nat. Chem.* **2011,** *3*, 409-414.

61. Kuroda, K.; DeGrado, W. F., Amphiphilic Polymethacrylate Derivatives as Antimicrobial Agents. *J. Am. Chem. Soc.* **2005,** *127*, 4128-4129.

62. Sambhy, V.; Peterson, B. R.; Sen, A., Antibacterial and Hemolytic Activities of Pyridinium Polymers as a Function of the Spatial Relationship between the Positive Charge and the Pendant Alkyl Tail. *Angew. Chem. Int. Ed.* **2008,** *47*, 1250-1254.

63. Mowery, B. P.; Lee, S. E.; Kissounko, D. A.; Epand, R. F.; Epand, R. M.; Weisblum, B.; Stahl, S. S.; Gellman, S. H., Mimicry of Antimicrobial Host-Defense Peptides by Random Copolymers. *J. Am. Chem. Soc.* **2007,** *129*, 15474-15476.

64. Abbas, A. K.; Murphy, K. M.; Sher, A., Functional Diversity of Helper T Lymphocytes. *Nature* **1996,** *383*, 787-793.

65. Wessels, S.; Ingmer, H., Modes of Action of Three Disinfectant Active Substances: A Review. *Regul. Toxicol. Pharmacol.* **2013,** *67*, 456-467.

66. Liu, L.; Huang, Y.; Riduan, S. N.; Gao, S.; Yang, Y.; Fan, W.; Zhang, Y., Main-Chain Imidazolium Oligomer Material as a Selective Biomimetic Antimicrobial Agent. *Biomaterials* **2012,** *33*, 8625-8631.

67. Ludtke, S.; He, K.; Huang, H., Membrane Thinning Caused by Magainin 2. *Biochemistry* **1995,** *34*, 16764-16769.

68. Lee, M.-T.; Sun, T.-L.; Hung, W.-C.; Huang, H. W., Process of Inducing Pores in Membranes by Melittin. *Proc. Natl. Acad. Sci. U.S.A.* **2013,** *110*, 14243-14248.

69. Eren, T.; Som, A.; Rennie, J. R.; Nelson, C. F.; Urgina, Y.; Nüsslein, K.; Coughlin, E. B.; Tew, G. N., Antibacterial and Hemolytic Activities of Polynorbornenes. *Macromol. Chem. Phys.* **2008,** *209*, 516-524.

70. Lienkamp, K.; Madkour, A. E.; Kumar, K.-N.; Nüsslein, K.; Tew, G. N., Antimicrobial Polymers Prepared by Ring-Opening Metathesis Polymerization: Manipulating Antimicrobial Properties by Organic Counterion and Charge Density Variation. *Chem. Eur. J.* **2009,** *15*, 11715-11722.

71. Yan, J.; Wang, K.; Dang, W.; Chen, R.; Xie, J.; Zhang, B.; Song, J.; Wang, R., Two Hits Are Better Than One: Membrane-Active and DNA Binding-Related Double-Action Mechanism of Nk-18, a Novel Antimicrobial Peptide Derived from Mammalian Nk-Lysin. *Antimicrob. Agents Chemother.* **2013,** *57*, 220-228.

CHAPTER 3

ANTIBACTERIAL AND BIOFILM-DISRUPTING COATINGS FROM RESIN ACID-DERIVED MATERIALS[4]

[4] Ganewatta, M. S.; Miller, K. P.; Singleton, S. P.; Mehrpouya-Bahrami, P.; Chen, Y. P.; Yan, Y.; Nagarkatti, M.; Nagarkatti, P.; Decho, A. W.; Tang, C., Antibacterial and Biofilm-Disrupting Coatings from Resin Acid-Derived Materials. *Biomacromolecules* **2015**, *16*, 3336-3344. Reprinted here with permission. Copyright (2015) American Chemical Society.

3.1 Abstract

We report antibacterial, anti-biofilm and biocompatible properties of surface-immobilized, quaternary ammonium-containing, resin acid-derived compounds and polycations that are known to be efficient antimicrobial agents with minimum toxicities to mammalian cells. Surface immobilization was carried out by the employment of two robust, efficient chemical methods: Copper-catalyzed azide-alkyne 1,3-dipolar cycloaddition click reaction, and surface-initiated atom transfer radical polymerization. Antibacterial and anti-biofilm activities against Gram-positive *Staphylococcus aureus* and Gram-negative *Escherichia coli* were strong. Hemolysis assays and the growth of human dermal fibroblasts on the modified surfaces evidenced their biocompatibility. We demonstrate that the grafting of quaternary ammonium-decorated abietic acid compounds and polymers from surfaces enables the incorporation of renewable biomass in an effective manner to combat bacteria and biofilm formation in biomedical applications.

3.2 Introduction

Microorganisms form biofilms on surfaces as a protective lifestyle in hostile environments.[1-3] These sessile communities often develop from single planktonic cells into a three-dimensionally organized and remarkably complex, community of microorganisms encapsulated within an emergent polymeric matrix.[4-7] Depending on the type of microorganisms and the environment in which they live, the biofilms are characterized by structural heterogeneity, genetic diversity and complex community interactions.[5, 8, 9]

Biofilms have become problematic in agricultural, industrial, environmental, and clinical settings.[10] Microbes in these resilient structures are inherently resistant to antimicrobial agents and have become a major cause of infectious diseases.[11-14] Many human diseases, such as dental caries, otitis, necrotizing fasciitis, and cystic fibrosis-related pneumonias, are related to bacterial biofilms.[13] Bacterial biofilms produced on the surfaces of medical implants including catheters, heart valves, pacemakers, stents, prosthetic joints, and contact lenses are a significant issue which pose considerable threats to patient morbidity and mortality, and incur substantial increases in health care costs each year.[12]

Despite the presence of advanced sterilization techniques, it is still difficult to eradicate biofilms and maintain sterility without frequent use of disinfectants. Therefore, there is an ever-growing demand for surfaces with inherent antimicrobial properties that can prevent bacterial colonization on them. Many methods for the antimicrobial modification of surfaces have been developed.[15, 16] Such methods include impregnating antimicrobial nanoparticles,[17] grafting small molecules having antimicrobial properties[18] or antimicrobial polymers on surfaces,[19-22] coatings with anti-quorum sensing molecules,[23] loading antibiotics into surface matrices for slow release,[24] photoactivated surfaces,[25] changing hydrophobicity,[26] and modifying surface nanotopography.[27]

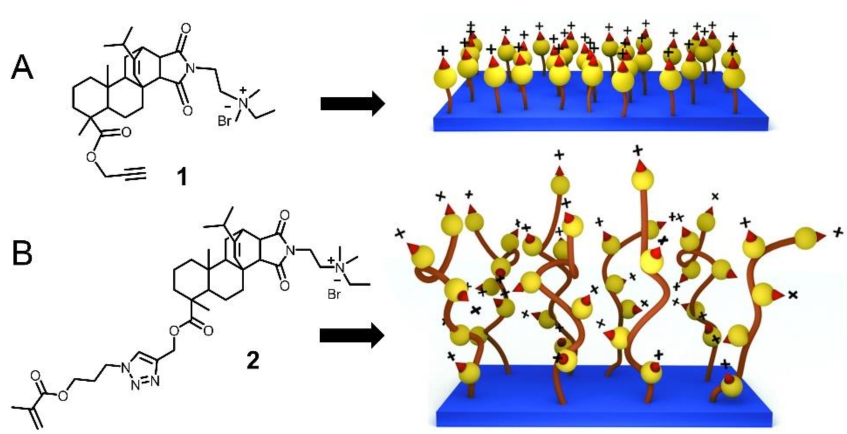

Figure 3.1. Illustration of resin acid derived cationic compounds and surfaces. (A) Compound 1 containing an alkyne functionality and the monolayer surface. (B) Methacrylate functionalized resin acid compound 2 and the polymer grafted surface.

Contact active coatings, which kill bacteria upon contact, can be fabricated with chemically immobilized quaternary ammonium antimicrobial agents. Cationic surfaces made up of covalently attached materials such as QA organosilanes,[28-30] antimicrobial peptides,[19, 31] and QA containing alkylated polymers such as polyvinylpyridines,[32] polyethylenimines,[33] poly(2-(dimethylamino)ethyl methacrylate),[34, 35] hyperbranced polyurea[36] and many others[37, 38] are known to be bactericidal. These materials are being studied extensively due to their ease of synthesis, self-sterilization properties, and long-lasting activities compared to other methods. Widespread utilization of such surfaces has necessitated the integration of sustainable materials for low-cost, non-cytotoxic and environmentally-friendly antimicrobial surfaces.

In earlier efforts, we found that the modification of natural resin acids (from gum rosin) into quaternary ammonium compounds is a promising method for the preparation of highly effective antimicrobial agents, which kill bacteria via selective bacterial membrane lysis while exhibiting high bio-compatibility.[39-41] Herein we report the surface modification using low-cost resin acid derived cationic compounds and polymers to obtain effective antimicrobial and antibiofilm surfaces (Figure 3.1).

The copper-catalyzed azide-alkyne 1,3-dipolar cycloaddition (CuAAC) click reaction was used to graft the cationic molecules to the substrate surfaces. Surface-initiated atom transfer radical polymerization (SI-ATRP) was used to functionalize substrate surfaces with cationic polymers. Although architecturally simple, these novel materials demonstrated promising antimicrobial properties with an increased resilience to bacterial biofilm formation against both Gram-positive and Gram-negative bacteria. Additional investigations revealed high levels of biocompatibility, illustrated by enhanced human dermal fibroblast (HDF) growth and low hemolysis of red blood cells.

3.3 Experimental section

Materials

Abietic acid (85%), maleic anhydride, *N*,*N*-dimethylaminoethylamine (DAEA), propargyl alcohol, triethylamine, *p*-toluene sulfonic acid (PTSA), bromoethane, α-bromoisobutyryl bromide (BIBB), (3-aminopropyl)triethoxysilane (APTES), sodium bicarbonate, calcium chloride, 3-chloroprapanol, sodium azide, methacryloyl chloride, copper(I) bromide, *N,N,N′,N′,N′′*-pentamethyldiethylenetriamine (PMDETA), sulfuric acid, hydrogen peroxide, ethyl acetate, copper sulfate pentahydrate, and sodium ascorbate were purchased from Sigma Aldrich, VWR, or Fisher Scientific and used as received. According to procedures reported in literature, (3-azidopropyl)trimethoxysilane (AzPTMS),[42] bromotriethylorthosilicate (BrTEOS),[43] and 3-azidopropyl methacrylate[44] were prepared. QA containing resin acid derived compound 1 was synthesized, following our recent report.[41] Acetic acid, dichloromethane (DCM), ethyl acetate, ethanol, hexane, diethyl ether, methanol, toluene, tetrahydrofuran (THF) and *N*,*N*-dimethylformamide (DMF) were obtained as ACS grade solvents. Standard protocols were followed to dry solvents or reagents. All other chemicals used for biological assays will be mentioned in the respective sections.

Methacrylate Monomer (Compound 2) Synthesis

Compound 1 (8.97 g, 14 mmol, 1.0 eq) and 3-azidopropyl methacrylate (3.07 g, 18 mmol, 1.25 eq) were charged to a 100 mL round bottom flask and dissolved in 60 mL of dry DMF. The flask was placed in an ice bath and stirred while bubbling nitrogen for 20 minutes. Cu(I)Br (80 mg, 0.558 mmol, 0.04 eq) and PMDETA (125 mg, 0.721 mmol, 0.05 eq) were dissolved in 2 mL of dry DMF under a nitrogen atmosphere and added to the reaction vessel. The flask was removed from the ice bath and allowed to heat to room temperature and react overnight. Upon completion of the reaction the crude product was diluted in DCM and washed several times with aqueous/brine solution. The organic layer was then concentrated by rotoevaporation, precipitated twice in cold diethyl ether and vacuum dried. Yield: 70%. ^{1}H and ^{13}C NMR were recorded on a Bruker Avance III HD 300 spectrometer. ^{1}H NMR (300 MHz, $CDCl_3$) δ (ppm): δ: 7.53 (s, 1H, C=C*H*N); 6.09 (s, 1H, CH*H*=CC=O); 5.60 (s, 1H, C*H*H=CCH_3); 5.33 (s, 1H, C*H*=C); 5.21 (m, 2H, $CC\mathit{H_2}OC$=O); 4.50 (t, 2H, $CH_2C\mathit{H_2}ONN$); 4.20 (t, 2H, $CH_2C\mathit{H_2}OC$=O); 3.79 (t, 2H, O=$CNC\mathit{H_2}CH_2$); 3.75 (t, 2H, O=$CNCH_2C\mathit{H_2}$); 3.60 (m, 2H, N+$C\mathit{H_2}CH_3$); 3.39 (s, 6H, N+$(C\mathit{H_3})_2$); 2.89 (m, 1H CHC*H*C=O); 2.56 (d, 1H $CH_2CC\mathit{H}C$=O); 2.36 (s, 3H, $C\mathit{H_3}C=CH_2$); 2.33 (m, 1H, $CH_2C\mathit{H}C$=CH). ^{13}C NMR (300 MHz, $CDCl_3$) δ (ppm): 178.5 ($CH_2C\mathit{C}$=OO); 178.2-177.1 (O=*C*N*C*=O); 167.1 ($CH_3C\mathit{C}$=OO); 147.3 (CH*C*=CHC); 143.1 (NCH=$\mathit{C}CH_2$); 136.0 ($CH_3\mathit{C}=CH_2$); 126.1 (N*C*H=CCH_2); 124.6 (CHC=*C*HC); 124.0 ($CH_3C=\mathit{C}H_2$); 61.2-59.9 ($CH_2\mathit{C}H_2N$+ and $CH_3\mathit{C}H_2N$+). Mass spectrometry was conducted on a Waters Micromass Q-Tof mass spectrometer, and the ionization source was positive ion electrospray. ES-MS: m/z 706.4540 (theoretical m/z: 706.4544 $+H^+$ without Br^-)

Preparation of Antimicrobial Surfaces

Figure 3.2 illustrates the synthetic route used for the preparation of the antimicrobial surfaces. As a fundamental study, glass substrates were used for the surface modifications. Glass slides were cut to the desired size (1.2 mm x 10 mm x 25 mm) and immersed in a solution of Piranha (H_2SO_4:H_2O_2, 3:1) at 50 °C for 3 h with occasional swirling. The surfaces were then carefully and thoroughly washed with deionized water until the pH reached to 7.0 and placed in an oven (120 °C) for 2 h. Later, they were transferred into a homemade reactor containing dry solutions of AzPTMS or BrTEOS (10 mM) in dry toluene. After assuring that all surfaces were completely immersed, the flask was heated at 110 °C for 24 h. The surfaces were purified by washing them thrice with toluene, ethanol and acetone, consecutively.

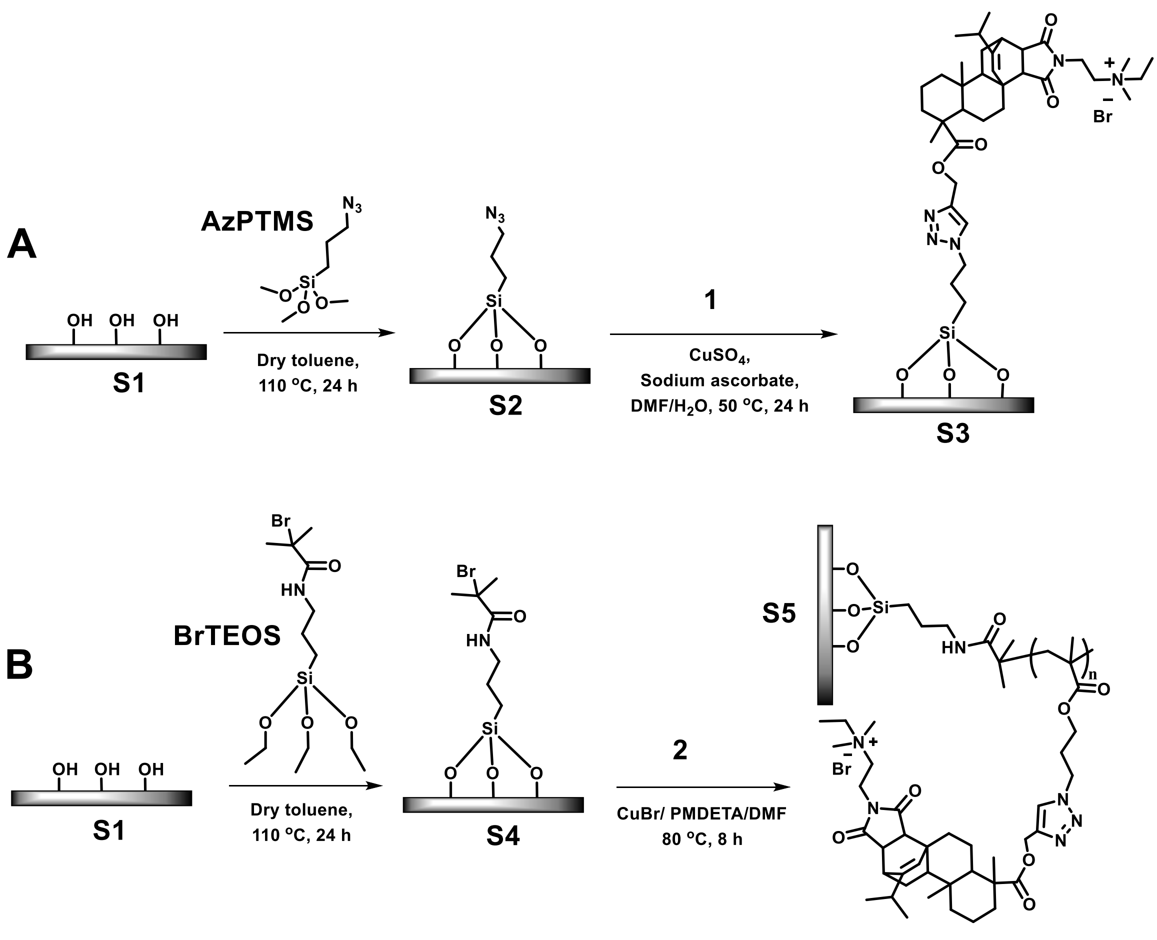

Figure 3.2 Grafting of antimicrobial materials on surfaces. (A) Grafting a monolayer of compound 1 and (B) Grafting the polymer with pendant cationic abietic acid derivative.

A 10 mM (final concentration) solution of compound 1 was prepared by dissolving it (318 mg, 0.5 mmol, 1.0 eq) in DMF (40 mL) and stirred for 10 min. Then azide grafted surfaces

(S2) were placed in the homemade reactor containing the solution along with $CuSO_4 \cdot 5H_2O$ (12.6 mg, 0.05 mmol, 0.1 eq) in water (5 mL). The flask was covered and purged with nitrogen for 15 min. Sodium ascorbate (20 mg, 0.1 mmol, 0.2 eq) in water (5 mL) was transferred using a needle. This flask was kept at 50 °C for 24 h. Compound 1 immobilized substrates were recovered from the reaction mixture and washed thoroughly first with DMF, ethanol and acetone, consecutively, and finally with deionized water. After drying under a stream of nitrogen, the modified glass slides were stored in a dry container.

ATRP initiator grafted substrates (S4) were kept in the homemade reactor and monomer 2 (4.716 g, 6 mmol, 1.0 eq) was added along with 18 mL of dry DMF and purged with N_2 for 15 mins. Then a mixture of CuBr (214.5 mg, 1.5 mmol, 0.25 eq) and PMDETA (259.5 mg, 1.5 mmol, 0.25 eq) in 12 mL of dry DMF was transferred. The reactor was immersed in a preheated oil bath at 80 ^{o}C and kept stirring for 8 h. After that the substrates were carefully washed with DMF, ethanol and acetone, consecutively, and finally with deionized water. After drying under a stream of nitrogen, the surface modified substrates were stored in a dry container.

Surface Characterizations

The chemical compositions of the surfaces were determined by X-ray photoelectron spectroscopy (XPS) using a Kratos AXIS Ultra DLD XPS system equipped with a monochromatic Al Kα source. Static water contact angles were measured using a VCA Optima (AST Products, Inc) system with a manual controller capable of casting 1 μL of Milli-Q water droplets. Static contact angles were recorded 5 seconds after placing the water drop on the surface. At least five replicate measurements were taken to calculate the average contact angle. Following reported procedures,[32, 45] the surface charge density was evaluated. Modified surfaces were dipped in a 1 wt % solution of fluorescein (Na salt) in deionized water for 10 min while shaking. Then the slides were thoroughly rinsed with deionized water, placed in 3 mL of 0.1 wt % cetyltrimethylammonium chloride in deionized water and shaken for 20 min to desorb the dye from the surface. The absorbance of the resultant aqueous solution was measured at 501 nm, after adding 10 vol % of 100 mM aqueous phosphate buffer at pH 8.0. The surface charge density was calculated using the surface area of the substrate and the extinction coefficient (77 $mM^{-1}cm^{-1}$).[32, 46, 47] This staining method was also used qualitatively to observe the presence of active material on the surface using the confocal laser scanning microscopy (CLSM). For comparison, the same polymerization procedure was conducted using glass beads instead of glass slides. The grafted polymer was cleaved from surface using HF acid, following a procedure reported in the literature.[48] Then the molecular weight was determined by gel permeation chromatography (GPC). It was performed with the eluent DMF at a flow rate of 1.0 mL/min at 50 °C on a Varian system equipped with a ProStar 210 pump and a Varian 356-LC RI detector and three phenogel columns (Phenomenex Co.) calibrated with narrow dispersed polystyrene standards.

Contact Active Anti-bacterial Properties

To rule out the presence of any physically adsorbed material on the surfaces, a standard diffusion assay was conducted using bacterial lawns of *E. coli* (ATCC 25922) and *S. aureus* (ATCC 25423) grown on tryptic soy agar. These bacterial strains were used throughout the study. To determine the antimicrobial activities of immobilized antimicrobial agent under dynamic contact conditions a modified test method was used.[49] Sterile conical tubes (15 mL) containing 5 mL of tryptic soy broth (TSB) were inoculated with 15 μL of log-phase cultures of either *E. coli* or *S. aureus*. Modified substrates were sterilized with ethanol. After drying, they were immersed vertically in the tubes containing the cultures and incubated at 37 °C with continuous shaking at 150 rpm. After 24 h, 1.0 mL from each well was serially diluted with phosphate buffered saline (PBS) and plated on tryptic soy agar. After incubating 24 h at 37 °C the bacterial colonies were counted to obtain the colony forming units (CFU). The glass slides in the conical tubes were carefully rinsed with PBS and stained with propidium iodide and SYTO 9 (Live/Dead BacLight viability kit, Life Technology, Carlsbad, CA, USA). These fluorescent nucleic acid stains indicate cell viability as a function of membrane integrity. Healthy cells with intact membranes will stain green, while dead or dying cells with compromised membranes will stain red. CLSM was used to visualize the samples. ImageJ software was used to calculate the number cells and CFUs observed from these experiments.

Anti-biofilm Activity in Solution

E. coli and *S. aureus* were sub-cultured for purity from a frozen glycerol stock on TSA at 37 °C, and subsequently used to inoculate 50 mL 10% TSB. The culture was incubated overnight at 37 °C with gentle shaking (150 rpm). Sterile MBEC Biofilm Assay plates with 96 well bases (Innovotech, Edmonton, Canada) were used to test for biofilm formation. In a typical procedure, 50 mL of the overnight culture was diluted into sterile 10% TSB for an approximate cell density of 10^5 CFU/mL to create the inoculum. Then 150 μL of the inoculum was added to each well and the peg lid was securely placed on the plate and sealed with parafilm. The plate was incubated for 24 hours at 37 °C, 110 rpm. A sterile 96-well plate was seeded with various concentrations of 1 (0-500 μg/mL) in 10% TSB. The MBEC peg lid was rinsed in deionized water three times and inserted onto the antimicrobial challenge plate. The plate was incubated at 37 °C and 110 rpm for 24 hours. After 24 hours, the biofilm was rinsed in deionized water for one minute and allowed to dry for 10 minutes at room temperature. The MBEC peg lid was then stained in 1% crystal violet for one minute to stain the biofilm and rinsed three times in fresh deionized water. The peg lid was then treated with 100% methanol (1 min) to dissolve the crystal violet. Dissolved crystal violet was then measured at 600 nm with a Power Wave 200 Microplate Scanning Spectrophotometer (Bio-Tek Instruments, Winooski, VT).

Anti-biofilm Activity of the Surfaces

Biofilms were grown on treated and untreated substrates separately within a flow-through CDC Biofilm Reactor (CBR, BioSurface Technol., Bozeman, MT, USA). CBRs are chemostat reactors that allow a gradual but constant refreshment of nutrients to facilitate continuous growth of attached biofilm communities.[50, 51] The bacteria *E. coli* was subcultured from a glycerol stock in 3 g/L tryptic soy broth (TSB, Sigma Aldrich, St. Louis, Missouri) at 37 °C. Three milliliters of an overnight culture were used to inoculate the sterile CBR containing 400 mL 3 g/L TSB. The CBR was maintained at room temperature with a constant stir speed of 120 rpm. The flow rate of sterile 3 g/L TSB into the CBR was maintained at 0.1 mL/min. Biofilms were quantified using a crystal violet (CV) staining assay. The substrate surfaces were extracted in duplicate at four and eight days post-inoculation. The slides were gently rinsed with PBS and treated with 1% crystal violet to stain the biofilm cells. Excess stain was rinsed with de-ionized water and crystal violet was extracted with methanol. Cell density of the biofilm was quantified by measuring the absorbance of crystal violet at 595 nm on a UV-2450PC UV-Vis Spectrophotometer (Shimadzu Corp., Kyoto, Japan).

Evaluation of Biocompatibility

Surface modified substrates were equilibrated in centrifuge tubes containing 10 mL of PBS and 0.2 mL of diluted mouse blood (800 μL of blood diluted with 1000 μL of PBS), following incubation at 37 °C for 1 h. PBS + 0.5% triton X100 and PBS were used as positive and negative controls, respectively. The tubes were centrifuged at 1500 rpm for 10 min and the optical absorbance of the supernatant was measured at 545 nm on a micro-plate reader. The hemolysis rate (HR) was calculated as follows: HR = (AS − AN)/ (AP − AN) here AS, AN, and AP are the optical absorbance of the supernatant of the solution containing modified glass, the negative control, and the positive control, respectively. Additionally, *in vitro* biocompatibility studies were carried out by utilizing HDF cell line which was obtained from Instrumentation Resources Facility, School of Medicine, University of South Carolina. HDF was propagated using Dulbecco's modified Eagle medium (DMEM, Sigma) supplemented with 7.5 mM of L-glutamine, 1% of penicillin/streptomycin solution, 10% of fetal bovine serum (complete DMEM). HDF (passage 30) was seeded in 12-wells of tissue culture polystyrene plates containing different surfaces at a density of 1×10^4 cells/cm^2 in a 1 mL volume of medium and allowed to proliferate for 96 h at 37 °C in a 10% CO_2 modified atmosphere until 60–70% confluence was reached as previously described.[52] Morphological observations of the HDF after 4 days of *in vitro* culture on the different surfaces were made by phase contrast microscopy and analyzed with Lumenera's INFINITY ANALYZE Software.

The HDF cells grown on different surfaces were fixed with 2% para formaldehyde for exactly 10 minutes. The fixed cells on the different surfaces were washed twice with PBS and then incubated with Alexa Fluor® 488 Phalloidin antibody (Life Technology) for actin staining (green) for 60 min at room temperature. After three times of PBS wash, the surfaces were stained for DNA with 4',6-diamidino-2-phenylindole (DAPI) (blue) for 15 min at room temperature. After rinsing thoroughly with PBS, the different surfaces were mounted on glass slides in Dabco (Sigma-Aldrich) and stored at 4 °C. The images from different surfaces were taken using CLSM.

3.4 Results and Discussion

Grafting Antimicrobial Agents on Substrate Surfaces

Current efforts toward the utilization of renewable resources to generate useful and functional materials are steadily increasing.[53-55] Diterpene resin acids produced largely by pine and conifer trees constitute a large bulk of biomass that can be effectively used to make novel materials. QA containing cationic compounds and polymers derived from these resin acids can act as highly effective antibacterial agents with remarkable biocompatibility (i.e. minimal cytotoxicity) towards mammalian cells.[39, 41, 56] Unlike other small QA compounds, this unusual activity of the QA abietic acid derivatives is related to the optimum balance between the hydrophenanthrene ring skeleton and the quaternary ammonium group. In the current study, we prepared antimicrobial surfaces using these resin acid-derived QA cationic compounds. Typically, QA compounds and polymers have been covalently attached onto various substrate surfaces such as glass, polymers, paper and metals.[57] In the present study, glass slides were used as the substrate since they are well known to be inert and biocompatible. However, it is possible to use the same chemistry for any substrate with hydroxyl functionality. Two strategies were followed to develop antimicrobial cationic surface systems. The surfaces with a monolayer of compound 1 were prepared via click chemistry between the surface immobilized azide groups and the alkyne moiety on the compound 1 (Figure 3.2A). Efficiency, versatility, and selectivity of the copper-catalyzed azide-alkyne cycloaddition (CuAAC) reaction is strongly demonstrated in a broad range of fields such as polymer and materials chemistry,[58-60] bioconjugate chemistry,[61] medicinal chemistry[62] and many other organic syntheses.[63] Furthermore, atom transfer radical polymerization (ATRP) is a widely utilized and versatile method for controlled radical polymerization that allows a diverse range of polymers and architectures to be prepared.[64] Surface initiated ATRP (SI-ATRP) is commonly used to prepare polymer brushes on surfaces.[65] This method is well explored to prepare antibacterial surfaces with high control, tunability and long-term effectiveness.[66] Therefore, SI-ATRP was used in this work, to graft cationic polymers from surfaces, which were modified with the ATRP initiator (Figure 3.2B).

Progress of the reactions were confirmed by determining the static water contact angle measurements (Figure 3.3A). Piranha treated glass surfaces (S1) were highly hydrophilic and had a water contact angle of 17°. When AzPTMS was immobilized (S2), the surface hydrophobicity increased which was evident from the contact angle increased to 85°. These results were in a good agreement with literature.[42, 45] Subsequent CuAAC click modification with the QA compound 1 amplified the surface hydrophilicity, leading to a final contact angle of 68°. Although there were positive charges on the compound 1 grafted surface (S3), the contact angle was much higher than that for pristine glass, which may be attributed to the hydrophilic/hydrophobic balance between the bulky hydrophenanthrene ring and the cationic groups. Surface attachment of ATRP initiator resulted in a surface (S4) with a contact angle of 60° which was later increased to 82° (**S5**) after the SI-ATRP of the Compound 2.

Additionally, XPS revealed the change of surface composition and the progression of the chemical modifications. The XPS survey scans illustrated the increase of carbon content and the appearance of nitrogen on Surface S2 and bromine on Surface S5**,** compared to that of the Surface S1 (Figure 3.3B). After the completion of CuAAC reaction and the SI-ATRP, the carbon content increased significantly on both surfaces S3 and S5. Depletion of silane peak intensity also confirmed the formation of a layer of material on top of the glass surface. XPS did not detect copper on the surfaces, thus nullifying the argument that residual catalyst from surface modifications may influence bactericidal properties. Also, previous control studies using copper against different strains of bacteria have not shown significant amounts of toxicity at low concentrations, indicating that our resin-acid derived compounds and polymers were responsible for the antimicrobial properties of the surfaces.[39] Grafting of cationic compound 1 and the cationic polymer resulted in surfaces that bear covalently attached cations. These cations can be stained with a negatively charged dye such as fluorescein. It is useful to qualitatively confirm the presence of cationic groups on surfaces. For the polymer grafted surface, the stain was visible even to the naked eye, indicating the increase of cationic groups on Surface **S5**. Figure 3.3C shows the CLSM images of different surfaces stained with fluorescein.

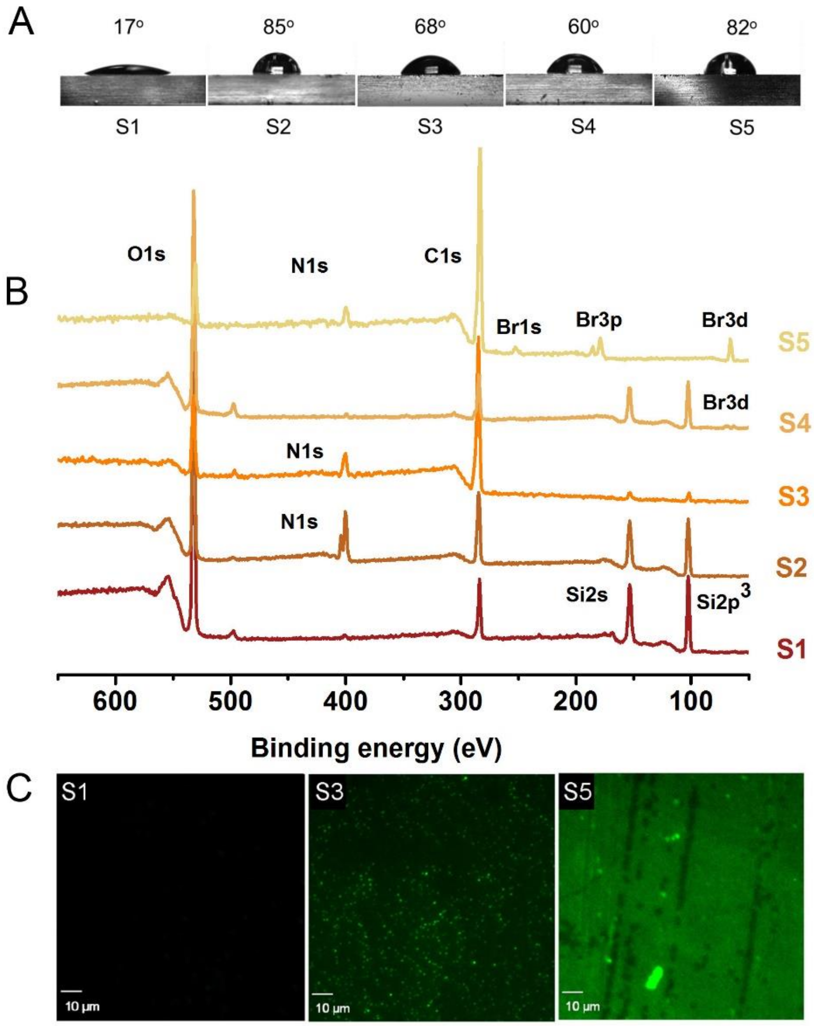

Figure 3.3. Surface characterization results. (A) Static water contact angles on various modified surfaces. (B) XPS survey spectra. (C) CLSM images of surfaces stained using fluorescein. S1, pristine glass; S2, azide-grafted; S3, compound 1-grafted; S4, ATRP initiator-grafted; and S5, polymer-grafted.

The density of QA groups on the glass surfaces was determined by a colorimetric method which is based on fluorescent complexation between fluorescein disodium salt and QA groups, as reported earlier.[32, 45] It can be envisioned that not all the cations could be exposed to fluorescein due to steric crowding, especially on the polymer grafted surface. Therefore, this method quantifies the 'solvent accessible' density of QA groups on the glass surfaces. Under the given conditions, fluorescein anions bind to QA groups via charge-

charge interactions. It is assumed that one dye molecule binds with one QA group. A stronger detergent such as cetyltrimethylammonium chloride can be used to remove the bound fluorescein from the surface. The stain can then be quantified by measuring the absorbance at 501 nm which is characteristic to fluorescein. There were approximately 0.5 cationic groups per nm^2 on the Surface S3. Surface S5 had a cationic group density of 6.3/ nm^2. Grafting density was approximated to 0.13/ nm^2, with respect to the molecular weight obtained from the cleaved polymer which was $M_{n,GPC}$ = 39,400 g/mol.

Although not studied in this work, it would be useful to explore the behavior of these cationic polymers grafted on surfaces using molecular dynamic simulations. Such study can predict how the cationic groups interact with the solution which is directly related to the biological property of such cationic surfaces.

Contact Active Antibacterial Activity of the Surfaces

In this work, we observed strong bactericidal effects upon contact of bacteria with QA resin acid derived cationic surfaces. It was found that there was no observable leakage of materials from the surfaces demonstrated by standard diffusion assays. The CLSM images (Figure 3.4) show the development of *S. aureus* and *E. coli* cells on surfaces after 24 h incubation with surfaces S1, S3 and S5. The Live/Dead kit used for this viability assay consists of two stains: propidium iodide (PI) and SYTO® 9, both of which stain nucleic acids. Green-fluorescing SYTO® 9 can enter all cells live or dead and is used for assessing total cell counts, whereas red fluorecing PI enters only cells with damaged cytoplasmic membranes (eg. dead cells). Therefore, bacteria observed from CLSM must result from pronounced growth on pristine glass surface.

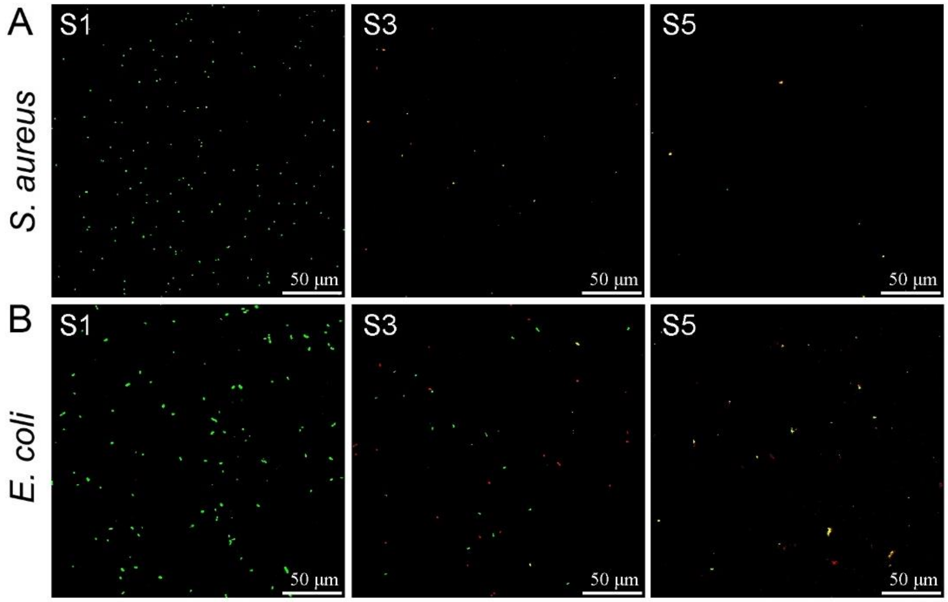

Figure 3.4 Stained (Live/Dead stain) surfaces after 24 h incubation with bacteria. (A) *S. aureus* and (B) *E. coli*. Green cells indicate live bacteria colonizing the surface while dead cells appear in red color. S1, pristine surface; S3, compound 1-grafted; and S5, polymer-grafted.

However, the number of cells attached to the surface remarkably reduced when the compound 1 was grafted (Figure 3.4 and 3.5A, B). This is possibly an anti-adherence property of these QA surfaces. Compared to S1, there is an 86% reduction of attached *S. aureus* cells and 47% reduction of attached *E. coli* cells on S3. Interestingly, S3 showed prominent bactericidal properties, observed in red-fluorescent cells (i.e. having compromised cell membranes). The modification with QA compound 1 resulted in a 61% loss in *S. aureus* viability and 49% in *E. coli* viability (Figure 3.5C, D). Further, surfaces with QA polymer prepared by SI-ATRP also exhibited a similar trend. However, the antibacterial activity was much higher in terms of bactericidal as well as anti-biofilm properties. There was a 94% reduction of *S. aureus* cells and a 59% reduction of *E. coli* cells attached on S5, compared S1. After incubation, most of the cells located on S5 fluoresced red, indicating membrane damage with 70% of *S. aureus* cells and 69% of *E.*

coli cells. In comparison with the results of S3, there was a notable increase in bactericidal activity of S5 against both *S. aureus* and *E. coli*. In addition, the modified glass surfaces were more bactericidal against Gram-positive *S. aureus* than they were against Gram-negative *E. coli*. This may be attributed to the bacterial cell envelope structural difference where Gram-negative *E. coli* has an additional outer membrane.

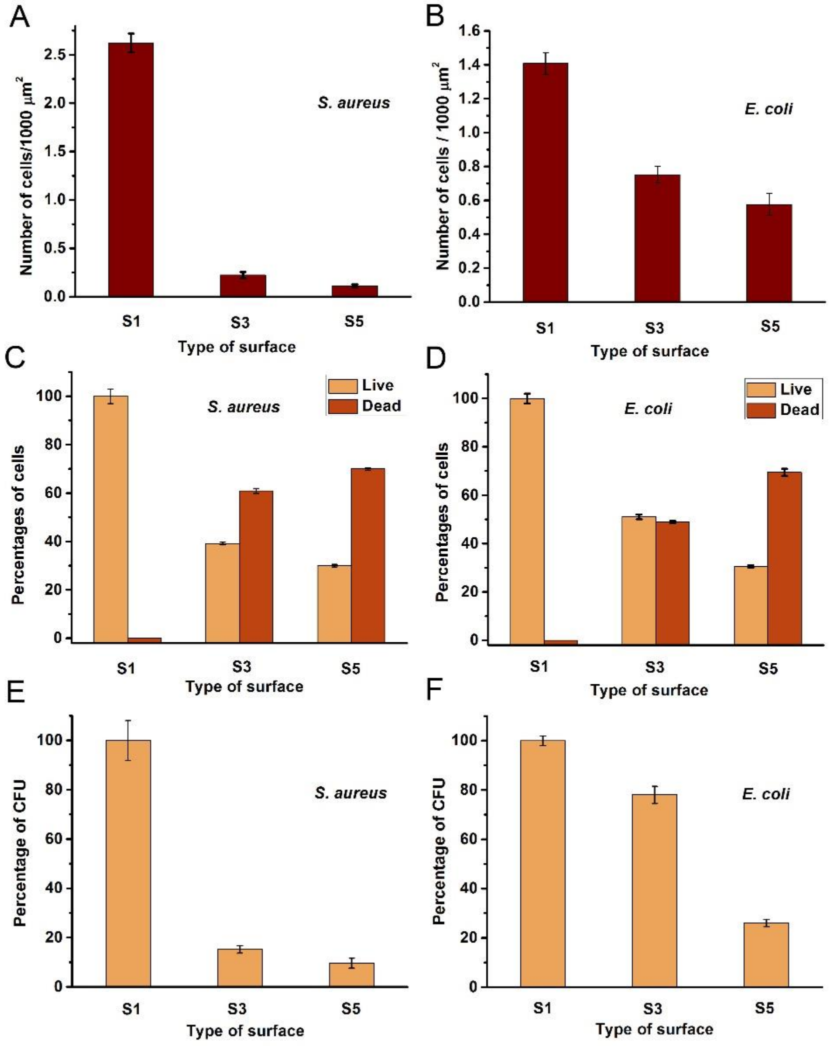

Figure 3.5 Antibacterial activity of the modified surfaces after 24 h. (A, B) Number of cells on the surface. (C, D) Percentages of live or dead cells on the surfaces. (E, F) Percentages of CFU obtained for the bacterial cultures exposed to surfaces. S1, pristine surface; S3, compound 1-grafted; and S5, polymer-grafted.

These cationic surfaces were able to kill planktonic bacterial cells that came in contact with them. This phenomenon was probed from CFU counts of the liquid bacterial media incubated in contact with the modified surfaces. *S. aureus* showed more susceptibility against both surfaces S3 and S5 with 84% or more reduction of CFU (Figure 3.5E, F). However, *E. coli* cells were less affected by the cationic surfaces resulting with the highest inhibition of 74% CFU in contact with S5 relative to control S1.

Anti-biofilm Properties

It has been demonstrated that QA compounds can effectively eradicate bacterial biofilm formation.[10] Since the material in this study showed strong antibacterial activities, a CDC bioreactor was used to study long-term antibiofilm activity. In most studies, relatively short periods of time (<1 day) are used to study biofilm growth on cationically modified surfaces. However, given that bacteria are dynamic and can adapt to their environment, we conducted experiments over longer periods of time. The results of the antimicrobial challenge assay indicated that compound 1 has strong anti-biofilm activity. The lowest concentration of compound 1, which prevented the growth of previously established *S. aureus* or *E. coli* biofilms on the pegs of the antimicrobial challenge plate, was 250 µg/mL. This was determined by measuring the mass of biofilm on each peg indirectly with dissolved crystal violet. The results for anti-biofilm activity of modified surfaces conducted with the CDC bioreactor are summarized in Figure 3.6. It should be noted that the model systems used for surface antimicrobial activity and antibiofilm properties are quite different, hence a direct comparison would not be meaningful. It is obvious that the unmodified surface S1 showed prominent and gradual growth of bacterial biofilm on the surface. However, QA-attached surfaces exhibited reduced growth of biofilm on them. For example, S3 with a monolayer of compound 1 showed 77 % less *S. aureus* biofilm biomass at 2 days of incubation and S5 with QA polymer demonstrated a 64 % reduction of that compared to the untreated glass S1. The cationic surfaces were more tolerant towards *S. aureus* biofilm growth compared to that of *E. coli*. This can be expected because the QA compounds have shown to be more antimicrobial towards Gram-positive bacteria. Over 8 days S3 and S5 demonstrated slow growth of biofilms, which was significantly less than that of the pristine surfaces. A similar or higher amount of biofilm on QA polymer coated-surface may be attributed to the fact that the increased surface area/roughness provided by the grafted polymer may provide more attachment sites.

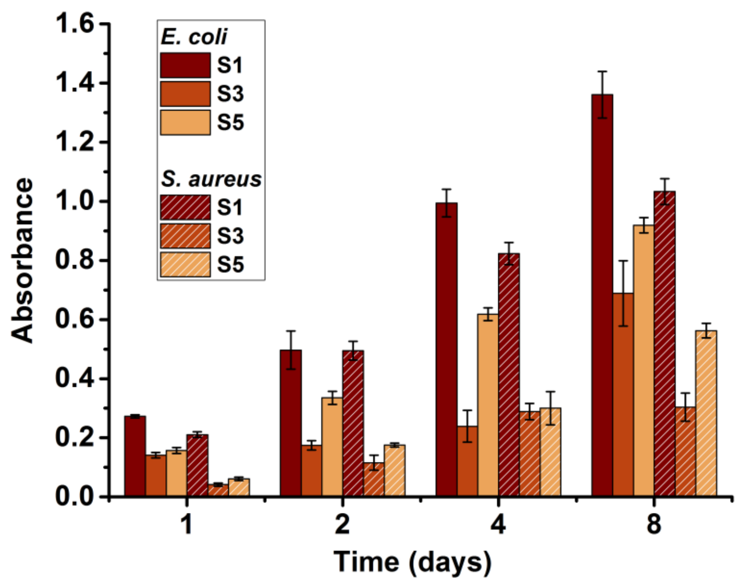

Figure 3.6 The amounts of *E. coli* and *S. aureus* biofilm biomass accumulated on the surfaces after incubating in the CDC bioreactor. S1, pristine surface; S3, compound 1-grafted; and S5, polymer-grafted.

The complicated process of biofilm formation is initially governed by physiochemical interactions between the bacterial cells and the target surface. Therefore, surface chemical composition, charge, hydrophobicity and contour operate as primary factors in the success or failure of colony initiation on a surface.[21, 22] Antibacterial surfaces may deactivate any planktonic cells that successfully interact with the surface, hence preventing the next stages of biofilm formation. We hypothesize that the reduction in bacterial growth was the result of two possible mechanisms (Figure 3.7). First, the cells are killed upon contact with the polymer and therefore cannot readily establish a biofilm. Second, the attachment of bacterial cells on the surface is reduced due to unfavorable surface properties such as charge and hydrophilic/hydrophobic balance. The antibacterial and antibiofilm assay results of this study indicated that the surface modification procedure induces both mechanisms.

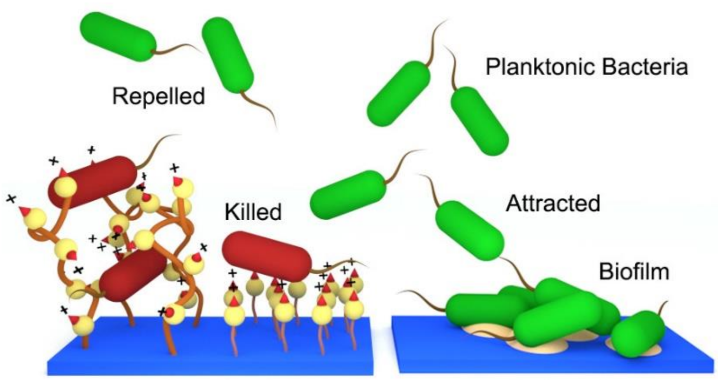

Figure 3.7 Comparison of antimicrobial mechanisms of the QA surfaces (left) and pristine surface (right). Resin acid containing cationic surfaces may act as a bactericidal and bacterial repelling coating.

Biocompatibility of the Surfaces

In our earlier reports, it was demonstrated that QA decorated abietic acid compounds and polymers are highly biocompatible while showing strong antimicrobial properties.[41] Here, additional biocompatibility evaluations were carried out for the modified surfaces utilizing hemolysis activity assays and surface cell growth assays. The hemolysis on chemically modified glass surfaces indicated a high degree of biocompatibility (i.e. non-cytotoxicity). Unmodified glass is known to have a negligible hemolytic effect. The hemolysis level of S3 was found to be <4%. The polymer grafted glass S5 resulted in insignificant hemolysis (< 0.1%). Interestingly the cationic surfaces showed improved proliferation of fibroblast cells. HDF cell proliferation over four days (Figure 3.8) showed continuous increase of cell density on the cationic surfaces.

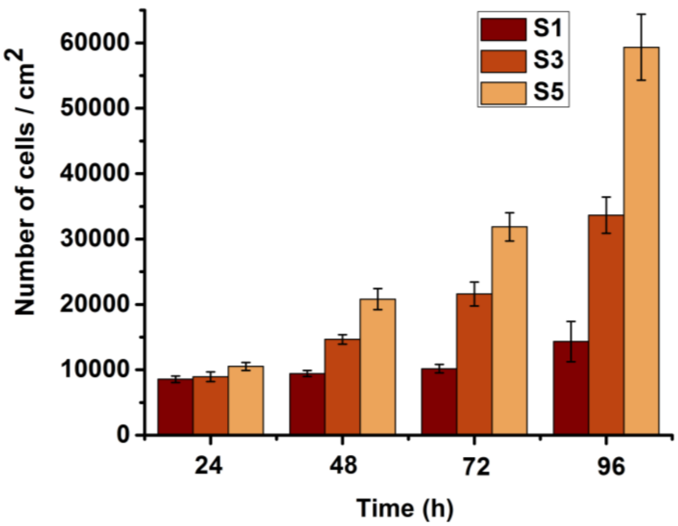

Figure 3.8 Amount of HDF cells proliferated on the surfaces. S1, Pristine surface; S3, Compound 1-grafted; and S5, Polymer-grafted.

Figure 3.9 shows the fluorescence microscopy and phase contrast images of the fibroblast cells grown on surfaces S1, S3 and S5. HDF cells were attached and spread well, with typical cell morphologies on surfaces S3 and S5. However, surface S1 did not show pronounced growth when compared to S3 or S5.

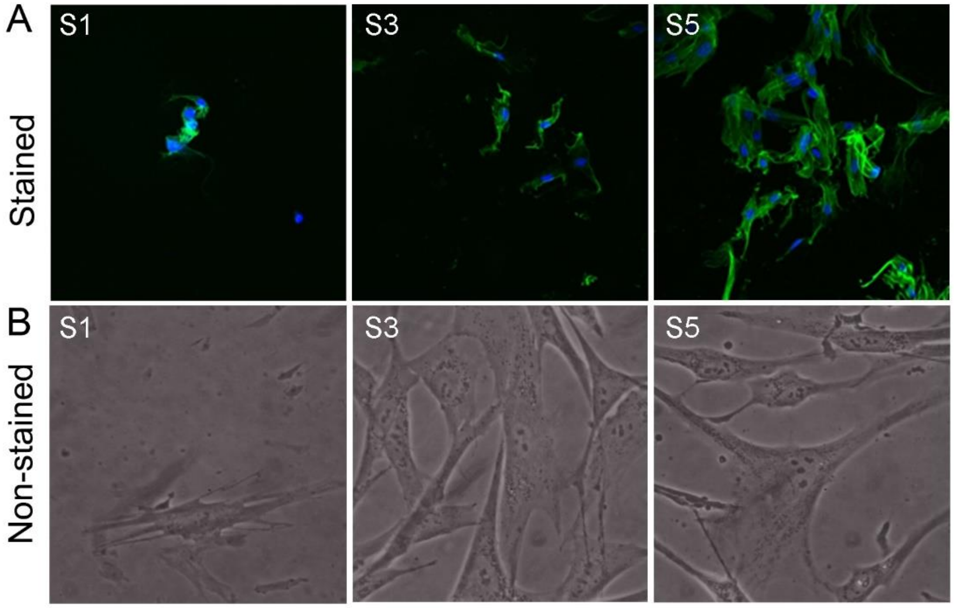

Figure 3.9 Morphology of HDF cells proliferated on the surfaces after 4 days. (A) Fluorescence microscopy images after staining. (B) Images under the phase contrast microscope. S1, Pristine surface; S3, Compound 1-grafted; and S5, Polymer-grafted.

After two days of seeding, cells changed their shape and began to spread. Cells on surfaces S3 and S5 had stretched out many filopodia, and most of them had further extended to be triangles and polygons, while the cells on Surface S1 spread to be flat with no or less ejection of filopodia. There was a difference in reaching confluence of the HDF cells within the different surfaces. Confluence of the HDF cells was observed on surfaces S3 and S5. There was a difference in cell proliferation on the surfaces, which was indicated by the varying extents of cell spreading observed on different surfaces. The Surface S5 was highly cell-adhesive. HDF, when attached to S5, proliferated to mature fibroblasts by extending their filopodia and having a branched cytoplasm surrounding their speckled nucleus. It was interesting to observe an improved proliferation of human fibroblast cells on the cationic surfaces which is consistent with previous reports, stating that cationic surfaces promote fibroblast spreading, proliferation and extracellular matrix production.[67,

[68] Therefore, it can be inferred that the resin acid containing cationic surfaces are able to provide suitable grounds for cell proliferation.

3.5 Conclusions

In conclusion, we have developed a simple and effective method to prepare antimicrobial surfaces using resin acid derived cationic compounds and polymers. The cationic compound 1 and polymer grafted surfaces showed strong antimicrobial activity against the bacteria, *S. aureus* and *E. coli*. The surfaces were more active against Gram-positive (i.e. *S. aureus*) bacteria. The surfaces were resistant to biofilm growth for longer durations of time as demonstrated by the CDC bioreactor assay. In addition, biocompatibility of surfaces was proven to be excellent, as demonstrated by hemolysis assays and HDF growth assays. These contact active coatings may be used to modify relevant surfaces to actively eliminate infectious microorganisms by destroying planktonic cells as well as controlling their biofilm growth. Therefore, this work presents a promising approach for the incorporation of renewable resources for developing surfaces that can control the spread of infectious diseases.

3.6 References

1. Costerton, J. W.; Cheng, K. J.; Geesey, G. G.; Ladd, T. I.; Nickel, J. C.; Dasgupta, M.; Marrie, T. J., Bacterial Biofilms in Nature and Disease. *Annu. Rev. Microbiol.* **1987,** *41*, 435-464.

2. Branda, S. S.; Vik, Å.; Friedman, L.; Kolter, R., Biofilms: The Matrix Revisited. *Trends Microbiol.* **2005,** *13*, 20-26.

3. Donlan, R. M., Biofilm Formation: A Clinically Relevant Microbiological Process. *Clin. Infect. Dis.* **2001,** *33*, 1387-1392.

4. Berk, V.; Fong, J. C. N.; Dempsey, G. T.; Develioglu, O. N.; Zhuang, X.; Liphardt, J.; Yildiz, F. H.; Chu, S., Molecular Architecture and Assembly Principles of Vibrio Cholerae Biofilms. *Science* **2012,** *337*, 236-239.

5. Davies, D. G.; Parsek, M. R.; Pearson, J. P.; Iglewski, B. H.; Costerton, J. W.;

Greenberg, E. P., The Involvement of Cell-to-Cell Signals in the Development of a Bacterial Biofilm. *Science* **1998,** *280*, 295-298.

6. Tuson, H. H.; Weibel, D. B., Bacteria–Surface Interactions. *Soft Matter* **2013,** *9*, 4368-4380.

7. Flemming, H.-C.; Wingender, J., The Biofilm Matrix. *Nat. Rev. Micro.* **2010,** *8*, 623-633.

8. Decho, A. W.; Frey, R. L.; Ferry, J. L., Chemical Challenges to Bacterial Ahl Signaling in the Environment. *Chem. Rev.* **2010,** *111*, 86-99.

9. Stewart, P. S.; Franklin, M. J., Physiological Heterogeneity in Biofilms. *Nat. Rev. Micro.* **2008,** *6*, 199-210.

10. Fletcher, M. H.; Jennings, M. C.; Wuest, W. M., Draining the Moat: Disrupting Bacterial Biofilms with Natural Products. *Tetrahedron* **2014,** *70*, 6373-6383.

11. Hall-Stoodley, L.; Costerton, J. W.; Stoodley, P., Bacterial Biofilms: From the Natural Environment to Infectious Diseases. *Nat. Rev. Micro.* **2004,** *2*, 95-108.

12. Høiby, N.; Bjarnsholt, T.; Givskov, M.; Molin, S.; Ciofu, O., Antibiotic Resistance of Bacterial Biofilms. *Int. J. Antimicrob. Agents* **2010,** *35*, 322-332.

13. Costerton, J. W.; Stewart, P. S.; Greenberg, E. P., Bacterial Biofilms: A Common Cause of Persistent Infections. *Science* **1999,** *284*, 1318-1322.

14. Hoyle, B.; Costerton, J. W., Bacterial Resistance to Antibiotics: The Role of Biofilms. *Prog. Drug Res.* **1991,** *37*, 91-105.

15. Hasan, J.; Crawford, R. J.; Ivanova, E. P., Antibacterial Surfaces: The Quest for a New Generation of Biomaterials. *Trends Biotechnol.* **2013,** *31*, 295-304.

16. Campoccia, D.; Montanaro, L.; Arciola, C. R., A Review of the Biomaterials Technologies for Infection-Resistant Surfaces. *Biomaterials* **2013,** *34*, 8533-8554.

17. Taglietti, A.; Arciola, C. R.; D'Agostino, A.; Dacarro, G.; Montanaro, L.; Campoccia, D.; Cucca, L.; Vercellino, M.; Poggi, A.; Pallavicini, P.; Visai, L., Antibiofilm Activity of a Monolayer of Silver Nanoparticles Anchored to an Amino-Silanized Glass Surface. *Biomaterials* **2014,** *35*, 1779-1788.

18. Swanson, T. E.; Cheng, X.; Friedrich, C., Development of Chitosan–Vancomycin Antimicrobial Coatings on Titanium Implants. *J. Biomed. Mater. Res. A* **2011,** *97*, 167-176.

19. Gao, G.; Lange, D.; Hilpert, K.; Kindrachuk, J.; Zou, Y.; Cheng, J. T. J.; Kazemzadeh-Narbat, M.; Yu, K.; Wang, R.; Straus, S. K.; Brooks, D. E.; Chew, B. H.; Hancock, R. E. W.; Kizhakkedathu, J. N., The Biocompatibility and Biofilm Resistance of Implant

Coatings Based on Hydrophilic Polymer Brushes Conjugated with Antimicrobial Peptides. *Biomaterials* **2011,** *32*, 3899-3909.

20. Muñoz-Bonilla, A.; Fernández-García, M., Polymeric Materials with Antimicrobial Activity. *Prog. Polym. Sci.* **2012,** *37*, 281-339.

21. Muñoz-Bonilla, A.; Fernández-García, M., The Roadmap of Antimicrobial Polymeric Materials in Macromolecular Nanotechnology. *Eur. Polym. J.* **2015,** *65*, 46-62.

22. Siedenbiedel, F.; Tiller, J. C., Antimicrobial Polymers in Solution and on Surfaces: Overview and Functional Principles. *Polymers* **2012,** *4*, 46-71.

23. Ho, K. K. K.; Chen, R.; Willcox, M. D. P.; Rice, S. A.; Cole, N.; Iskander, G.; Kumar, N., Quorum Sensing Inhibitory Activities of Surface Immobilized Antibacterial Dihydropyrrolones Via Click Chemistry. *Biomaterials* **2014,** *35*, 2336-2345.

24. Brohede, U.; Forsgren, J.; Roos, S.; Mihranyan, A.; Engqvist, H.; Strømme, M., Multifunctional Implant Coatings Providing Possibilities for Fast Antibiotics Loading with Subsequent Slow Release. *J. Mater. Sci. Mater. Med.* **2009,** *20*, 1859-1867.

25. Foster, H.; Ditta, I.; Varghese, S.; Steele, A., Photocatalytic Disinfection Using Titanium Dioxide: Spectrum and Mechanism of Antimicrobial Activity. *Appl. Microbiol. Biotechnol.* **2011,** *90*, 1847-1868.

26. Zhang, X.; Wang, L.; Levanen, E., Superhydrophobic Surfaces for the Reduction of Bacterial Adhesion. *RSC Adv.* **2013,** *3*, 12003-12020.

27. Ivanova, E. P.; Hasan, J.; Webb, H. K.; Gervinskas, G.; Juodkazis, S.; Truong, V. K.; Wu, A. H. F.; Lamb, R. N.; Baulin, V. A.; Watson, G. S.; Watson, J. A.; Mainwaring, D. E.; Crawford, R. J., Bactericidal Activity of Black Silicon. *Nat. Commun.* **2013,** *4*.

28. Isquith, A. J.; Abbott, E. A.; Walters, P. A., Surface-Bonded Antimicrobial Activity of an Organosilicon Quaternary Ammonium Chloride. *Appl. Microbiol.* **1972,** *24*, 859-863.

29. Gottenbos, B.; van der Mei, H. C.; Klatter, F.; Nieuwenhuis, P.; Busscher, H. J., In Vitro and in Vivo Antimicrobial Activity of Covalently Coupled Quaternary Ammonium Silane Coatings on Silicone Rubber. *Biomaterials* **2002,** *23*, 1417-1423.

30. Li, Z.; Lee, D.; Sheng, X.; Cohen, R. E.; Rubner, M. F., Two-Level Antibacterial Coating with Both Release-Killing and Contact-Killing Capabilities. *Langmuir* **2006,** *22*, 9820-9823.

31. Gabriel, M.; Nazmi, K.; Veerman, E. C.; Nieuw Amerongen, A. V.; Zentner, A., Preparation of Ll-37-Grafted Titanium Surfaces with Bactericidal Activity. *Bioconj. Chem.* **2006,** *17*, 548-550.

32. Tiller, J. C.; Liao, C.-J.; Lewis, K.; Klibanov, A. M., Designing Surfaces That Kill

Bacteria on Contact. *Proc. Natl. Acad. Sci. U.S.A.* **2001,** *98*, 5981-5985.

33. Lin, J.; Qiu, S.; Lewis, K.; Klibanov, A. M., Mechanism of Bactericidal and Fungicidal Activities of Textiles Covalently Modified with Alkylated Polyethylenimine. *Biotechnol. Bioeng.* **2003,** *83*, 168-172.

34. Huang, J.; Murata, H.; Koepsel, R. R.; Russell, A. J.; Matyjaszewski, K., Antibacterial Polypropylene Via Surface-Initiated Atom Transfer Radical Polymerization. *Biomacromolecules* **2007,** *8*, 1396-1399.

35. Dong, H.; Huang, J.; Koepsel, R. R.; Ye, P.; Russell, A. J.; Matyjaszewski, K., Recyclable Antibacterial Magnetic Nanoparticles Grafted with Quaternized Poly(2-(dimethylamino)ethyl methacrylate) Brushes. *Biomacromolecules* **2011,** *12*, 1305-1311.

36. Asri, L. A. T. W.; Crismaru, M.; Roest, S.; Chen, Y.; Ivashenko, O.; Rudolf, P.; Tiller, J. C.; van der Mei, H. C.; Loontjens, T. J. A.; Busscher, H. J., A Shape-Adaptive, Antibacterial-Coating of Immobilized Quaternary-Ammonium Compounds Tethered on Hyperbranched Polyurea and Its Mechanism of Action. *Adv. Funct. Mater.* **2014,** *24*, 346-355.

37. Klibanov, A. M., Permanently Microbicidal Materials Coatings. *J. Mater. Chem.* **2007,** *17*, 2479-2482.

38. Ferreira, L.; Zumbuehl, A., Non-Leaching Surfaces Capable of Killing Microorganisms on Contact. *J. Mater. Chem.* **2009,** *19*, 7796-7806.

39. Wang, J.; Chen, Y. P.; Yao, K.; Wilbon, P. A.; Zhang, W.; Ren, L.; Zhou, J.; Nagarkatti, M.; Wang, C.; Chu, F.; He, X.; Decho, A. W.; Tang, C., Robust Antimicrobial Compounds and Polymers Derived from Natural Resin Acids. *Chem. Commun.* **2012,** *48*, 916-918.

40. Chen, Y.; Wilbon, P. A.; Chen, Y. P.; Zhou, J.; Nagarkatti, M.; Wang, C.; Chu, F.; Decho, A. W.; Tang, C., Amphipathic Antibacterial Agents Using Cationic Methacrylic Polymers with Natural Rosin as Pendant Group. *RSC Adv.* **2012,** *2*, 10275-10282.

41. Ganewatta, M. S.; Chen, Y. P.; Wang, J.; Zhou, J.; Ebalunode, J.; Nagarkatti, M.; Decho, A. W.; Tang, C., Bio-Inspired Resin Acid-Derived Materials as Anti-Bacterial Resistance Agents with Unexpected Activities. *Chem. Sci.* **2014,** *5*, 2011-2016.

42. Godula, K.; Rabuka, D.; Nam, K. T.; Bertozzi, C. R., Synthesis and Microcontact Printing of Dual End-Functionalized Mucin-Like Glycopolymers for Microarray Applications. *Angew. Chem. Int. Ed.* **2009,** *48*, 4973-4976.

43. Beltrán-Osuna, Á. A.; Cao, B.; Cheng, G.; Jana, S. C.; Espe, M. P.; Lama, B., New Antifouling Silica Hydrogel. *Langmuir* **2012,** *28*, 9700-9706.

44. Yan, Y.; Zhang, J.; Qiao, Y.; Tang, C., Facile Preparation of Cobaltocenium-Containing Polyelectrolyte Via Click Chemistry and Raft Polymerization. *Macromol. Rapid Commun.* **2014,** *35*, 254-259.

45. Huang, J.; Koepsel, R. R.; Murata, H.; Wu, W.; Lee, S. B.; Kowalewski, T.; Russell, A. J.; Matyjaszewski, K., Nonleaching Antibacterial Glass Surfaces Via "Grafting Onto": The Effect of the Number of Quaternary Ammonium Groups on Biocidal Activity. *Langmuir* **2008,** *24*, 6785-6795.

46. Sjöback, R.; Nygren, J.; Kubista, M., Absorption and Fluorescence Properties of Fluorescein. *Spectrochim. Acta Mol. Biomol. Spectrosc.* **1995,** *51*, L7-L21.

47. Murata, H.; Koepsel, R. R.; Matyjaszewski, K.; Russell, A. J., Permanent, Non-Leaching Antibacterial Surfaces-2: How High Density Cationic Surfaces Kill Bacterial Cells. *Biomaterials* **2007,** *28*, 4870-4879.

48. Li, Y.; Benicewicz, B. C., Functionalization of Silica Nanoparticles Via the Combination of Surface-Initiated Raft Polymerization and Click Reactions. *Macromolecules* **2008,** *41*, 7986-7992.

49. Lee, S. B.; Koepsel, R. R.; Morley, S. W.; Matyjaszewski, K.; Sun, Y.; Russell, A. J., Permanent, Nonleaching Antibacterial Surfaces-1: Synthesis by Atom Transfer Radical Polymerization. *Biomacromolecules* **2004,** *5*, 877-882.

50. Donlan, R. M.; Piede, J. A.; Heyes, C. D.; Sanii, L.; Murga, R.; Edmonds, P.; El-Sayed, I.; El-Sayed, M. A., Model System for Growing and Quantifying Streptococcus Pneumoniae Biofilms in Situ and in Real Time. *Appl. Environ. Microbiol.* **2004,** *70*, 4980-4988.

51. Goeres, D. M.; Loetterle, L. R.; Hamilton, M. A.; Murga, R.; Kirby, D. W.; Donlan, R. M., Statistical Assessment of a Laboratory Method for Growing Biofilms. *Microbiology* **2005,** *151*, 757-762.

52. Zhang, Y. Z.; Venugopal, J.; Huang, Z. M.; Lim, C. T.; Ramakrishna, S., Characterization of the Surface Biocompatibility of the Electrospun Pcl-Collagen Nanofibers Using Fibroblasts. *Biomacromolecules* **2005,** *6*, 2583-2589.

53. Yao, K.; Tang, C., Controlled Polymerization of Next-Generation Renewable Monomers and Beyond. *Macromolecules* **2013,** *46*, 1689-1712.

54. Wilbon, P. A.; Chu, F.; Tang, C., Progress in Renewable Polymers from Natural Terpenes, Terpenoids, and Rosin. *Macromol. Rapid Commun.* **2013,** *34*, 8-37.

55. Chen, Y.; Wilbon, P. A.; Zhou, J.; Nagarkatti, M.; Wang, C.; Chu, F.; Tang, C., Multifunctional Self-Fluorescent Polymer Nanogels for Label-Free Imaging and Drug Delivery. *Chem. Commun.* **2013,** *49*, 297-299.

56. Ganewatta, M. S.; Tang, C., Controlling Macromolecular Structures Towards

Effective Antimicrobial Polymers. *Polymer* **2015,** *63*, A1-A29.

57. Madkour, A. E.; Dabkowski, J. M.; Nüsslein, K.; Tew, G. N., Fast Disinfecting Antimicrobial Surfaces. *Langmuir* **2008,** *25*, 1060-1067.

58. Fournier, D.; Hoogenboom, R.; Schubert, U. S., Clicking Polymers: A Straightforward Approach to Novel Macromolecular Architectures. *Chem. Soc. Rev.* **2007,** *36*, 1369-1380.

59. Binder, W. H.; Sachsenhofer, R., 'Click' Chemistry in Polymer and Material Science: An Update. *Macromol. Rapid Commun.* **2008,** *29*, 952-981.

60. Nandivada, H.; Jiang, X.; Lahann, J., Click Chemistry: Versatility and Control in the Hands of Materials Scientists. *Adv. Mater.* **2007,** *19*, 2197-2208.

61. Breinbauer, R.; Köhn, M., Azide–Alkyne Coupling: A Powerful Reaction for Bioconjugate Chemistry. *ChemBioChem* **2003,** *4*, 1147-1149.

62. Tron, G. C.; Pirali, T.; Billington, R. A.; Canonico, P. L.; Sorba, G.; Genazzani, A. A., Click Chemistry Reactions in Medicinal Chemistry: Applications of the 1,3-Dipolar Cycloaddition between Azides and Alkynes. *Med. Res. Rev.* **2008,** *28*, 278-308.

63. Kolb, H. C.; Finn, M. G.; Sharpless, K. B., Click Chemistry: Diverse Chemical Function from a Few Good Reactions. *Angew. Chem. Int. Ed.* **2001,** *40*, 2004-2021.

64. Matyjaszewski, K.; Tsarevsky, N. V., Macromolecular Engineering by Atom Transfer Radical Polymerization. *J. Am. Chem. Soc.* **2014,** *136*, 6513-6533.

65. Pyun, J.; Kowalewski, T.; Matyjaszewski, K., Synthesis of Polymer Brushes Using Atom Transfer Radical Polymerization. *Macromol. Rapid Commun.* **2003,** *24*, 1043-1059.

66. Lee, S. B.; Koepsel, R. R.; Morley, S. W.; Matyjaszewski, K.; Sun, Y.; Russell, A. J., Permanent, Nonleaching Antibacterial Surfaces. 1. Synthesis by Atom Transfer Radical Polymerization. *Biomacromolecules* **2004,** *5*, 877-882.

67. Kishida, A.; Iwata, H.; Tamada, Y.; Ikada, Y., Cell Behaviour on Polymer Surfaces Grafted with Non-Ionic and Ionic Monomers. *Biomaterials* **1991,** *12*, 786-792.

68. De Rosa, M.; Carteni, M.; Petillo, O.; Calarco, A.; Margarucci, S.; Rosso, F.; De Rosa, A.; Farina, E.; Grippo, P.; Peluso, G., Cationic Polyelectrolyte Hydrogel Fosters Fibroblast Spreading, Proliferation, and Extracellular Matrix Production: Implications for Tissue Engineering. *J. Cell. Physiol.* **2004,** *198*, 133-143.

CHAPTER 4

Facially Amphiphilic Antimicrobial Polymers Containing Lithocholic Acid in the Main-Chain

4.1 Abstract

Bacterial infections have become a global issue that needs timely attention. Specially, multidrug-resistant Gram-negative bacteria has become very problematic. We developed lithocholic acid containing main-chain polyionenes that show antimicrobial activity against several bacterial species. Interestingly, by choosing appropriate monomers, these cationic polymers can form core-shell micelles where the hydrophobic core is composed of lithocholic acid structure. These nanoparticles can be developed into carriers to deliver hydrophobic antibiotics to have a dual functional antimicrobial system.

4.2 Introduction

Microbial infections have become problematic due to the difficulty to treat them with conventional antibiotics. The use and misuse of antibiotics and well as the lack of new molecule discovery over the last few decades have resulted in the rise of antibiotic resistant pathogenic microorganisms that circumvent the well-being of humans worldwide. Specially, the rise of drug-resistant Gram-negative bacteria is of particular concern given the limited number of antimicrobial agents that can be used for such infections.[1, 2] The cell wall structure and the presence of an outer envelope is often responsible for the less sensitivity of Gram-negative bacteria to antimicrobial agents.[3] Antimicrobial polymers are a class of hydrophilic cationic macromolecules that can selectively destroy microorganisms such as bacteria, fungi or protozoans with low or no toxicity to mammalian cells.[4]

In our group, we have developed several antimicrobial macromolecules utilizing natural rosin with impressive activities.[5-8] There the cationic charge was implemented as pendent groups on polymer chains. However, antimicrobial agents such as antimicrobial peptides and antimicrobial polymers favor a facially amphiphilic orientation during their mechanism of action. In search for facially amphiphilic biomolecules, we noted bile acids as potential candidates to prepare effective antimicrobial polymers. Bile of mammals and other vertebrates are rich in bile acids that are amphiphilic steroid acids. They typically stay conjugated with taurine or glycine in the liver forming bile salts that serve as surfactants to solubilize dietary lipids and fats by the formation of micelles allowing digestion of food. Liver cells produce primary bile acids such as cholic acid and chenodeoxycholic acid in humans via oxidation of cholesterol in a multi-step pathway. Bacterial partial dihydroxylation in the intestine results in secondary bile acids such as deoxycholic acid and lithocholic acid. Bile acids have been utilized for many areas including drug delivery,[9] sensing,[10] polymeric gels,[11] antimicrobial[12, 13] and other biological applications.[14]. Bile acid based amphiphiles demonstrate strong interactions with cell membranes.[15]

The 5β framework of bile acids or the cis A - B ring junction imparts a curvature to the ring system resulting in two faces with dramatically different properties.[16] Hydroxyl groups of bile acid molecules are positioned in the α-face while their methyl groups are in the β-face, thereby creating facial amphiphilicity (Figure 4.1). The steroidal nucleus with four fused rings provide the hydrophobic core that can preferentially embed into cell membranes. The presence of hydroxyl and carboxylic acid group offer hydrophilic chemical functionalization to achieve robust and scalable molecular designs and architectures to investigate key determinants of its surface activity and the ability to selectively solubilize membrane lipids.

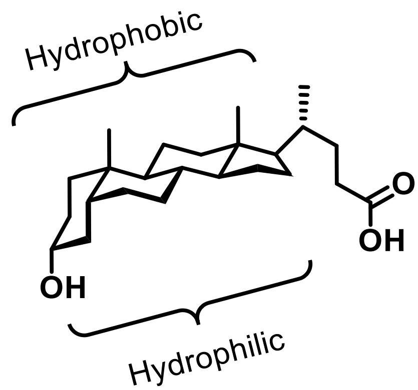

Figure 4.1 Facially amphiphilic structure of lithocholic acid.

Recent advances on bile acid in macromolecular research include a broad variety of structures with bile acids as repeating units in the polymer backbone, as pendant groups along the polymer chain in block or statistical polymer and chain end-functional polymers.[17, 18] Notable research on bile acid polymers have been carried out by X. X. Zhu and coworkers.[18] Biopolymers containing bile acids in the main chain have been widely prepared using step-growth polymerization via incorporating a variety of linkers, such as esters, amides, triazoles, urethanes, and imines. Polycondensations are useful to prepare highly efficacious and inexpensive antimicrobial polymers for wide scale applications.[19] A unique class of polyelectrolytes known as polyionenes can be prepared by polycondensation to have cations in the main chain at regular and specific sites. Polyionenes have many applications in fields such as gene transfection, cancer drug delivery and antimicrobial. They are generally prepared from a reaction between ditertiary amines and dihalides via Menschutkin reaction.[20, 21] With the proper combination of cationic and hydrophobic units, such polymers have been developed into antimicrobial agents with strong antimicrobial activities with good biocompatibility.[22, 23] However, there is little research done to prepare hydrophobic polyionenes that incorporate biomass derived chemicals targeted for antimicrobial applications.

We envisioned the possibility to develop ditertiary amines and dihalides monomers from bile acids such as lithocholic acid that can be used to prepare polyionenes. Water soluble cationic polymers with a degradable backbone can be easily developed using lithocholic acid in the main chain. In this study, we developed difunctional monomers from LCA and used them to make cationic polymers that contain quaternary ammonium groups along the polymer backbone. These polymers formed micelles in water at low concentrations. The antimicrobial activity and the drug loading capability were investigated.

4.3 Experimental section

Materials

Lithocholic acid (95%, Aldrich), lithium aluminum hydride (95%, Aldrich) and 6-bromohexanoyl chloride (97%, Aldrich) were used as received. *N*,*N*,*N*',*N*'-tetramethyl-1,2-ethanediamine (99%, TCI) and *N*,*N*,*N*',*N*'-tetramethyl-1,6-hexanediamine (99%, Aldrich) were distilled before used. Tetrahydrofuran (THF) and *N*, *N*-dimethylformamide (DMF) were dried over drying columns. Ampicillin was purchased from VWR as the pure form. All other reagents and solvents were from commercial resources and used as received unless otherwise mentioned. Spectrum Spectra/Por® 3 Dialysis Membranes with MWCO 3500 was purchased from VWR.

Characterization

^{1}H NMR (300 MHz) spectra were recorded on a Bruker Avance III HD 300. Zetasizer Nano ZS, Malvern Instruments Corporate was used for the determination of micelle size and surface charge. The morphology of the polymer nanoparticles was recorded by using the Field-Emission Scanning Electron Microscopy (FE-SEM, Zeiss UltraPlus). UV-vis spectra were recorded on a Shimadzu UV 2450 spectrophotometer.

Synthesis of 3α,5β-cholane-3,24-diol

A suspension of $LiAlH_4$ powder (2.0 g, 0.053 mol, 2.0 equiv.) was added to dry THF 100 mL in a round-bottom flask, slowly and carefully at 0 °C. Then lithocholic acid (10 g, 0.027 mol, 1.0 equiv.) was added to the suspension in small quantities at 0 °C while stirring vigorously. After keeping at room temperature for 30 min, the mixture was refluxed for 18 h. Then the reaction mixture was transferred carefully to a 10 % HCl(aq) 1 L in a conical flask. The product was extracted to diethyl ether 3 times. After drying with anhydrous $MgSO_4$, the solvent was removed by rotary evaporation. Then it was kept in a vacuum oven at 50 ^{o}C over night to obtain a white crystalline powder 9.6 g (yield = 99 %).

Synthesis of Lithocholic Dibromide Compounds

3α,5β-cholane-3,24-diol (10.0 g, 0.275 mol, 1 equiv.) was transferred to a solution of 6-bromohexanoyl chloride (23.5 g, 0.11 mol, 4.0 equiv.) in dry THF at 0 °C. The flask was sealed and stirred at room temperature for 24 h. Then it was washed with $NaHCO_3$, water and brine against DCM. The product was concentrated by rotary evaporation and precipitated into methanol three times. Then the product was filtered and vacuum oven dried to obtain a white powder 15.0 g (yield = 75 %).

Synthesis of Main-chain Cationic Polymers

Stoichiometric amounts of the dibromide and the diamine were used for the condensation polymerization. In a typical procedure, the dibromide (500 mg, 0.698 mmol, 1 equiv.) was transferred to a 25 mL round-bottom flask. It was added with *N*,*N*,*N*',*N*'-tetramethyl-1,6-hexanediamine (121.4 mg, 0.698 mmol, 1 equiv.) using dry DMF 5.0 mL.

The flask was sealed using a rubber septum and heated to 60 ^{o}C for 24 h. After the completion of the reaction, the mixture was dialyzed against 3 L of water for 24 h. Then the remaining solution was freeze-dried for 2 days to obtain a white powder 485 mg (yield = 78 %)

Critical Micelle Concentration

The CMC value of the polymer was determined using the fluorescence of pyrene as the probe. A stock solution of pyrene (0.1 mg/mL) in acetone. Then, 20 µL of the pyrene solution was added to glass vials and left to dry. Next, a series of polymer solutions were made at concentrations ranging from 0.3 mg/mL to 0.0001 mg/mL using serial dilution. Afterwards, 10.0 mL of each polymer solution was added to pyrene containing vials, vortex for 1 min and left at room temperature for 24 h for the system to reach equilibrium. The polymer solutions were excited using 334 nm excitation wavelength and emission was recorded at 372 nm and 392 nm with slit width kept at 2.5 nm.

Antimicrobial Assay

Actively-growing cultures of each bacterial strain on Mannitol salt agar (MSA) were inoculated on Tryptic Soy Broth (TSB) agar plates. The bacterial growth culture (cell concentrations were 1.0 x 10^{6} CFU/mL) 10 µL was diluted to 1 mL in TSB and 100 µL of that was spread on TSB agar plates to form a bacterial lawn covering the plate surface. Then 6 mm (diameter) sterile discs were placed on the plate surface, followed by adding the polymers and compounds at different concentrations in DMSO was added to disks. The plates were incubated at 37 ^{o}C for 18 h. The development of a clear zone around the disk was indicative of the ability of materials to kill bacteria.

Antibiotic Loaded Micelles and Drug Release

The hydrophobic antibiotic ampicillin was used to demonstrate the drug loading capability of these polymers. Drug loaded micelles were prepared by a membrane dialysis method. The polymer P2 10.0 mg was mixed with ampicillin 10.0 mg and dissolved in 5 mL of DMSO. Then the solution was dialyzed against deionized water 3 L at room temperature. The water was replaced three times over 24 h. Then the dialysis bag containing the drug loaded micelles was immersed in a graduated glass media bottle containing PBS solution 150 mL at 37 ^{o}C. The stirring was kept at 300 rpm. At specific time intervals, 3 mL of the solution was taken out for UV-vis analysis. After the measurements, the solution was returned to the bottle. The cumulative release was calculated based on the total release of the contents from the dialysis bag.

4.4 Results and Discussion

Reduction of lithocholic acid utilizing $LiAlH_4$ is a robust and high yielding route to obtain 3α,5β-cholane-3,24-diol. This diol compound is converted to a dibromide using fatty acyl bromides with different lengths. The cationic polymers were synthesized by the stoichiometric copolymerization of dibromocholane derivatives with the corresponding ditertiary amines according to the Menschutkin reaction (Figure 4.2). As we envisioned there is a wide range of ditertiary amines that can be used for the polymerization allowing us to explore several different polymers for potential antimicrobial applications. However, initially few structural variations were investigated to obtain a polymeric system that can produce cationic micelles at fairly low critical micellar concentration (CMC). Such micelles can be used to deliver hydrophobic antibiotics such as ampicillin or ciprofloxacin in to microbial cells.[24]

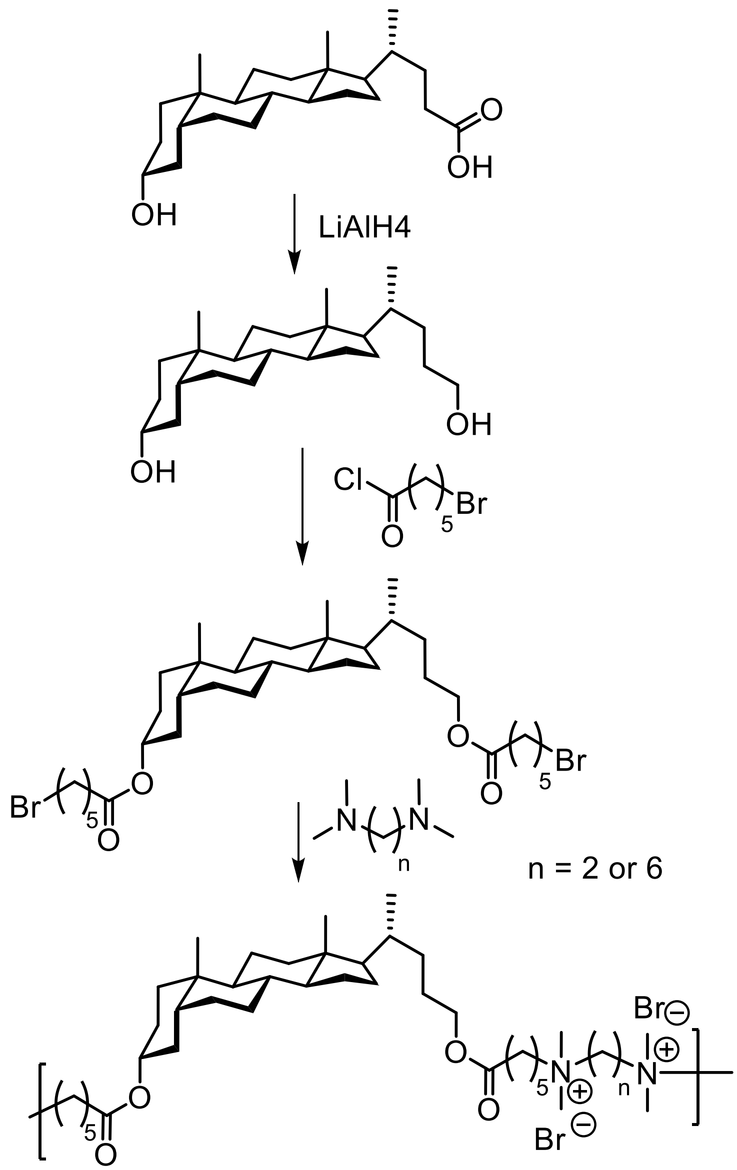

Figure 4.2 Synthesis of main-chain cationic polymers from lithocholic acid. Polymer P1, n=2 and polymer P2, n=6.

The intermediate compounds were purified by simple precipitation because the hydrophobic steroidal structure made the compounds insoluble in methanol. After the polymerization reaction was completed, dialysis against deionized water was employed to remove oligomeric molecules and unreacted amines. The products were characterized by ^1H NMR (Figure 4.3).

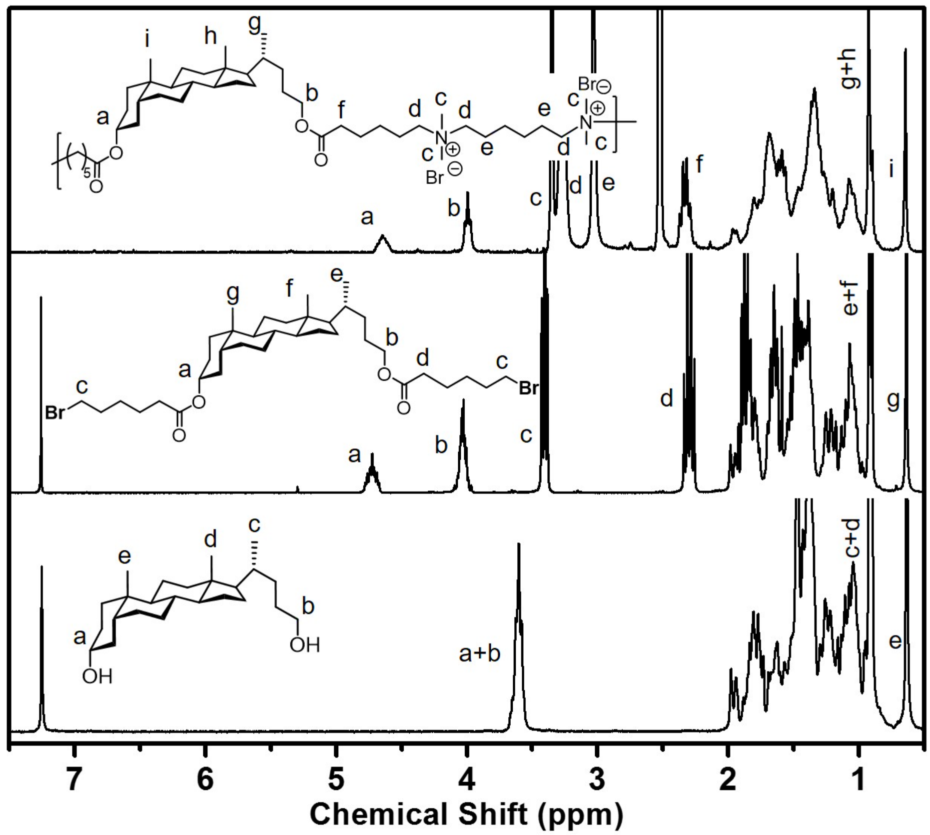

Figure 4.3 ^1H NMR spectra of the compounds and polymer in each step of the synthesis.

Interestingly, after dialysis the polymers form micelles (Figure 4.4A) as observable by turbid solution that showed Tindall scattering. This demonstrated that the polymers can form particles in water. In addition, the micelles were observed using SEM (Figure 4.4B). The particles size was in a broad range because they were prepared by redispersing the freeze-dried polymer powder. Amphiphilic polymers that contain hydrophobic and cationic regions can self-assemble to form core-shell structure in aqueous solutions. Here in the lithocholic polymer micelles, the hydrophobic core is composed of the steroidal rings while the cationic linkers form the shell (Figure 4.4C)

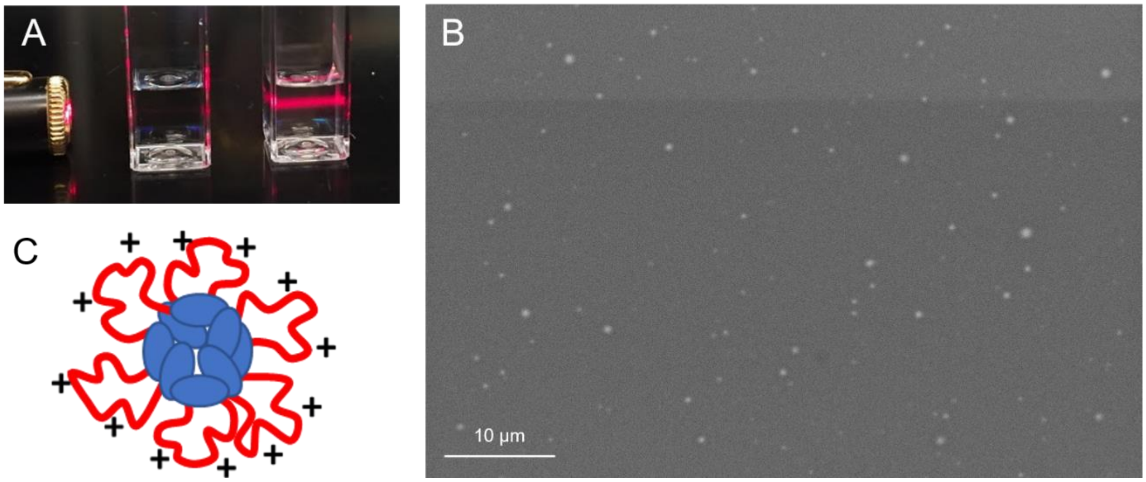

Figure 4.4 Polymer nanoparticle characterization. (A) An image of polymer P2 (n=6) in water (right) and filtered deionized water (left) against a laser. Only the polymer solution shows light scattering. (B) SEM image of the polymer micelles. The samples were prepared by drop-casting. (C) An illustration of the polymer micelle where the hydrophobic core is made of the steroidal rings and the cationic groups make the hydrophilic shell.

Dynamic light scattering (DLS) was used to measure the size of the micelles (Figure 4.5). The size of the micelles depend on the size of the linker amine. The polymer P2 formed smaller micelles (average diameter ~ 296 nm) while the polymer with shorter linker formed larger micelles (average diameter ~1000 nm). Micelles made from 24 h dialysis showed narrow dispersity while the ones made by redispersing the freeze-dried samples were broader in size distribution. This may be due to the shorter equilibration times allowed in the latter method. Given the smaller size of the nanoparticles polymer P2 was investigated more for the CMC, antimicrobial activity and drug loading capabilities. In addition, the average surface zeta potential of the micelles was about +64 mV.

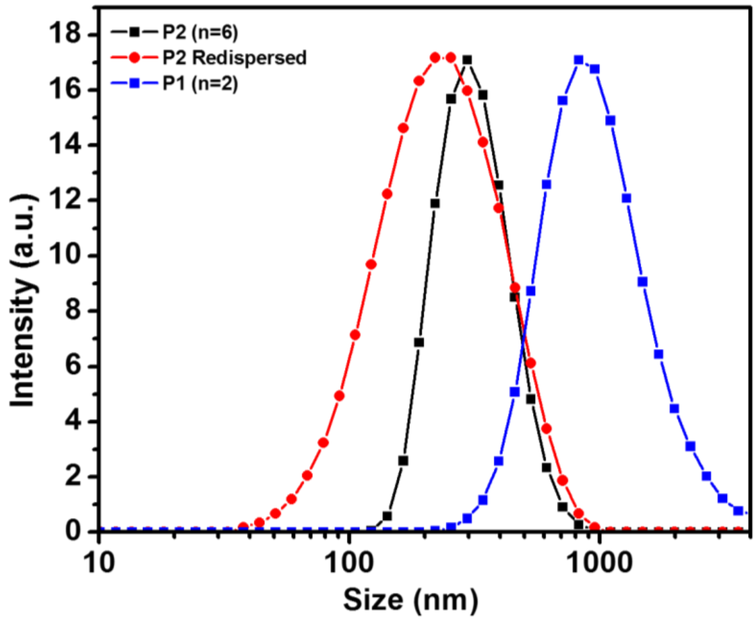

Figure 4.5 Polymer micelle characterization using DLS.

The CMC of the polymer P2 was measured using pyrene as a spatially sensitive floroscent probe. Pyrene florscence peak ratios at 372 nm (I1)and 391 nm (I3) can be used to probe the hydrophobicity of the environment (Figure 4.6). The concentration of pyrene was kept at 1×10^{-7} M to make sure excimer formation is avoided. The peak intensity at 391 nm increased significantly with increasing amount of polymer concentration indicating the partition of pyrene molecules into the hydrophobic core of the polymer micelles. The CMC for P2 was estimated to be 16.2 µg/mL. Such a low CMC value is useful to maintain the micellar morphology in dilute media used for antimcirobial applications.

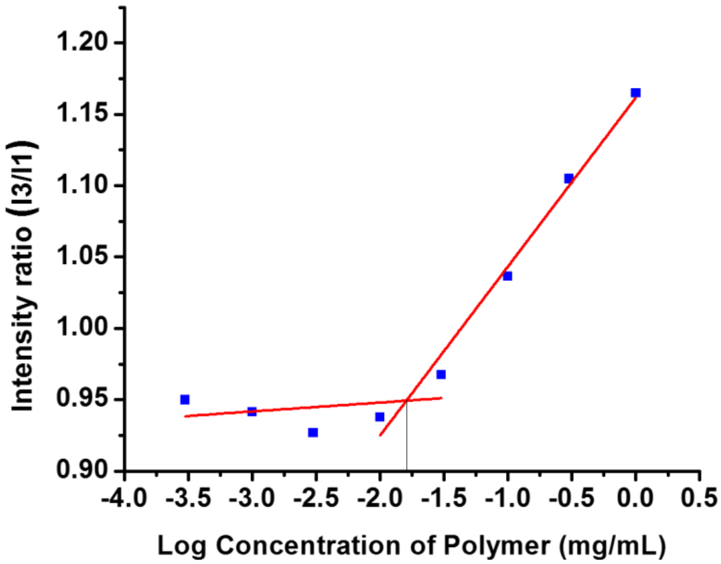

Figure 4.6 Polymer critical micellar concentration evaluation using pyrene as a probe.

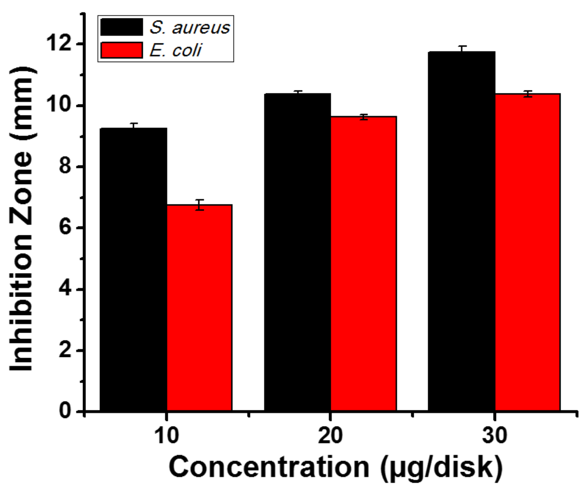

Figure 4.7 Antimicrobial activities of polymer P2. Inhibition zone measurements vs concentration (µg/disk).

The antimicrobial activity was evaluated using disk diffusion assays against Gram-positive *S. aureus* and Gram-negative *E. coli* (Figure 4.7). The starting lithocholic acid or the dibromide did not show any activity. Interestingly the micellar solutions show strong activity against both classes of bacterial at low concentrations demonstrating its broad-spectrum activity.

Low biocompatibility, poor bacterial cell penetration and unwanted side effects and susceptibility to microbial resistance mechanisms are some of the causes leading to the clinical failure of novel antibiotics. Polymeric micelles and other nano structures that can incorporate antibiotics as carriers are considered as a promising approach to address such issues. [25, 26] In this study, the antibiotic ampicillin was successfully loaded to polymer micelles via a dialysis method. As a demonstration of such capability, only a single initial loading was explored although more studies are in progress. Figure 4.8 shows the release profile of the drug under physiological conditions. The release profile indicated a sustained release. After 10 h period, the cumulative release reached to about 77 %. Such behavior shows that the hydrophobic drug molecules were encapsulated into the hydrophobic core of the polymer micelles.

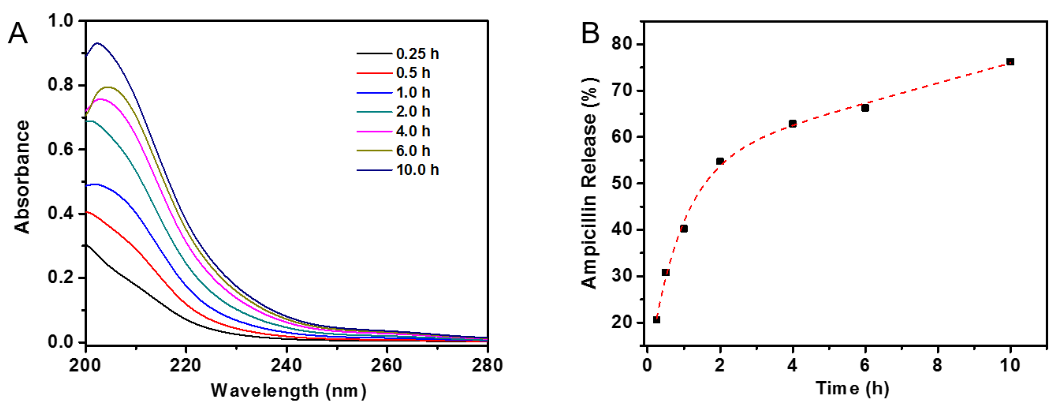

Figure 4.8 Release profile of the antibiotic ampicillin in PBS buffer at 37 ^{o}C. (A) UV-vis measurements. (B) Cumulative release profile.

4.5 Conclusions

In conclusion, main-chain quaternary ammonium containing antimicrobial polymers were developed using lithocholic acid as the hydrophobic structure. The synthesis involved only three simple steps that show the potential to be synthesized at large scale. The polymers formed micelles in aqueous media at low CMCs. The particles sizes can be controlled by varying the length of the amine linkers. These polymers showed prominent antimicrobial activities and show promise as broad-spectrum antimicrobial agents. It was demonstrated that the polymer micelles can incorporate hydrophobic drugs and release over long periods of time under physiological conditions. Additional research is needed to explore the drug loading capacity of the micelles and their dual functional antimicrobial activity as well as biocompatibility with mammalian cells.

4.6 References

1. Peleg , A. Y.; Hooper , D. C., Hospital-Acquired Infections Due to Gram-Negative Bacteria. *N. Engl. J. Med.* **2010,** *362*, 1804-1813.

2. Tamma, P. D.; Cosgrove, S. E.; Maragakis, L. L., Combination Therapy for Treatment of Infections with Gram-Negative Bacteria. *Clin. Microbiol. Rev.* **2012,** *25*, 450-470.

3. Denyer, S. P.; Maillard, J. Y., Cellular Impermeability and Uptake of Biocides and Antibiotics in Gram-Negative Bacteria. *J. Appl. Microbiol.* **2002,** *92*, 35S-45S.

4. Ganewatta, M. S.; Tang, C., Controlling Macromolecular Structures Towards Effective Antimicrobial Polymers. *Polymer* **2015,** *63*, A1-A29.

5. Wang, J.; Chen, Y. P.; Yao, K.; Wilbon, P. A.; Zhang, W.; Ren, L.; Zhou, J.; Nagarkatti, M.; Wang, C.; Chu, F.; He, X.; Decho, A. W.; Tang, C., Robust Antimicrobial Compounds and Polymers Derived from Natural Resin Acids. *Chem. Commun.* **2012,** *48*, 916-918.

6. Chen, Y.; Wilbon, P. A.; Chen, Y. P.; Zhou, J.; Nagarkatti, M.; Wang, C.; Chu, F.; Decho, A. W.; Tang, C., Amphipathic Antibacterial Agents Using Cationic Methacrylic Polymers with Natural Rosin as Pendant Group. *RSC Adv.* **2012,** *2*, 10275-10282.

7. Ganewatta, M. S.; Chen, Y. P.; Wang, J.; Zhou, J.; Ebalunode, J.; Nagarkatti, M.; Decho, A. W.; Tang, C., Bio-Inspired Resin Acid-Derived Materials as Anti-Bacterial Resistance Agents with Unexpected Activities. *Chem. Sci.* **2014,** *5*, 2011-2016.

8. Ganewatta, M. S.; Miller, K. P.; Singleton, S. P.; Mehrpouya-Bahrami, P.; Chen, Y. P.; Yan, Y.; Nagarkatti, M.; Nagarkatti, P.; Decho, A. W.; Tang, C., Antibacterial and Biofilm-Disrupting Coatings from Resin Acid-Derived Materials. *Biomacromolecules* **2015,** *16*, 3336-3344.

9. Patil, S.; Patil, S.; Gawali, S.; Shende, S.; Jadhav, S.; Basu, S., Novel Self-Assembled Lithocholic Acid Nanoparticles for Drug Delivery in Cancer. *RSC Adv.* **2013,** *3*, 19760-

19764.

10. Khatri, V. K.; Chahar, M.; Pavani, K.; Pandey, P. S., Bile Acid-Based Cyclic Bisbenzimidazolium Receptors for Anion Recognition: Highly Improved Receptors for Fluoride and Chloride Ions. *J. Org. Chem.* **2007,** *72*, 10224-10226.

11. Pal, A.; Basit, H.; Sen, S.; Aswal, V. K.; Bhattacharya, S., Structure and Properties of Two Component Hydrogels Comprising Lithocholic Acid and Organic Amines. *J. Mater. Chem.* **2009,** *19*, 4325-4334.

12. Ye, W.; Li, Y.; Zhou, Z.; Wang, X.; Yao, J.; Liu, J.; Wang, C., Synthesis and Antibacterial Activity of New Long-Chain-Alkyl Bile Acid-Based Amphiphiles. *Bioorg. Chem.* **2013,** *51*, 1-7.

13. do Nascimento, P. G. G.; Lemos, T. L. G.; Almeida, M. C. S.; de Souza, J. M. O.; Bizerra, A. M. C.; Santiago, G. M. P.; da Costa, J. G. M.; Coutinho, H. D. M., Lithocholic Acid and Derivatives: Antibacterial Activity. *Steroids* **2015,** *104*, 8-15.

14. Hofmann, A. F., Bile Acids: Trying to Understand Their Chemistry and Biology with the Hope of Helping Patients. *Hepatology* **2009,** *49*, 1403-1418.

15. Singh, M.; Singh, A.; Kundu, S.; Bansal, S.; Bajaj, A., Deciphering the Role of Charge, Hydration, and Hydrophobicity for Cytotoxic Activities and Membrane Interactions of Bile Acid Based Facial Amphiphiles. *Biochim. Biophys. Acta* **2013,** *1828*, 1926-1937.

16. Li, Y.; Dias, J. R., Dimeric and Oligomeric Steroids. *Chem. Rev.* **1997,** *97*, 283-304.

17. Cunningham, A. J.; Zhu, X. X., Polymers Made of Bile Acids: From Soft to Hard Biomaterials. *Can. J. Chem.* **2016,** *94*, 659-666.

18. Zhu, X.-X.; Nichifor, M., Polymeric Materials Containing Bile Acids. *Acc. Chem. Res.* **2002,** *35*, 539-546.

19. Zhang, M.; Teo, J. J.; Liu, S.; Liang, Z. C.; Ding, X.; Ono, R. J.; Breyta, G.; Engler, A. C.; Coady, D. J.; Garcia, J., Simple and Cost-Effective Polycondensation Routes to Antimicrobial Consumer Products. *Polym. Chem.* **2016,** *7*, 3923-3932.

20. Casson, D.; Rembaum, A., Solution Properties of Novel Polyelectrolytes. *Macromolecules* **1972,** *5*, 75-81.

21. Abboud, J.-u. M.; Notario, R.; Bertrán, J.; Solà, M., One Century of Physical Organic Chemistry: The Menshutkin Reaction. In *Progress in Physical Organic Chemistry*, John Wiley & Sons, Inc.: 2007; pp 1-182.

22. Liu, S.; Ono, R. J.; Wu, H.; Teo, J. Y.; Liang, Z. C.; Xu, K.; Zhang, M.; Zhong, G.; Tan, J. P. K.; Ng, M.; Yang, C.; Chan, J.; Ji, Z.; Bao, C.; Kumar, K.; Gao, S.; Lee, A.; Fevre, M.; Dong, H.; Ying, J. Y.; Li, L.; Fan, W.; Hedrick, J. L.; Yang, Y. Y., Highly

Potent Antimicrobial Polyionenes with Rapid Killing Kinetics, Skin Biocompatibility and In vivo Bactericidal Activity. *Biomaterials* **2017,** *127*, 36-48.

23. Strassburg, A.; Kracke, F.; Wenners, J.; Jemeljanova, A.; Kuepper, J.; Petersen, H.; Tiller, J. C., Nontoxic, Hydrophilic Cationic Polymers—Identified as Class of Antimicrobial Polymers. *Macromol. Biosci.* **2015,** *15*, 1710-1723.

24. Liu, L.; Venkatraman, S. S.; Yang, Y.-Y.; Guo, K.; Lu, J.; He, B.; Moochhala, S.; Kan, L., Polymeric Micelles Anchored with Tat for Delivery of Antibiotics across the Blood–Brain Barrier. *Biopolymers* **2008,** *90*, 617-623.

25. Xiong, M.-H.; Bao, Y.; Yang, X.-Z.; Zhu, Y.-H.; Wang, J., Delivery of Antibiotics with Polymeric Particles. *Adv. Drug Del. Rev.* **2014,** *78*, 63-76.

26. Stebbins, N. D.; Ouimet, M. A.; Uhrich, K. E., Antibiotic-Containing Polymers for Localized, Sustained Drug Delivery. *Adv. Drug Del. Rev.* **2014,** *78*, 77-87.

CHAPTER 5

BIOBASED PLASTICS AND ELASTOMERS FROM RENEWABLE ROSIN VIA "LIVING" RING-OPENING METATHESIS POLYMERIZATION[5]

[5] Ganewatta, M. S.; Ding, W.; Rahman, M. A.; Yuan, L.; Wang, Z.; Hamidi, N.; Robertson, M. L.; Tang, C., Biobased Plastics and Elastomers from Renewable Rosin Via "Living" Ring-Opening Metathesis Polymerization. *Macromolecules* **2016**, *49*, 7155-7164. Reprinted here with permission. Copyright (2016) American Chemical Society.

5.1 Abstract

Utilization of biomass for commodity polymers has gained tremendous interest. We report a method to prepare high molecular weight renewable homopolymers and block copolymers derived from natural rosin. Monomers with high renewable content (70 wt %) were prepared via a simple esterification reaction between dehydroabietic alcohol and 5-*exo*-norbornene carboxylic acid. Living and controlled polymerization of these monomers were achieved by ring-opening metathesis polymerization (ROMP) to obtain polymers with molecular weight up to ~500 kg/mol. These homopolymers exhibit structure-dependent glass transition temperatures, excellent thermal stabilities and thermoplastic properties. Chain entanglement molecular weight was determined via rheological assessments for such polymers with bulky side moieties. Using the living ROMP, dehydroabietic-based homopolymer was chain-extended with a soybean oil-derived norbornene monomer to yield triblock copolymers, which show behaviors of thermoplastic elastomers.

5.2 Introduction

With the decline of fossil reserves and aggravated change of environmental conditions, there is a remarkable interest in both academia and industry for generating a leap towards sustainable materials derived from renewable biomass feedstock.[1-3] Therefore, the development of sustainable chemicals and polymers from biomass has witnessed a sharp increase during the past decade.[4, 5] Incorporation of sustainable polymers in commodity applications steadily increases in the pursuit of a biobased polymer market.[6, 7] However, there is some divergence between sustainable polymers and petroleum-derived counterparts in terms of relative cost and performance that should be addressed to meet the current market demands.[8]

Non-food biomass derived chemicals are more appealing as building blocks for polymers.[9] Especially, chemicals from forestry products such as lignin,[10, 11] cellulose[12] and rosin[13] are of more interest due to their wide abundance and low-cost. Rosin is produced by conifer trees, especially pine tree as a defense against herbivore and pathogen attacks.[14] Rosin based materials are used for decades as adhesives, paints and coatings, inks, soaps and detergents, lubricants, fuel additives, and food additives. Rosin consists of several resin acids (or rosin acids) such as abietic, dehydroabietic, palustric, pimaric and neoabietic acid. The worldwide production of rosin is more than 1 million metric tons per year.[13] Resin acids are obtained by several sources such as gum rosin that is the exudate of wounded pine trees, or tall oil rosin via fractionation of crude tall oil from the Kraft pulping process or wood rosin by extracting pines tree stumps.[13]

Over the past few years, several research groups including ours have produced a variety of well-defined polymeric materials based on resin acids.[13, 15, 16] We have prepared various types of rosin acid-containing sustainable polymers via techniques such as ATRP, ROP, and ADMET.[17-21] Polymers with cationically modified resin acids were developed as effective antimicrobial biomaterials.[22-25] Sacripante et al. reported the synthesis of polyester resins from dehydroabietic acid.[26] In addition, Cramil et al. studied the cationic dimerization of abietic acid to design polymers by ADMET.[27] However, in all cases it is challenging to obtain high molecular weight homopolymers (>50 kg/mol) that contain resin acids, largely due to the unfavorable steric influence by the bulky tricyclic structure. The presence of bulky hydrophenanthrene structure significantly increases chain entanglement molecular weight to a degree not achievable via the reported strategies. Therefore, mechanically robust and ductile polymer products have not been reported from these resin acids.

Synthesis of unsaturated polymers from cycloolefins via ROMP has made a great impact on polymer science.[28] Monomers having considerable ring strain such as norbornene, cyclopentene, and cyclooctene have been demonstrated to undergo ROMP.[29] Renewable cyclic molecules such as caryophyllene, humulene[30] and apopinene[31] are found to undergo ROMP to produce polyterpenes. However, resin acids require additional functionality that has enough ring strain to undergo metathesis. Herein, we report a robust method to synthesize high molecular weight (HMW) resin acid-derived norbornene polymers which contain up to 70 wt. % of renewable biomass via controlled and living ring-opening metathesis polymerization (ROMP). The living polymerization was demonstrated by kinetic studies as well as by the successful chain extension to prepare triblock copolymers. The fibrous polymers have high glass transition temperatures (T_g), impressive mechanical properties and thermal stability. Furthermore, the chain entanglement molecular weight was, for the first time, investigated using rheological measurements.

Biobased building blocks for the design of sustainable block copolymers has become a hot topic in thermoplastic elastomer (TPE) research.[32] Renewable biomass and their derivatives including lactide,[33, 34] plant oils,[35, 36] methinide,[37] ε-caprolactone,[38] ε-decalactone,[39] isosorbide,[40] glucose,[41] vanillin[42, 43] are used to make TPEs. The ability of the high T_g resin acid blocks to serve as rigid domains for TPE applications is also explored in this work.

5.3 Experimental section

Materials

Dehydroabietic acid (DHAA, ~90%) was obtained from Wuzhou Chemicals, China and used as received. Lithium aluminum hydride (95%, Aldrich), *exo*-5-norbornenecarboxylic acid (97%, Aldrich), Hoveyda-Grubbs catalyst 2nd generation (HG2, 97%, Aldrich), trimethylacetic anhydride (99%, Aldrich), 4-dimethylaminopyridine (DMAP, 99%, Aldrich), ethanolamine (99%, Aldrich), 3-amino-1-propanol (99%, Aldrich), methacrylic anhydride (94%, Aldrich), triethylamine (TEA, 99%, Alfa Aesar), 3-chloroperbenzoic acid (mCPBA, 70 − 75%, Alfa Aesar), were used as received. Grubbs catalyst 3rd generation (G3) was synthesized following a procedure reported in literature.[44] Soybean oil-containing monomer (M3) was prepared following our previous report.[45] Dichloromethane (DCM) was dried over drying columns. All other reagents were from commercial resources and used as received unless otherwise mentioned.

Molecular Characterization

Nuclear magnetic resonance (^{1}H NMR and ^{13}C NMR) experiments were performed on a Bruker Avance III HD 300 using deuterated chloroform as the solvent. The Fourier transform infrared spectrometry (FTIR) spectra were taken on a PerkinElmer spectrum 100 FTIR spectrometer. Mass spectrometry was conducted on a Waters Micromass Q-Tof mass spectrometer. Molecular weight and molecular weight distribution of polymers were determined using a gel permeation chromatography (GPC) equipped with a Waters 1525 Binary Pump, three Styragel columns and a Waters 2414 Refractive Index (RI) detector. HPLC grade THF solvent was used as eluent at 35 °C with a flow rate of 1.0 mL/min. The system was calibrated with narrow dispersed polystyrene standards obtained from Polymer

Laboratories. GPC samples were prepared by dissolving the polymer in THF at a concentration of 3-5 mg/mL and passing through PTFE micro filters with average pore size of 0.2 μ m. The injection volume was 50 μL. Absolute molecular weight determination was carried out using light scattering measurements similar to our earlier report.[46]

Thermal, Mechanical and Rheological Properties

Glass transition temperature (T_g) of polymers was characterized by a TA Instruments Q2000 differential scanning calorimeter (DSC) calibrated for temperature with an indium standard. About 10 mg of each sample was used for the DSC test with a nitrogen flow rate at 50 mL/min. Samples were heated from -50 °C to 200 °C at a rate of 10 °C /min and cooled down to -50 °C at the same rate. The data were collected from the second heating scan. The thermal degradation properties were investigated by thermogravimetric analysis (TGA), using TA Instruments Q5000 TGA system. The sample (~10 mg) was heated from room temperature to 150 °C at a rate of 10 °C/min under nitrogen and kept at 150 °C for 10 min. The balance purge flow was kept at 10.0 mL/min and the sample purge flow was 25 mL/min. Then the sample was cooled to 30 °C and heated to 800 °C at the same rate. Tensile stress-strain testing was carried out with an Instron 5543A testing instrument. The films were prepared by dissolving ~750 mg polymer in THF, centrifugation at 5000 rpm to remove any particles and casting the THF solution in a PTFE mold. After the evaporation of solvent, the film was kept under vacuum for 18 hours at room temperature, 12 hours at 60 °C under nitrogen and 12 hours at 60 °C under vacuum. The dog-bone shape films with a width of 5 mm and a length of 22 mm were tested at room temperature with the crosshead speed of 5 mm/mm for thermoplastics and 20 mm/min for thermoplastic elastomers. The cyclic tensile deformation was conducted stepwise up to 100%

strain. In a typical cycle, when the sample reached 100% strain, the crosshead direction was reversed and the strain was decreased at the same rate until stress was reached to zero. Entanglement molecular weight of the polymer was characterized through measurement of frequency-dependencies of the dynamic moduli (G', G") using a TA Instruments DHR-2 rheometer. A polymer was compression molded at 130 °C into a 25 mm disk using an evacuable pellet die. The disk was then placed between 25 mm parallel plates, and heated up to 130 °C. The linear region was firstly determined by a strain sweep from 0.1% to 10% at a frequency of 10 rad/s. A frequency sweep was then performed within the linear region from 0.1 rad/s to 100 rad/s. The strain sweep and frequency sweep were performed every 10 °C from 130 °C to 230 °C. The master curve was then obtained by time-temperature superposition at a reference temperature of 180 °C.

Morphological Characterization

Atomic force microscopy (AFM) was performed using a Multimode Nanoscope V system (Bruker, Santa Barbara, CA). Tapping mode AFM was used to map the topography by tapping the surface using an oscillating tip. The measurements were performed using commercial Si cantilevers with a nominal spring constant and resonance frequency at 20–80 N m^{-1} and 230–410 kHz, respectively (TESP, Bruker AFM Probes, Santa Barbara, CA). Small-angle X-ray scattering (SAXS) experiment of bulk samples were conducted using SAXS LAB Ganesha at the South Carolina SAXS Collaborative of the University of South Carolina. A Xenocs GeniX3D microfocus source and a copper target were used to generate a monochromic beam with a 0.154 nm wavelength. The instrument was calibrated using a silver behenate reference with the first order scattering vector $q^* = 1.076$ nm^{-1}, where q =

$4\pi\lambda^{-1}$ sin θ and a total scattering angle of 2θ. The data were collected for 1 hour in the transmission mode with an incident X-ray flux of ~1.5 M photons/s.

Density Measurement

The polymer was dissolved in dichloromethane and cast on a microscope slide. The sample was air-dried for several hours and then dried under vacuum at 120 °C overnight to remove all solvents and air within the sample. Two solutions were prepared: 1) an aqueous sodium chloride solution (24 wt% sodium chloride) and 2) a methanol/water solution (35% vol% methanol). A tall graduated glass column was placed in a water bath maintained at 23 °C. A density gradient of the two solutions was created within the column. The prepared column was stabilized in the water bath overnight prior to use. Calibration beads of known density were placed in the column to generate a density-height calibration curve. Finally, the degassed polymer was placed in the column and the density was determined using density-height calibration curve, after equilibration for 1-2 days. Measurements on three separate specimens were taken to ensure reproducibility.

Synthesis of Dehydroabietane-18-ol (1)

Dehydroabietic acid (15.0 g, 0.05 mol, 1.0 equiv.) was dissolved in anhydrous THF (50 mL) in a round-bottom flask and kept in an ice bath at 0 °C. Then $LiAlH_4$ powder (5.9 g, 0.15 mol, 3.0 equiv.)) was added to the THF solution slowly and carefully. It was stirred at room temperature for 30 min and later keep under reflux for 12 h. Then the reaction flask was kept in an ice bath and quenched with 10 % HCl. The THF was removed by rotary evaporation and the product was extracted with DCM 3 times, washed with $NaHCO_3$ and brine. After drying with anhydrous $MgSO_4$, the solvent was removed by rotary evaporation and vacuum dried to obtain a viscous colorless product 12.0 g (yield = 84%). ^{1}H NMR (300

MHz, CDCl3, δ (ppm)): 7.18 (d, *J* = 8.2 Hz, 1H; Ar), 6.99 (d, *J* = 8.1 Hz, 1H; Ar), 6.89 (s, 1H; Ar), 3.36 (ddd, J = 97.5, 10.9, 5.3 Hz, 2H; C*H*$_2$OH), 2.96-2.82 (br, 2H; C*H*$_2$Ar), 2.88-2.75 (m, 2H; ArC*H*(CH_3)$_2$), 2.29 (m, 1H; CC*H*C), 0.89 (s, 3H; CC*H*$_3$). ^{13}C NMR (75 MHz, $CDCl_3$, δ (ppm)): 147.35, 145.55, 134.79, 126.83, 124.27, 123.82, 72.26, 43.95, 38.47, 37.86, 37.36, 35.13, 33.48, 30.14, 25.32, 24.04, 18.89, 18.68, 17.43. MS (EI), m/z calc. 286.2297; obs. 286.2296.

Synthesis of Dehydroabietanyl Norborn-5-ene-2-carboxylate (M1)

A typical synthetic procedure included the following steps. Reduced dehydroabietic acid (1) (1.0 g, 3.5 mmol, 1 equiv.) was dissolved in anhydrous THF (15 mL). It was added with *exo*-5-norbornene carboxylic acid (532 mg, 3.85 mmol, 1.1 equiv.), trimethylacetic anhydride (731 mg, 3.85 mmol, 1.1 equiv.) and 4-dimethylaminopyridine (DMAP) (4.3 mg, 0.035 mmol, 0.01 equiv.). The round bottom flask was purged with nitrogen for 10 min and kept stirring at 60 °C for 24 h. Afterwards, 1 mL of water was added and stirred 15 min at 60 °C to quench the remaining anhydride. The workup step involved the removal of THF by rotary evaporation, washing with a saturated solution of $NaHCO_3$ twice, brine once, drying the DCM layer with anhydrous $MgSO_4$, and rotary evaporation of solvent to obtain the partially pure product. Further purification was carried out by column chromatography (silica gel, eluent: hexane: ethyl acetate, 9.5:0.5) to yield the pure product as a viscous oil 1.2 g (yield = 85%). ^{1}H NMR (300 MHz, CDCl3, δ (ppm)): 7.19 (d, *J* = 8.2 Hz, 1H; Ar), 7.00 (d, *J* = 8.2 Hz, 1H; Ar), 6.90 (s, 1H; Ar), 6.20 – 5.98 (m, 2H; C*H*C*H*), 3.85 (ddd, *J* = 18.5, 11.0, 7.1 Hz, 2H; C*H*$_2$O), 3.01 (s, 1H; COCHC*H*), 2.96-2.72 (m, 4H; C*H*$_2$Ar, ArC*H*(CH_3)$_2$), CH_2C*H*CH), 2.29 (m, 1H; CC*H*C), 2.22 (dd, *J* = 9.3, 4.2 Hz, 1H; COC*H*), 0.96 (s, 3H; ArCC*H*$_3$). MS (EI), m/z calc. 406.2872; obs. 406.2870.

Synthesis of 4'-Hydroxybutyl Dehydroabietate (2)

Dehydroabietic acid (5 g, 0.017 mol, 1.0 equiv.) in a round bottom flask was kept in an ice bath. Then 10 mL $SOCl_2$ (excess) was added slowly to the flask. While stirring, it was added with two drops of dry DMF. After 30 min, the reaction flask was fixed with a condenser and kept under reflux for 3 h. Excess $SOCl_2$ was removed by rotary evaporation, redissolved in anhydrous DCM and transferred to a flask containing 1,4-butanediol (3.0 g, 0.050 mol, 3.0 equiv.) and triethylamine (5.1 g, 0.050 mol, 3 equiv.) at 0 °C. Then it was heated to 40 °C for 18 h. To purify the product, the crude mixture was washed with a saturated solution of $NaHCO_3$, water and brine. Later, the organic layer was dried with anhydrous $MgSO_4$. After removal of the solvent a viscous pale yellow product was obtained (yield = 73 %) ^{1}H NMR (300 MHz, $CDCl_3$, δ (ppm)): 7.18 (d, J = 8.2 Hz, 1H; Ar), 7.01 (d, J = 8.2 Hz, 1H; Ar), 6.89 (s, 1H; Ar), 4.18-4.02 (m, 2H; COCH_2), 3.67 (t, J = 6.2 Hz, 2H; CH_2OH), 3.01 (s, 1H; COCHC*H*), 2.96-2.73 (m, 3H; CH_2Ar, ArC*H*(CH_3)$_2$)), 2.27 (m, 1H; CCH_2). MS (EI), m/z calc. 372.2664; obs. 372.2669.

Synthesis of 4-((Norborn-5-ene-2-carbonyl)oxy)butyl Dehydroabietate (M2)

A similar protocol to the synthesis of HBDA was followed here. *exo*-5-norbornene carboxylic acid and HBDA was used as the reactants. For the purification after extraction, column chromatography (silica gel, eluent: hexane: dichloromethane, 1:1) was used. (yield = 82 %) ^{1}H NMR (300 MHz, CDCl3, δ (ppm)): 7.19 (d, J = 8.2 Hz, 1H; Ar), 7.01 (d, J = 8.2 Hz, 1H; Ar), 6.88 (s, 1H; Ar), 6.27 – 6.01 (m, 2H; C*H*C*H*), 4.10 (p, J = 11.0 Hz, 4H; 2xCOCH_2), 3.01 (s, 1H; COCHC*H*), 2.96-2.74 (m, 4H; CH_2Ar, ArC*H*(CH_3)$_2$), CH_2C*H*CHCH), 2.36-2.17 (m, 3H; COC*H*, C*H*HCC*H*C). MS (EI), m/z calc. 492.3240; obs. 492.3236.

Synthesis of Polymers P1 and P2 by ROMP

Polymers were synthesized using G3 or HG2 catalysts. A typical procedure for the synthesis of a polymer with a monomer to catalyst ratio 250:1 is as follows. Catalyst HG2 (6.19 mg, 9.85 mmol, 1 equiv.) was dissolved in 4.0 mL of anhydrous DCM in a round bottom flask under nitrogen. The monomer M1 (1.0 g, 2.46 mmol, 250 equiv.) was dissolved in 16 mL of DCM. The monomer was cannula-transferred into the catalyst under vigorous stirring of the catalyst solution. After confirming the complete conversion using ^{1}H NMR, the reaction was quenched with 1 mL ethyl vinyl ether (EVE). The polymer solution was concentrated about two times and precipitated into methanol twice. Then it was vacuum dried to obtain the product.

Kinetic Study of ROMP of Monomer M1

The living and controlled polymerization of M1 was studied. Investigation of the time and conversion to develop semilogarithmic plots was carried out as following. M1 (200 mg, 0.49 mmol, 250 equiv.) was dissolved in anhydrous DCM at room temperature and transferred to a solution of G3 catalyst (1.43 mg, 0.002 mmol, 1 equiv.) at a final monomer concentration of 50 mg/mL. Samples were taken out at 1 min intervals into a vial containing 0.5 mL of EVE to terminate the polymerization. The conversion of monomer was calculated by comparing integration of the norbornene double bond peak (~6.0 ppm) to aromatic proton peak (~6.9 ppm). Several polymerizations with different molar feed ratio of monomer to catalyst were conducted to explore the controlled behavior. G3 catalyst was also used for this experiment similar to the protocol as mentioned above. All polymerizations led to >99 % conversion after about 45 min. The degree of polymerization was calculated from the molecular weight obtained via GPC. Living polymerization was demonstrated via a chain extension of a polymer that was not quenched. In this experiment the polymerization was conducted using G3 catalyst and a monomer to catalyst ratio of 125:1 was used. M1 (51 mg, 0.126 mmol, 125 equiv.) was dissolved in anhydrous DCM at room temperature and transferred to a solution of G3 catalyst (0.73 mg, 0.001 mmol, 1 equiv.). The complete consumption of monomer was confirmed by ^{1}H NMR. Then additional amount of monomer (51 mg) dissolved in DCM was transferred to the same reaction flask. After 1 h, EVE was added to quench the reaction. Samples were analyzed using GPC and ^{1}H NMR.

Hydrogenation of P1 to Obtain P3

The hydrogenation was carried out using *p*-toluenesulfonyl hydrazide (TSH). In a typical experiment, 6 mol equivalent of TSH was used to make sure the complete reduction of homopolymer. However, it should be noted that the aromaticity remains intact throughout the reduction procedure. A representative experiment is outlined here. P1 homopolymer (1.0 g, 2.46 mmol double bonds, 1.0 equiv.) was dissolved in 20 mL of anhydrous toluene. Then, TSH (2.75 g, 14.78 mmol, 6.0 equiv.) and triethylamine (2.0 g, 19.8 mmol, 8.0 equiv.) were transferred. The flask was connected to a reflux condenser and kept under nitrogen. The flask was placed in an oil bath set at 120 °C and kept under vigorous stirring for 6 hours. After confirming the conversion by ^{1}H NMR, the reaction was stopped by cooling to room temperature. The polymer was recovered by precipitating the concentrated reaction mixture in methanol twice. A white fibrous material was obtained (yield = 96%).

Synthesis of Triblock Copolymers (P4-P11)

Triblock copolymers were synthesized following a similar procedure to the homopolymer preparation. However, sequential monomer addition was used before quenching the reaction. In a typical experiment, appropriate amount of catalyst (G3) was dissolved in dry DCM under nitrogen. Then monomer M1 in DCM (<50 mg/mL) was transferred to the catalyst. After 1 h, an adequate amount of sample was taken out for NMR and GPC characterizations. Next, soybean oil monomer M3 was transferred to the polymerization system. Similarly, the third block was also made using M1. Finally, the reaction was quenched using EVE and the polymer was purified by precipitation into methanol. The composition of each polymer was confirmed by ^{1}H NMR and GPC.

Thin film Preparation and AFM

Thin films were prepared by spin-coating a 2 mg/mL THF solution of triblock copolymers onto oxidized silicon wafer (100 nm thick thermal oxide) at 1500 rpm. The silicon wafers were cleaned using ethanol and then plasma cleaning. The thin films were annealed at room temperature for 24 hours under THF solvent chamber. Atomic force microscopy (AFM) was accomplished using a Multimode Nanoscope V system (Bruker, Santa Barbara, CA) in tapping mode.

5.4 Results and Discussion

Synthesis of Monomers and Polymers

We used widely available dehydroabietic acid (DHAA) as a substrate to prepare norbornene-containing monomers. Two monomers were prepared where the first monomer dehydroabietanyl norborn-5-ene-2-carboxylate (M1) is a direct combination of reduced DHAA and *exo*-5-norbornene carboxylic acid, and the second monomer 4-((norborn-5-

ene-2-carbonyl)oxy)butyl dehydroabietate (M2) has 1,4-butanediol as the spacer (Figure 5.1). This spacer is used to vary the steric effect between the polymer backbone and the bulky multicyclic side-group. Such modifications can be used to finely tune thermal (e.g., T_g) and mechanical properties.

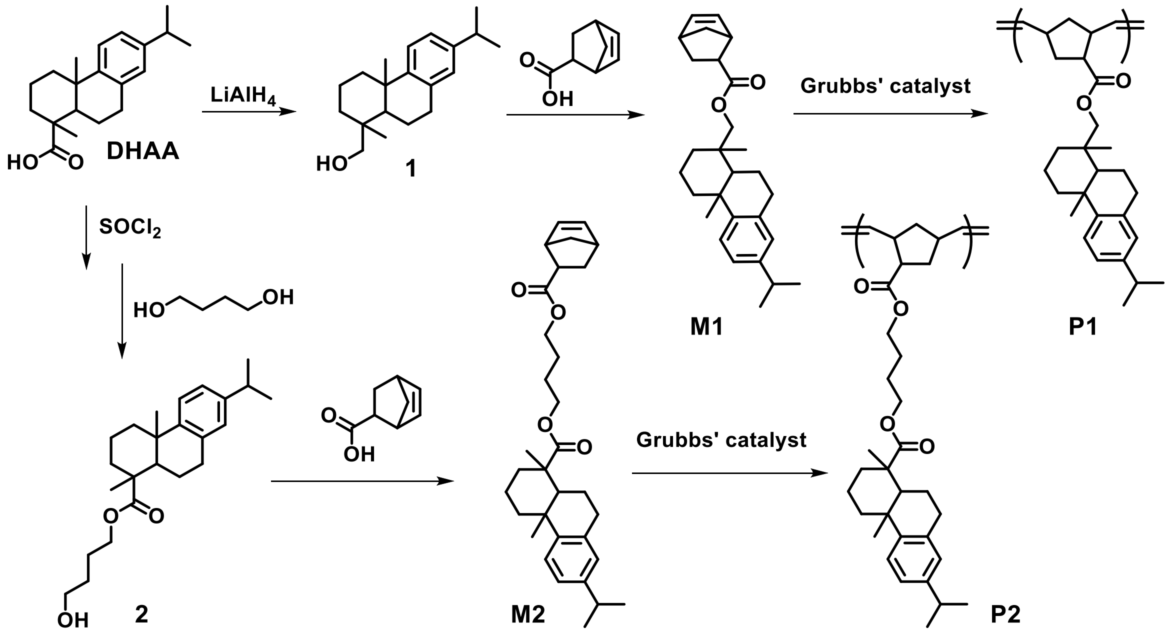

Figure 5.1 Synthesis of dehydroabietic-containing norbornene monomers M1 and M2 and their polymers P1 and P2.

The structures of both monomers were confirmed by ^1H NMR, ^{13}C NMR, IR and mass spectra. Figure 5.2A and 5.2B illustrates the ^1H NMR spectra of the monomers that unambiguously show the high purity as confirmed by the chemical shifts of aromatic, alkene and methylene protons that correlate with the DHAA, norbornene, the spacer group respectively. For example, in Figure 5.2A the three sharp peaks around 6.80-7.20 ppm correspond to the aromatic protons on the rosin moiety. The double bond in norbornene appears at 6.10 ppm. The peaks for the methylene protons next to the ester bond in M1 at 3.70-4.10 ppm shows splitting due to restricted rotation at the neighboring quaternary carbon. In addition, IR spectra showed the formation of esters bonds (C=O peak at 1715 cm^{-1}, C-O peak at 1150 cm^{-1}) and the disappearance of the broad carboxylic peak at 2500-3300 cm^{-1}.

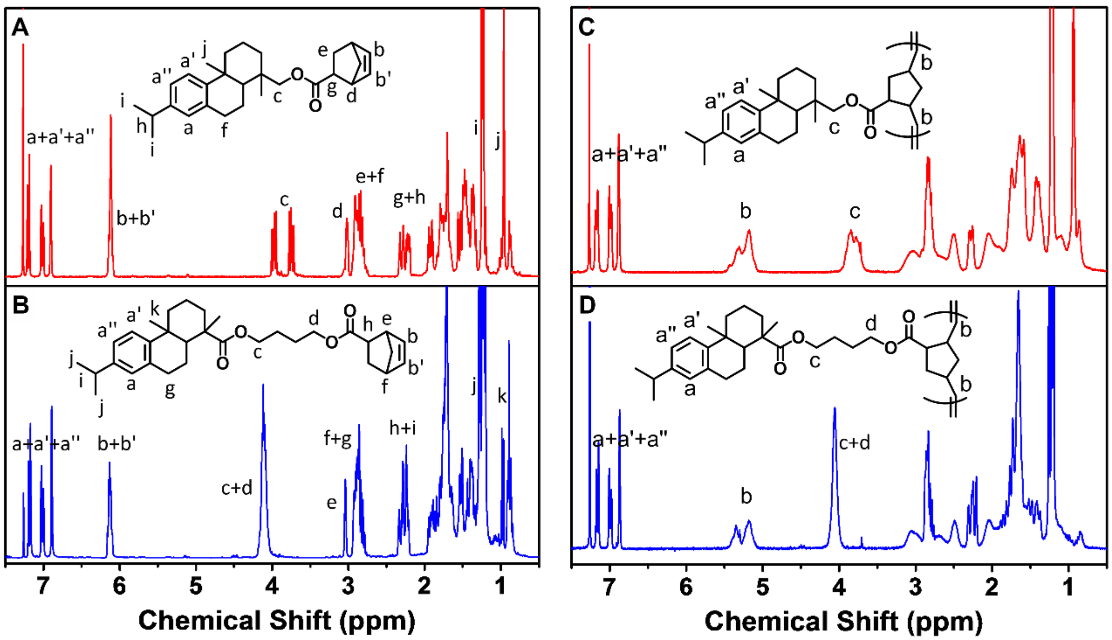

Figure 5.2 ^{1}H NMR spectra of monomers and polymers. (A) Rosin acid derived monomer M1. (B) Monomer with a spacer M2. (C) Homopolymer P1. (D) Homopolymer P2.

The polymerization was carried out using Grubbs' third generation catalyst (G3) or Hoveyda-Grubbs' second generation catalyst (HG2) to achieve complete monomer conversion and high polymer yields in very short periods of time. The full conversion (>99 %) was confirmed using the disappearance of the ^{1}H NMR peak at 6.10 ppm of monomers. Figure 5.2C and 5.2D illustrates the ^{1}H NMR spectrum of homopolymer P1 and P2. There are two overlapping broad peaks at 4.98-5.42 ppm which correspond to the cis and trans double bonds on the polymer backbone. It should be noted that polymers with high molecular weight even up to ~500 kg/mol can be prepared by adjusting ratio of monomer to catalyst. These HMW polymers appear to be fibrous and white color. The polymer made with a ratio of monomer to catalyst at 1250:1 has a relative molecular weight M_n = 396 kg/mol and $Đ$ = 1.79 in the Gel Permeation Chromatography (GPC) with a RI detector and calibrated with polystyrene standards. However, with a light scattering detector, M_n was found to be 594 ± 7 kg/mol which is close to the theoretical molecular weight. When preparing HMW homopolymers, HG2 catalyst resulted in higher dispersity compared to G3 catalyst.

The double bonds in the norbornene polymer backbone are prone to thermo-oxidative degradation that may discolor and crosslink polymers, although the polymers made in this study did not show color changes nor become insoluble during storage at ambient conditions. This potential problem can be overcome by hydrogenation of such polymers.[47] Typically, hydrogenation of unsaturated polymers enhances their thermal stability and durability. Diimide hydrogenation offers an efficient and robust route to remove the unsaturation of polymers.[48-50] Thermal decomposition of *p*-toluenesulfonyl hydrazide, which was used in this work, generated diimide reducing agent in situ, that efficiently reduced the unsaturated backbone of polymer. Hydrogenation of homopolymer P1 resulted in P3 with a similar physical appearance. The alkene protons in the ^{1}H NMR spectrum at 4.98-5.42 ppm completely disappeared, indicating the complete hydrogenation.

Thermal properties of resultant polymers were characterized using differential scanning calorimetry (DSC) and thermogravimetric analysis (TGA). As expected, all the homopolymers in this study are amorphous and exhibit only a T_g without any melting temperature. Interestingly, P1 has an exceedingly higher T_g (110 °C) (Figure 5.8A), compared to polynorbornene T_g (~45 °C) and a resin acid containing methacrylate polymer we reported earlier that has a T_g ~90 °C.[17] Also norbornene polymers with linear pendant stearic acid showed T_g -32 °C.[51] This may be attributed to the rigid multicyclic pendent rosin group in close proximity to the unsaturated polymer backbone. This steric strain was relieved when the rosin group was placed further away from the backbone as the T_g of P2 appeared at 55 °C.

Table 5.1 Homopolymer synthesis and characterizations.

Polymer	Molar ratio^a	Conversion^b (%)	$M_n{}^c$ (kg/mol)	$Đ^c$	$T_g{}^d$ (°C)	$T_d{}^e$(°C)
P1	1250:1	> 99	396	1.79	110	421
P2	200:1	> 99	136	1.96	55	362
P3	1250:1	> 99	384	1.87	85	431

^{a}Molar ratio: monomer:catalyst(HG2). ^{b}Measured by ^{1}H NMR. ^{c}Relative molecular weight measured by GPC with refractive index detector and calibrated with polystyrene standards. ^{d}Measured by DSC. ^{e}Decomposition temperature at 10 wt. % loss determined by TGA.

Hydrogenation improves the chain motion and thus lowers the T_g, as demonstrated by P3 (T_g = 85 °C). However, a melting temperature, which is typically present for hydrogenated polynorbornene,[52] was not observed in the rosin-based polymers. These polymers were heated under a continuous flow of nitrogen to investigate the thermal resistance (Table 5.1). Hydrogenated polymer P3 showed enhanced thermal stability compared to unsaturated polymer P1. In contrast, P2 decomposed at a much lower temperature. The presence of two ester bonds in the repeating unit may be the reason.

Controlled and Living ROMP

The controlled and living polymerization was examined using several kinetic experiments. The polymerization reactions were conducted utilizing the G3 catalyst which showed very rapid conversion (>90% within five minutes). First, a kinetic study of polymerization of M1 was carried out. The monomer conversions were calculated by comparing ^{1}H NMR signals of vinyl protons and aromatic protons of M1. The semilogarithmic plot (Figure 5.3A) shows a linear relationship between the reaction time and $\ln([M_0]/[M])$, indicating the controlled/living polymerization. In a second study, the feed ratio of monomer to catalyst was varied, and polymerizations were allowed for complete conversion. The plot of molar feed ratio vs. degree of polymerization (Figure 5.3B) shows a linear increase of molecular weight with the feed ratio, further confirming the controlled polymerization. Also, monomodal GPC curves demonstrated the facile control of polymerization (Figure 5.3C). Typically, living ROMP allows chain extension of a polymer to synthesize block copolymers.[53, 54] We were able to observe smooth chain extension when an additional amount of monomer M1 was added sequentially. GPC curves exhibited the successful chain extension (Figure 5.3D).

Chain Entanglement Molecular Weight

The chain entanglement molecular weight (M_e) is a critical property governing physical behaviors of a polymer in both glassy and rubbery states. Rheology was employed to characterize M_e of homopolymer P1, which contains bulky rosin side-chain anticipated to increase M_e. The frequency (ω) dependencies of the dynamic moduli (G', G") were characterized at various temperatures, and time temperature superposition was employed to create a master curve, presented in Figure 5.4.

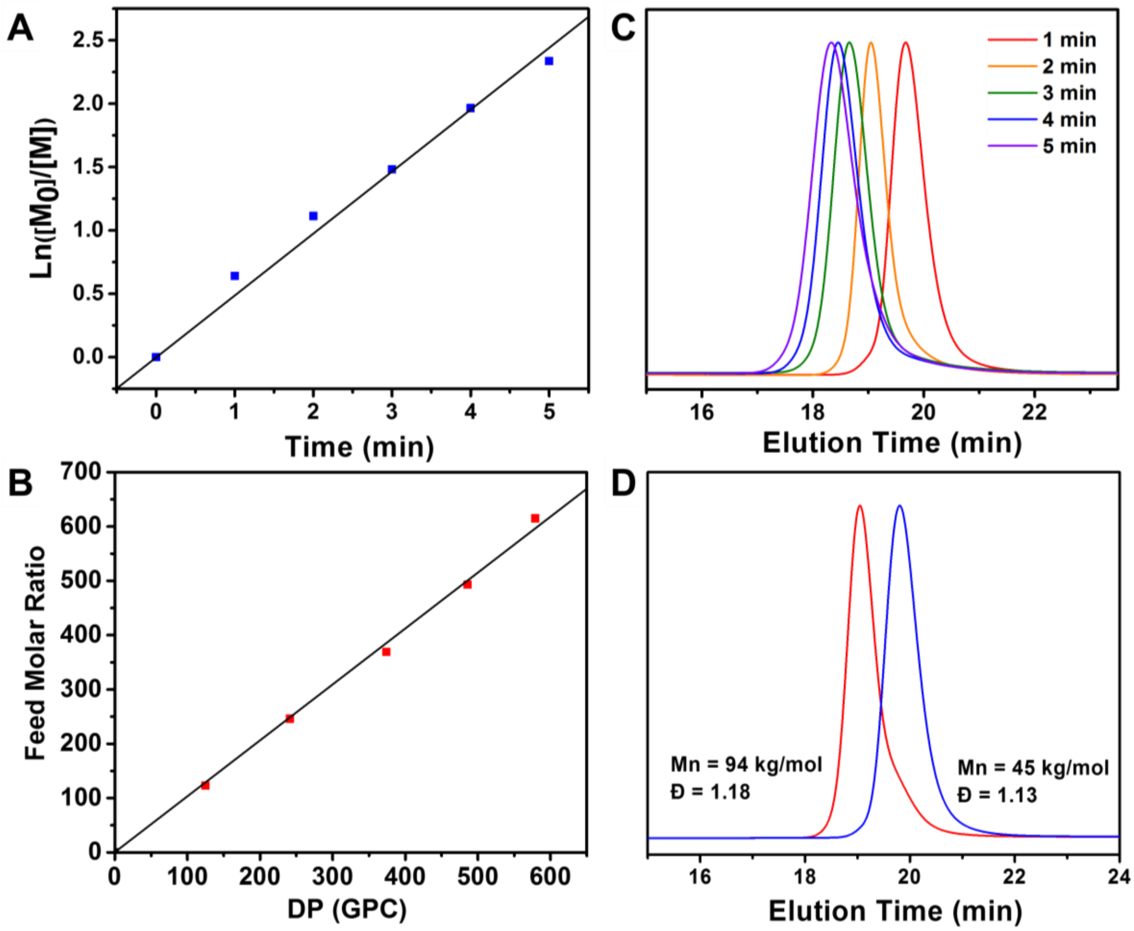

Figure 5.3 Controlled and living polymerization of M1. (A) Kinetic plot of polymerization of M1 with Grubbs' 3rd catalyst (Reaction conditions: molar ratio M1:G3 = 250:1, in dichloromethane and at 23 °C); (B) plot of degree of polymerization vs feeding ratio; (C) Evolution of GPC traces; and (D) GPC traces before and after chain extension (Reaction conditions: molar ratio M1:G3 = 125:1, in dichloromethane and at 23 °C).

The temperature dependence of the shift factor was in good agreement with the Williams-Landel-Ferry equation (Figure 5.5). The terminal flow region, where the storage modulus (G') is proportional to ω^2 and loss modulus (G'') is proportional to ω, is not observed in Figure 5.4, as the experiments were stopped at temperature of T = 230 °C to avoid thermal degradation. The master curve shows a rubbery plateau in the intermediate frequency region, which is a signature of entanglements.

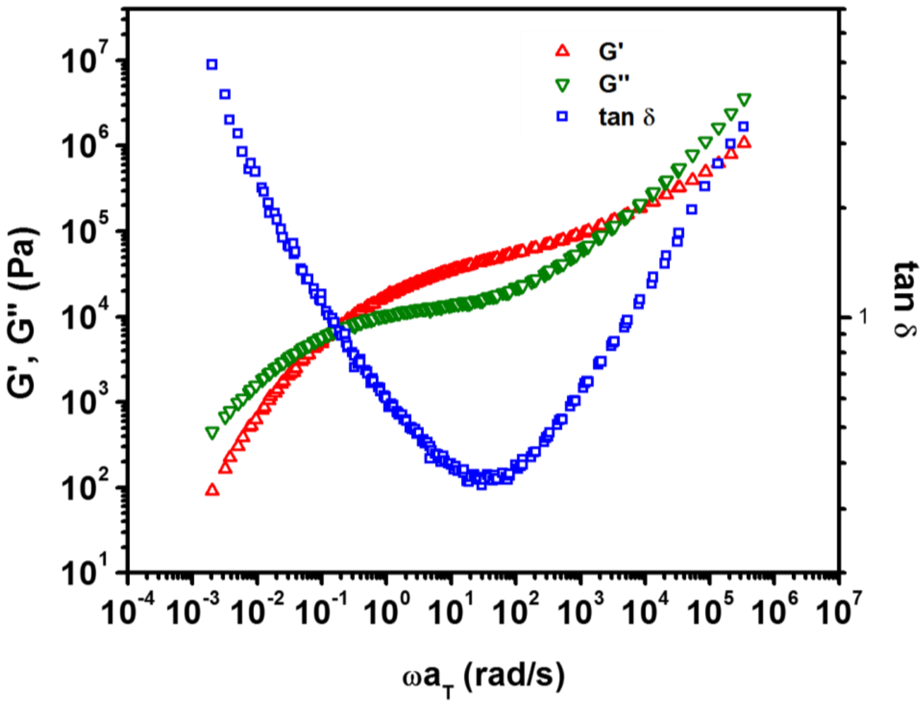

Figure 5.4 Master curve of G', G", and tan δ versus reduced angular frequency at the reference temperature T = 180 °C for the HMW homopolymer P1.

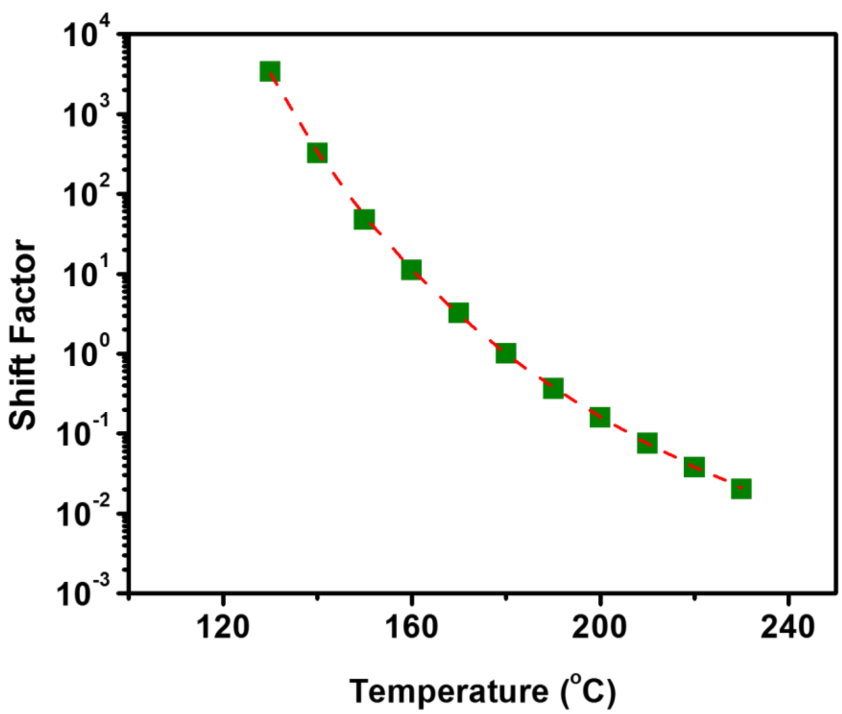

Figure 5.5 Temperature dependence of the shift factor (squares) and fit of the Williams-Landel-Ferry equation (dashed curve, C_1=6.44058, C_2=142.002 K).

M_e is determined through equation 1 where ρ is the density of the polymer at temperature T, R is the gas constant, and G_N^0 is the plateau modulus at temperature T.

$$M_e = \frac{\rho RT}{G_N^0} \qquad (1)$$

The rubbery plateau in Figure 5.4 is frequency-dependent due to the polydispersity of polymer. Following prior literature for polydisperse polymers, G_N^0 was taken to be the storage modulus (G') at the frequency where tan δ exhibits a minimum value.[55-58] Following this method, G_N^0 was determined to be 4.4×10^4 Pa (at the reference temperature of 180 °C).

Characterization of M_e from the plateau modulus (equation 1) requires measurement of the density of polymer. The polymer density at room temperature was measured to be 1.0696 g/ml using a density gradient column. The density at the reference temperature (180 °C) was estimated using the empirical temperature-dependence of polymer densities described by Van Krevelen.[59]

The resulting calculated density at the reference temperature of 180 °C was 1.001 g/cm^3. This density was input into equation 1, along with the measured G_N^0, resulting in M_e = 86 kg/mol. This M_e value is much higher than that of conventional polymers such as polynorbornene (M_e = 41.0 kg/mol)[60] polystyrene (M_e = 16.6 kg/mol) or poly(methyl methacrylate) (M_e = 16.6 kg/mol), but comparable to (or less than) polymethacrylates with bulky side-groups, such as poly(octylmethyl methacrylate) (M_e = 86.7 kg/mol) or poly(dodecyl methacrylate) (M_e = 144 kg/mol).[61] Register et al. reports M_e for hydrogenated poly(alkylnorbornene)s (e.g., poly(decylnorbornene) M_e = 11.0 kg/mol), where M_e increases with alkyl chain length.[62] Therefore, it is not surprising that the sterically demanding rosin moiety result in such a high M_e for its polymer.

Tensile Properties

Plastics with molecular weight lower than M_e are absence of chain entanglements and long-range intermolecular interaction, resulting in brittle behaviors as observed from many previously reported (meth)acrylate polymers with pendent resin acid groups. In the current study, the HMW homopolymers with ~500 kg/mol molecular weight, almost 5 times higher than M_e, readily form free-standing films. Dog-bone specimens cut from the solvent cast and dried films were transparent (Figure 5.6A). The films were flexible and non-tacky. Summary of the monotonic uniaxial tensile results are given in Table 5.2. As illustrated in the Figure 5.6B, nominal stress-strain curves the homopolymers exhibited though thermoplastic properties. The homopolymer P1 had an ultimate tensile strength as high as 25.7 ± 0.3 MPa and a Young's Modulus of 1.18 ± 0.03 GPa. The elongation at break was found to be 6.8 ± 0.4 % with the stress at break 23.8 ± 1.1 MPa (Figure 5.6B).

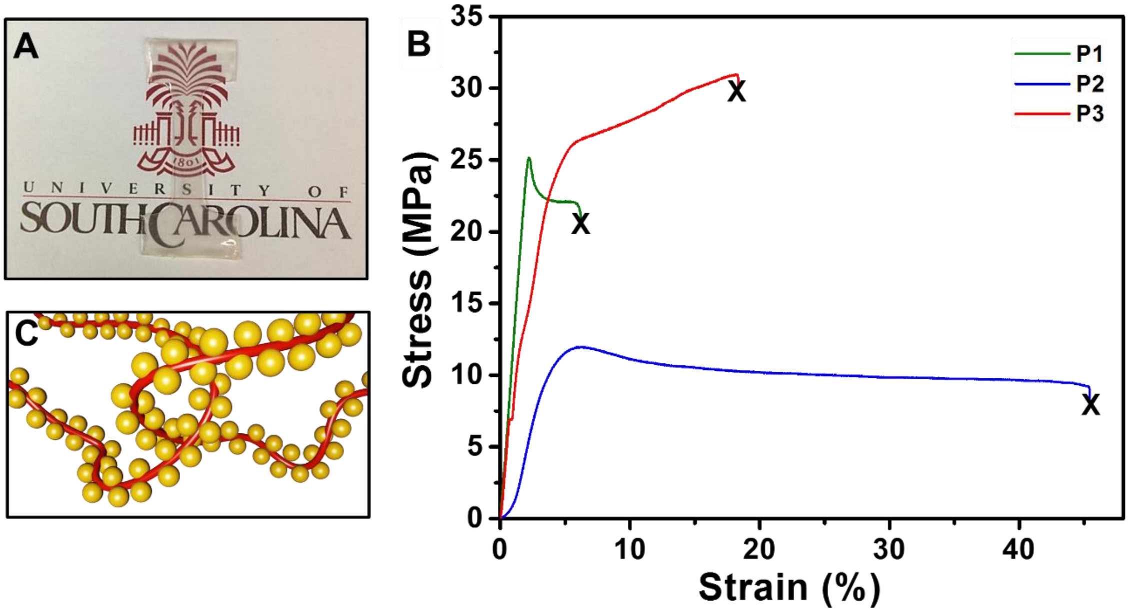

Figure 5.6 Representative tensile test data of the homopolymers. (A) Dog-bone sample of homopolymer P1, (B) Representative examples of monotonic uniaxial stress-strain curves for the homopolymers P1, P2 and P3, (C) Illustration of chain entanglements in the bulky pendant containing polymer.

Table 5.2. Tensile properties of homopolymers P1, P2 and P3.[a]

Polymer	Yield strength 63	Strain at beak (ε) (%)	Stress at break (σ) 63	Young's Modulus (E) (GPa)
P1	25.7 ± 0.3	6.8 ± 0.4	23.8 ± 1.1	1.18 ± 0.03
P2	11.7 ± 0.2	49.4 ± 2.8	8.9 ± 0.2	0.61 ± 0.02
P3	24.2 ± 1.4	18.4 ± 0.1	28.6 ± 1.6	0.31 ± 0.05

[a]Average measurements for duplicate samples are shown in the table. Young's Modulus calculated for the linear response until 2 % elongation.

The polymer P2 with the longer linker appeared as a softer plastic material than P1. It had a lower yield strength of 11.7 ± 0.2 MPa and a higher elongation at break of 49.4 ± 2.8 %. Interestingly, the hydrogenated polymer, P3 showed whitening during the tensile test, and its tensile stress increased up to 28.6 ± 1.6 MPa after the yield point meanwhile its elongation at break reached 18.4 ± 0.1 %. This may be attributed to strain induced chain orientation during the deformation, which could be investigated further in the future.

Application in Thermoplastic Elastomers

TPEs are reprocessable materials that bridge rubber and thermoplastics. The most common TPEs consist of block copolymers with a general structure of ABA, where A is a thermoplastic block with a high T_g and B is an elastomeric block with low T_g. Microphase separation occurs where the rubbery middle block constituting a three-dimensional elastomeric network and the dispersed end block self-assemble into minority domains that serve as multi-junction points.

The high T_g of P1 makes it favorable for TPE applications. We envisioned that a triblock copolymer with a soft middle block (low T_g) end-capped with P1 could generate thermoplastic elastomer properties. With this regard, we chose a soybean oil based norbornene monomer (M3) that we reported recently.[45] Hard-soft-hard type triblock copolymer, where end block is derived from rosin and middle block is predominantly derived from soybean oil, was prepared in a one-pot strategy through sequential monomer addition (Figure 5.7). The composition of the resulting triblock copolymer (denoted as R-*b*-S-*b*-R) could be easily controlled by adjusting the feed ratios of monomer.

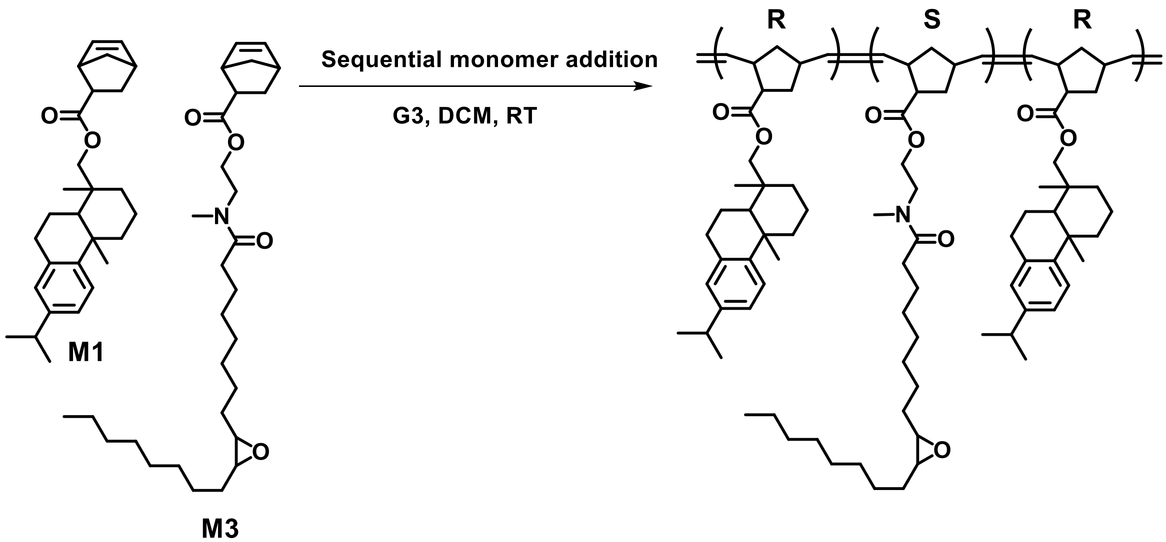

Figure 5.7 Synthesis of triblock copolymers by ROMP with sequential monomer addition. Resin acid derived block is denoted as R and soybean oil derived block denoted as S.

The completion of polymerization reaction was confirmed by ^{1}H NMR and GPC. The DSC curves showed two T_gs for polymers with the composition of rosin monomer M1 ranging from 15.5 to 45.8 wt% (P4-P8) while the molecular weight was adjusted from ~30 to ~70 kg/mol. This indicated the microphase separation between the partially immiscible blocks. Most desirable TPE properties were observed when the M1 content was 30.0 wt % (P10). Two other polymers with 44.4 wt % (P9) and 16.2 wt % (P11) of rosin monomer were also evaluated for thermal and tensile properties for comparison. The triblock copolymer characterizations are summarized in Table 5.3. The DSC curves of these are given in Figure 5.8B. When the end block percentage is increased, the glass transition corresponding to the end blocks became sharp and the thermal decomposition temperature of the polymer also improved.

Table 5.3 Characterizations, thermal and tensile properties of the triblock copolymers R-*b*-S-*b*-R.

Sample	Molar ratio[a]	Rosin content[b]		M_n[c] (kg/mol)	$Đ$[c]	T_g[d] (°C)		T_d[e] (°C)	Stress at break (σ)[f] 63	Strain at beak (ε)[f] (%)
		(wt %)	(mol %)			R block	S block			
P9	50:105:50:1	44.4	48.4	95.6	1.38	96	-32	319	2.2 ± 0.1	60.2 ± 1.1
P10	25:105:25:1	30.0	33.4	70.2	1.18	90	-31	309	4.7 ± 0.6	258.5 ± 26.5
P11	25:210:25:1	16.2	18.6	121.9	1.17	89	-34	302	0.76 ± 0.04	478.4 ± 16.7

[a]Molar ratio: M1/M3/M1/G3. [b]The percentages were calculated by ^{1}H NMR. [c]Triblock molecular weight measured by GPC. [d]Measured by DSC. [e]Decomposition temperature at 10 wt. % loss determined by TGA. [f]Average measurements for duplicate samples are shown.

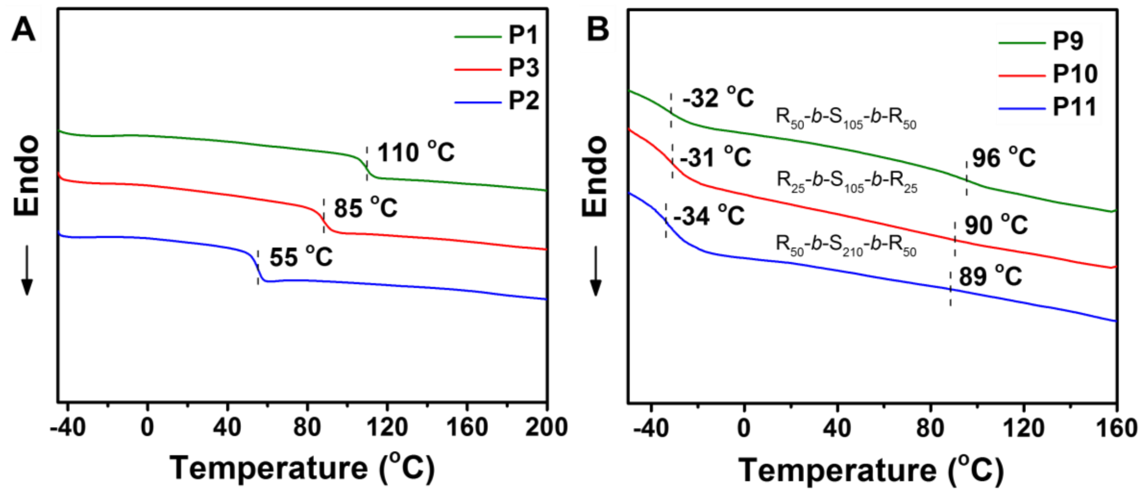

Figure 5.8 DSC curves of the polymers. (A) Homopolymers P1, P2 and P3. (B) Triblock copolymers P9, P10 and P11. Composition of the triblock copolymers based on feed ratios are shown.

To further investigate the microphase separation behavior, thin films of P10 were prepared on silicon wafers and imaged using atomic force microscopy (AFM) (Figure 5.9A). It clearly indicated a microphase-separated morphology. SAXS pattern of the bulk film showed a distinct first-order peak with a minor overlapping peak and a broad shoulder peak (Figure 5.9B). Although a well-ordered morphology was not observed, the results indicated sufficient microphase separation in the bulk sample. The average feature size was ~ 106 nm from SAXS which is consistent with AFM result. The higher molecular weight of the polymers may have kinetically trapped the polymer chains preventing long range ordering of the domains.

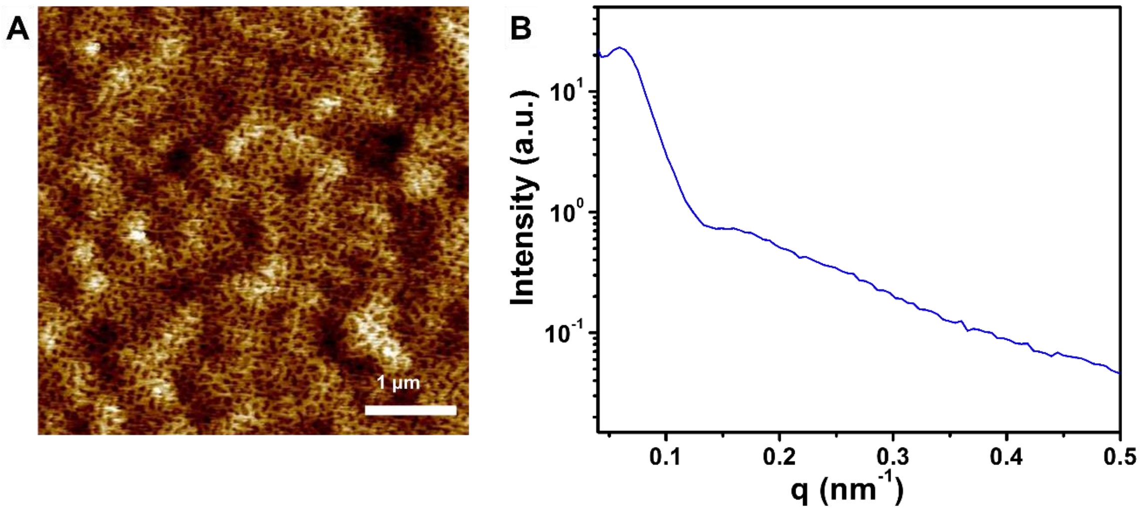

Figure 5.9 Morphological characterization of triblock copolymer P10. (A) AFM phase image indicating microphase separated features. (B) SAXS profile with a sharp first-order peak and a broad shoulder peak.

Mechanical properties of these triblock copolymers were characterized by monotonic tensile tests (Figure 5.10A and Table S3). At 30.0 wt % of monomer M1, the polymer (P10) behaved as a thermoplastic elastomer with elongation as high as 258.5 ± 26.5 % and the ultimate stress at 4.4 ± 0.6 MPa. The rosin content has a strong influence on the mechanical behavior of the polymer. When there is a high fraction of rosin (P9), plastic properties were evident while the lower fraction of rosin content (P11) resulted in elastic properties.

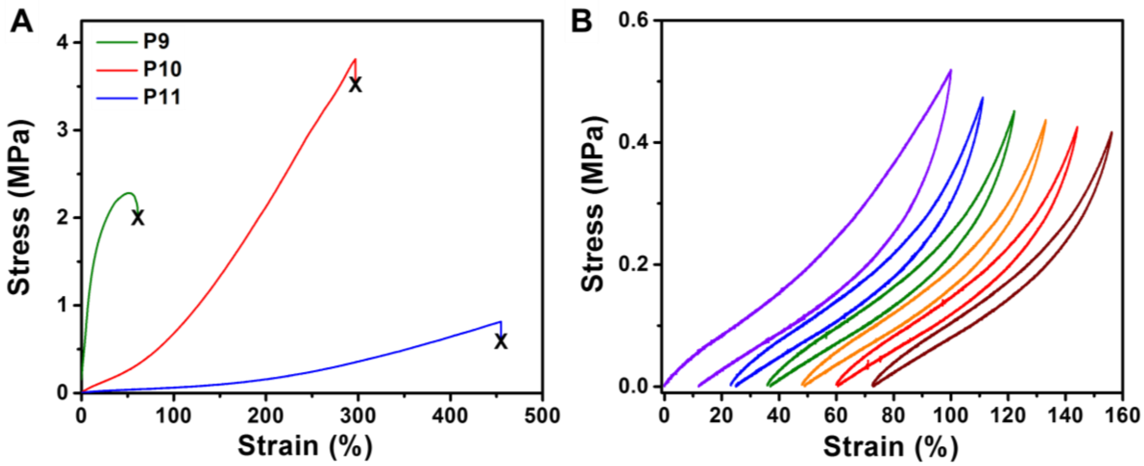

Figure 5.10 Representative tensile test data of triblock copolymers (A) Monotonic uniaxial stress–strain curves of triblock copolymers P9, P10 and P11. (B) Cyclic stress–stain curves of P10. For clarity, the curves are shifted on the strain axis.

The elastic properties of polymer P10 were examined by repetitive cyclic tensile deformation to a strain of 100% (Figure 5.10B). After the first cycle, about 88.0 % of the deformation was recovered. Such a plastic deformation may be attributed to the rearrangement of the rosin domains. The transient behavior was stabilized after several cycles of deformation as indicated by the peak stress and hysteresis. The energy loss under cyclic loading and unloading is reduced from 33.9 % in the first cycle to 17.3 % in the second cycle. After the third cycle the polymer demonstrated excellent elastic recovery >99 %.

5.5 Conclusions

In summary, we demonstrated that rosin-containing HMW polymers can be prepared by controlled and living ROMP. The homopolymers showed tough thermoplastic properties. The T_gs can be modulated from 110 °C to 55 °C via hydrogenation or by controlling the spacer between the polymer backbone and the bulky dehydroabietic acid moiety. The chain entanglement molecular weight for rosin-containing polymers was determined for the first time to be 86 kg/mol. The high T_g of polymers was utilized to make thermoplastic elastomers that included a soft middle block derived from soybean oil. Thermoplastic elastomers with high elastic recovery can be developed using these novel monomers.

5.6 References

1. Miller, S. A., Sustainable Polymers: Replacing Polymers Derived from Fossil Fuels. *Polym. Chem.* **2014,** *5*, 3117-3118.

2. Gandini, A.; Lacerda, T. M., From Monomers to Polymers from Renewable Resources: Recent Advances. *Prog. Polym. Sci.* **2015,** *48*, 1-39.

3. Wool, R.; Sun, X. S., *Bio-Based Polymers and Composites*. Academic Press: Boston, 2011.

4. Sheldon, R. A., Green and Sustainable Manufacture of Chemicals from Biomass: State of the Art. *Green Chem.* **2014,** *16*, 950-963.

5. Gandini, A., The Irruption of Polymers from Renewable Resources on the Scene of Macromolecular Science and Technology. *Green Chem.* **2011,** *13*, 1061-1083.

6. Miller, S. A., Sustainable Polymers: Opportunities for the Next Decade. *ACS Macro Lett.* **2013,** *2*, 550-554.

7. Shen, L.; Worrell, E.; Patel, M., Present and Future Development in Plastics from Biomass. *Biofuels, Bioprod. Biorefin.* **2010,** *4*, 25-40.

8. Mülhaupt, R., Green Polymer Chemistry and Bio-Based Plastics: Dreams and Reality. *Macromol. Chem. Phys.* **2013,** *214*, 159-174.

9. Zhang, Y.; Chen, E. Y.-X., Polymerization of Nonfood Biomass-Derived Monomers to Sustainable Polymers. In *Selective Catalysis for Renewable Feedstocks and Chemicals*, Nicholas, M. K., Ed. Springer International Publishing: Cham, 2014; pp 185-227.

10. Chung, H.; Washburn, N. R., Chemistry of Lignin-Based Materials. *Green Mater.* **2013,** *1*, 137-160.

11. Isikgor, F. H.; Becer, C. R., Lignocellulosic Biomass: A Sustainable Platform for the Production of Bio-Based Chemicals and Polymers. *Polym. Chem.* **2015,** *6*, 4497-4559.

12. Habibi, Y.; Lucia, L. A.; Rojas, O. J., Cellulose Nanocrystals: Chemistry, Self-Assembly, and Applications. *Chem. Rev.* **2010,** *110*, 3479-3500.

13. Wilbon, P. A.; Chu, F.; Tang, C., Progress in Renewable Polymers from Natural Terpenes, Terpenoids, and Rosin. *Macromol. Rapid Commun.* **2013,** *34*, 8-37.

14. Bohlmann, J.; Keeling, C. I., Terpenoid Biomaterials. *Plant J.* **2008,** *54*, 656-669.

15. Yao, K.; Tang, C., Controlled Polymerization of Next-Generation Renewable Monomers and Beyond. *Macromolecules* **2013,** *46*, 1689-1712.

16. Winnacker, M.; Rieger, B., Recent Progress in Sustainable Polymers Obtained from Cyclic Terpenes: Synthesis, Properties, and Application Potential. *ChemSusChem* **2015,** *8*, 2455-2471.

17. Zheng, Y.; Yao, K.; Lee, J.; Chandler, D.; Wang, J.; Wang, C.; Chu, F.; Tang, C., Well-Defined Renewable Polymers Derived from Gum Rosin. *Macromolecules* **2010,** *43*, 5922-5924.

18. Wilbon, P. A.; Zheng, Y.; Yao, K.; Tang, C., Renewable Rosin Acid-Degradable Caprolactone Block Copolymers by Atom Transfer Radical Polymerization and Ring-Opening Polymerization. *Macromolecules* **2010,** *43*, 8747-8754.

19. Yao, K.; Wang, J.; Zhang, W.; Lee, J. S.; Wang, C.; Chu, F.; He, X.; Tang, C., Degradable Rosin-Ester–Caprolactone Graft Copolymers. *Biomacromolecules* **2011,** *12*, 2171-2177.

20. Wilbon, P.; Gulledge, A. L.; Benicewicz, B. C.; Tang, C., Renewable Rosin Fatty Acid Polyesters: The Effect of Backbone Structure on Thermal Properties. *Green Mater.* **2013,** *1*, 96-104.

21. Wang, J.; Yao, K.; Korich, A. L.; Li, S.; Ma, S.; Ploehn, H. J.; Iovine, P. M.; Wang, C.; Chu, F.; Tang, C., Combining Renewable Gum Rosin and Lignin: Towards Hydrophobic Polymer Composites by Controlled Polymerization. *J. Polym. Sci., Part A: Polym. Chem.* **2011,** *49*, 3728-3738.

22. Chen, Y.; Wilbon, P. A.; Chen, Y. P.; Zhou, J.; Nagarkatti, M.; Wang, C.; Chu, F.; Decho, A. W.; Tang, C., Amphipathic Antibacterial Agents Using Cationic Methacrylic Polymers with Natural Rosin as Pendant Group. *RSC Adv.* **2012,** *2*, 10275-10282.

23. Wang, J.; Chen, Y. P.; Yao, K.; Wilbon, P. A.; Zhang, W.; Ren, L.; Zhou, J.; Nagarkatti, M.; Wang, C.; Chu, F.; He, X.; Decho, A. W.; Tang, C., Robust Antimicrobial Compounds and Polymers Derived from Natural Resin Acids. *Chem. Commun.* **2012,** *48*, 916-918.

24. Ganewatta, M. S.; Chen, Y. P.; Wang, J.; Zhou, J.; Ebalunode, J.; Nagarkatti, M.; Decho, A. W.; Tang, C., Bio-Inspired Resin Acid-Derived Materials as Anti-Bacterial Resistance Agents with Unexpected Activities. *Chem. Sci.* **2014,** *5*, 2011-2016.

25. Ganewatta, M. S.; Miller, K. P.; Singleton, S. P.; Mehrpouya-Bahrami, P.; Chen, Y. P.;

Yan, Y.; Nagarkatti, M.; Nagarkatti, P.; Decho, A. W.; Tang, C., Antibacterial and Biofilm-Disrupting Coatings from Resin Acid-Derived Materials. *Biomacromolecules* **2015,** *16*, 3336-3344.

26. Sacripante, G. G.; Zhou, K.; Farooque, M., Sustainable Polyester Resins Derived from Rosins. *Macromolecules* **2015,** *48*, 6876-6881.

27. Llevot, A.; Grau, E.; Carlotti, S.; Grelier, S.; Cramail, H., Dimerization of Abietic Acid for the Design of Renewable Polymers by Admet. *Eur. Polym. J.* **2015,** *67*, 409-417.

28. Bielawski, C. W.; Grubbs, R. H., Living Ring-Opening Metathesis Polymerization. *Prog. Polym. Sci.* **2007,** *32*, 1-29.

29. Sutthasupa, S.; Shiotsuki, M.; Sanda, F., Recent Advances in Ring-Opening Metathesis Polymerization, and Application to Synthesis of Functional Materials. *Polym. J.* **2010,** *42*, 905-915.

30. Grau, E.; Mecking, S., Polyterpenes by Ring Opening Metathesis Polymerization of Caryophyllene and Humulene. *Green Chem.* **2013,** *15*, 1112-1115.

31. Strick, B. F.; Delferro, M.; Geiger, F. M.; Thomson, R. J., Investigations into Apopinene as a Biorenewable Monomer for Ring-Opening Metathesis Polymerization. *ACS Sustainable Chem. Eng.* **2015,** *3*, 1278-1281.

32. Holmberg, A. L.; Reno, K. H.; Wool, R. P.; Epps III, T. H., Biobased Building Blocks for the Rational Design of Renewable Block Polymers. *Soft Matter* **2014,** *10*, 7405-7424.

33. Wanamaker, C. L.; O'Leary, L. E.; Lynd, N. A.; Hillmyer, M. A.; Tolman, W. B., Renewable-Resource Thermoplastic Elastomers Based on Polylactide and Polymenthide. *Biomacromolecules* **2007,** *8*, 3634-3640.

34. Zhang, J.; Li, T.; Mannion, A. M.; Schneiderman, D. K.; Hillmyer, M. A.; Bates, F. S., Tough and Sustainable Graft Block Copolymer Thermoplastics. *ACS Macro Lett.* **2016,** *5*, 407-412.

35. Wang, S.; Vajjala Kesava, S.; Gomez, E. D.; Robertson, M. L., Sustainable Thermoplastic Elastomers Derived from Fatty Acids. *Macromolecules* **2013,** *46*, 7202-7212.

36. Wang, Z.; Yuan, L.; Trenor, N. M.; Vlaminck, L.; Billiet, S.; Sarkar, A.; Du Prez, F. E.; Stefik, M.; Tang, C., Sustainable Thermoplastic Elastomers Derived from Plant Oil and Their "Click-Coupling" Via Tad Chemistry. *Green Chem.* **2015,** *17*, 3806-3818.

37. Hillmyer, M. A.; Tolman, W. B., Aliphatic Polyester Block Polymers: Renewable, Degradable, and Sustainable. *Acc. Chem. Res.* **2014,** *47*, 2390-2396.

38. Nakayama, Y.; Aihara, K.; Yamanishi, H.; Fukuoka, H.; Tanaka, R.; Cai, Z.; Shiono,

T., Synthesis of Biodegradable Thermoplastic Elastomers from E-Caprolactone and Lactide. *J. Polym. Sci., Part A: Polym. Chem.* **2015,** *53*, 489-495.

39. Martello, M. T.; Schneiderman, D. K.; Hillmyer, M. A., Synthesis and Melt Processing of Sustainable Poly(E-Decalactone)-Block-Poly(Lactide) Multiblock Thermoplastic Elastomers. *ACS Sustainable Chem. Eng.* **2014,** *2*, 2519-2526.

40. Gallagher, J. J.; Hillmyer, M. A.; Reineke, T. M., Acrylic Triblock Copolymers Incorporating Isosorbide for Pressure Sensitive Adhesives. *ACS Sustainable Chem. Eng.* **2016,** *4*, 3379-3387.

41. Nasiri, M.; Reineke, T. M., Sustainable Glucose-Based Block Copolymers Exhibit Elastomeric and Adhesive Behavior. *Polym. Chem.* **2016,** *7*, 5233-5240.

42. Holmberg, A. L.; Stanzione, J. F.; Wool, R. P.; Epps, T. H., A Facile Method for Generating Designer Block Copolymers from Functionalized Lignin Model Compounds. *ACS Sustainable Chem. Eng.* **2014,** *2*, 569-573.

43. Firdaus, M.; Meier, M. A. R., Renewable Co-Polymers Derived from Vanillin and Fatty Acid Derivatives. *Eur. Polym. J.* **2013,** *49*, 156-166.

44. Sanford, M. S.; Love, J. A.; Grubbs, R. H., A Versatile Precursor for the Synthesis of New Ruthenium Olefin Metathesis Catalysts. *Organometallics* **2001,** *20*, 5314-5318.

45. Yuan, L.; Wang, Z.; Trenor, N. M.; Tang, C., Robust Amidation Transformation of Plant Oils into Fatty Derivatives for Sustainable Monomers and Polymers. *Macromolecules* **2015,** *48*, 1320-1328.

46. Yuan, L.; Hamidi, N.; Smith, S.; Clemons, F.; Hamidi, A.; Tang, C., Molecular Characterization of Biodegradable Natural Resin Acid-Substituted Polycaprolactone. *Eur. Polym. J.* **2015,** *62*, 43-50.

47. Lee, L.-B. W.; Register, R. A., Hydrogenated Ring-Opened Polynorbornene: A Highly Crystalline Atactic Polymer. *Macromolecules* **2005,** *38*, 1216-1222.

48. Hahn, S. F., An Improved Method for the Diimide Hydrogenation of Butadiene and Isoprene Containing Polymers. *J. Polym. Sci., Part A: Polym. Chem.* **1992,** *30*, 397-408.

49. Sohn, B. H.; Gratt, J. A.; Lee, J. K.; Cohen, R. E., Hydrogenation of Ring Opening Metathesis Polymerization Polymers. *J. Appl. Polym. Sci.* **1995,** *58*, 1041-1046.

50. Mahittikul, A.; Prasassarakich, P.; Rempel, G. L., Noncatalytic Hydrogenation of Natural Rubber Latex. *J. Appl. Polym. Sci.* **2007,** *103*, 2885-2895.

51. Mutlu, H.; Meier, M. A. R., Ring-Opening Metathesis Polymerization of Fatty Acid Derived Monomers. *J. Polym. Sci., Part A: Polym. Chem.* **2010,** *48*, 5899-5906.

52. Esteruelas, A. M.; González, F.; Herrero, J.; Lucio, P.; Oliván, M.; Ruiz-Labrador, B., Thermal Properties of Polynorbornene (Cis- and Trans-) and Hydrogenated Polynorbornene. *Polym. Bull.* **2007,** *58*, 923-931.

53. Ren, L.; Zhang, J.; Bai, X.; Hardy, C. G.; Shimizu, K. D.; Tang, C., Preparation of Cationic Cobaltocenium Polymers and Block Copolymers by "Living" Ring-Opening Metathesis Polymerization. *Chem. Sci.* **2012,** *3*, 580-583.

54. Pitet, L. M.; Zhang, J.; Hillmyer, M. A., Sequential Romp of Cyclooctenes as a Route to Linear Polyethylene Block Copolymers. *Dalton Trans.* **2013,** *42*, 9079-9088.

55. Liu, C.; He, J.; Ruymbeke, E. v.; Keunings, R.; Bailly, C., Evaluation of Different Methods for the Determination of the Plateau Modulus and the Entanglement Molecular Weight. *Polymer* **2006,** *47*, 4461-4479.

56. Wu, S., Entanglement, Friction, and Free Volume between Dissimilar Chains in Compatible Polymer Blends. *J. Polym. Sci. Part B Polym. Phys.* **1987,** *25*, 2511-2529.

57. Wu, S., Chain Structure and Entanglement. *J. Polym. Sci. Part B Polym. Phys.* **1989,** *27*, 723-741.

58. Wu, S.; Beckerbauer, R., Effect of Tacticity on Chain Entanglement in Poly(Methyl Methacrylate). *Polym. J.* **1992,** *24*, 1437-1442.

59. Van Krevelen, D. W.; Te Nijenhuis, K., *Properties of Polymers: Their Correlation with Chemical Structure; Their Numerical Estimation and Prediction from Additive Group Contributions*. Elsevier: Amsterdam, 2009.

60. Mark, J. E., *Polymer Data Handbook*. Oxford University Press: New York, 1999.

61. Fetters, L.; Lohse, D.; Colby, R., Chain Dimensions and Entanglement Spacings. In *Physical Properties of Polymers Handbook*, Springer: New York,: 2007; pp 447-454.

62. Hatjopoulos, J. D.; Register, R. A., Synthesis and Properties of Well-Defined Elastomeric Poly(Alkylnorbornene)S and Their Hydrogenated Derivatives. *Macromolecules* **2005,** *38*, 10320-10322.

63. Som, A.; Vemparala, S.; Ivanov, I.; Tew, G. N., Synthetic Mimics of Antimicrobial Peptides. *Biopolymers* **2008,** *90*, 83-93.

CHAPTER 6

SUMMARY AND OUTLOOK

6.1 Dissertation Summary

In this dissertation work, two major research frontiers were explored. First, antimicrobial biomaterials were developed using natural biomass-derived chemicals. Pine rosin-derived cationic compounds and polymers were prepared as antimicrobial agents in solution and on surfaces. The antimicrobial efficacy was tested against a range of bacteria including MRSA, and the results were promising. These novel materials were highly biocompatible with mammalian cells. The mechanism of action was elucidated using MDS and well as dye-leakage assays. The cationic materials were able to disrupt lipid membranes that may be the major mechanism of action. Contact-active antimicrobial coatings were prepared using resin acid containing compounds and polymers. They were antimicrobially active against bacteria and biocompatible with mammalian cells. In addition, these surfaces reduced the biofilm growth considerably. Antimicrobial main-chain polyionenes were explored using bile acids as the hydrophobic core. They formed cationic micelles in water that demonstrated antimicrobial activity. In addition, the antibiotic loaded micelles showed slow release over longer period of times. More recently, ring-opening metathesis polymerization was utilized to synthesize high molecular weight polymers from resin acids. Molecular weight of polymers as high as half a million Daltons was achieved. Flexible and mechanically robust films from these resin acid polymers were developed. Thermoplastic elastomers were prepared by combining resin acids and soybean oil derived compounds.

6.2 Future Work

Exploration of renewable biomass as a source of building blocks for sustainable material development has gained tremendous momentum during the past decade, and will keep growing in the future. Antimicrobial biomaterial development using the hydrocarbon rich biomass such as rosin and bile acids has more avenues for future developments to make them more effective antimicrobial agents with low toxicity. There are several polymer architectures such as brush, star and comb and other cationic groups such as phosphonium, sulfonium and metallo-cations are at their infancy for antimicrobial applications. In addition, the exploration of microbial response for such cationic antimicrobial polymers can be useful to predict future antimicrobial resistance developments. Cationic bile acid polymers can be developed as hydrophobic antibiotic carriers, which have dual action against bacteria. Improving the performance of biobased polymeric materials is very important to compete with the petrochemical analogues. Compared to other renewable biomass, rosin chemistry has to be developed in several directions before it gains wide spread applications as polymeric materials. Although this dissertation demonstrated a promising way to enhance the performance of rosin polymers as thermoplastics and elastomers, further investigations are required to find lower cost monomers. In addition, other block copolymer architectures can be explored to improve mechanical robustness (tensile strength, elasticity, etc.).

Appendix A – Permission to Reprint

Copyright Clearance Center RightsLink®

Home | Account Info | Help

WILEY

Book: Sustainable Polymers from Biomass
Chapter: Introduction
Author: Mitra S. Ganewatta, Chuanbing Tang, Chang Y. Ryu
Publisher: John Wiley and Sons
Date: Feb 24, 2017

Logged in as:
Mitra Ganewatta
Account #:
3000859345
LOGOUT

Order Completed

Thank you for your order.

This Agreement between Mitra Ganewatta ("You") and John Wiley and Sons ("John Wiley and Sons") consists of your license details and the terms and conditions provided by John Wiley and Sons and Copyright Clearance Center.

Your confirmation email will contain your order number for future reference.

Printable details.

License Number	4066801399986
License date	Mar 12, 2017
Licensed Content Publisher	John Wiley and Sons
Licensed Content Publication	Wiley oBooks
Licensed Content Title	Introduction
Licensed Content Author	Mitra S. Ganewatta, Chuanbing Tang, Chang Y. Ryu
Licensed Content Date	Feb 24, 2017
Licensed Content Pages	9
Type of use	Dissertation/Thesis
Requestor type	Author of this Wiley chapter
Format	Print and electronic
Portion	Full chapter
Will you be translating?	No
Title of your thesis / dissertation	ANTIMICROBIAL BIOMATERIALS AND SUSTAINABLE POLYMERS FROM RENEWABLE BIOMASS
Expected completion date	May 2017
Expected size (number of pages)	165
Requestor Location	Mitra Ganewatta 631 Sumter St COLUMBIA, SC 29208 United States Attn: Mitra Ganewatta
Publisher Tax ID	EU826007151
Billing Type	Invoice
Billing address	Mitra Ganewatta 631 Sumter St COLUMBIA, SC 29208 United States Attn: Mitra Ganewatta
Total	0.00 USD

Copyright Clearance Center RightsLink®

Account Info | Help

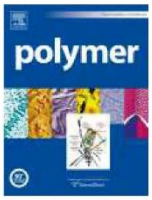

Title: Controlling macromolecular structures towards effective antimicrobial polymers
Author: Mitra S. Ganewatta,Chuanbing Tang
Publication: Polymer
Publisher: Elsevier
Date: Apr 20, 2015

Logged in as:
Mitra Ganewatta
Account #:
3000859345
LOGOUT

Order Completed

Thank you for your order.

This Agreement between Mitra Ganewatta ("You") and Elsevier ("Elsevier") consists of your order details and the terms and conditions provided by Elsevier and Copyright Clearance Center.

License number	Reference confirmation email for license number
License date	Mar, 17 2017
Licensed Content Publisher	Elsevier
Licensed Content Publication	Polymer
Licensed Content Title	Controlling macromolecular structures towards effective antimicrobial polymers
Licensed Content Author	Mitra S. Ganewatta,Chuanbing Tang
Licensed Content Date	20 April 2015
Licensed Content Volume	63
Licensed Content Issue	n/a
Licensed Content Pages	29
Type of Use	reuse in a thesis/dissertation
Portion	full article
Format	both print and electronic
Are you the author of this Elsevier article?	Yes
Will you be translating?	No
Order reference number	
Title of your thesis/dissertation	ANTIMICROBIAL BIOMATERIALS AND SUSTAINABLE POLYMERS FROM RENEWABLE BIOMASS
Expected completion date	May 2017
Estimated size (number of pages)	165
Elsevier VAT number	GB 494 6272 12
Requestor Location	Mitra Ganewatta 631 Sumter St COLUMBIA, SC 29208 United States Attn: Mitra Ganewatta
Publisher Tax ID	98-0397604
Billing Type	Invoice
Billing address	Mitra Ganewatta 631 Sumter St COLUMBIA, SC 29208 United States Attn: Mitra Ganewatta
Total	0.00 USD

CLOSE WINDOW

RSC | Advancing the Chemical Sciences

Royal Society of Chemistry
Thomas Graham House
Science Park
Milton Road
Cambridge
CB4 0WF

Tel: +44 (0)1223 420 066
Fax: +44 (0)1223 423 623
Email: contracts-copyright@rsc.org

www.rsc.org

Acknowledgements to be used by RSC authors

Authors of RSC books and journal articles can reproduce material (for example a figure) from the RSC publication in a non-RSC publication, including theses, without formally requesting permission providing that the correct acknowledgement is given to the RSC publication. This permission extends to reproduction of large portions of text or the whole article or book chapter when being reproduced in a thesis.

The acknowledgement to be used depends on the RSC publication in which the material was published and the form of the acknowledgements is as follows:

- For material being reproduced from an article in *New Journal of Chemistry* the acknowledgement should be in the form:
    - [Original citation] - Reproduced by permission of The Royal Society of Chemistry (RSC) on behalf of the Centre National de la Recherche Scientifique (CNRS) and the RSC
- For material being reproduced from an article *Photochemical & Photobiological Sciences* the acknowledgement should be in the form:
    - [Original citation] - Reproduced by permission of The Royal Society of Chemistry (RSC) on behalf of the European Society for Photobiology, the European Photochemistry Association, and RSC
- For material being reproduced from an article in *Physical Chemistry Chemical Physics* the acknowledgement should be in the form:
    - [Original citation] - Reproduced by permission of the PCCP Owner Societies
- For material reproduced from books and any other journal the acknowledgement should be in the form:
    - [Original citation] - Reproduced by permission of The Royal Society of Chemistry

The acknowledgement should also include a hyperlink to the article on the RSC website.

The form of the acknowledgement is also specified in the RSC agreement/licence signed by the corresponding author.

Except in cases of republication in a thesis, this express permission does not cover the reproduction of large portions of text from the RSC publication or reproduction of the whole article or book chapter.

A publisher of a non-RSC publication can use this document as proof that permission is granted to use the material in the non-RSC publication.

Copyright Clearance Center RightsLink®

Home | Account Info | Help

ACS Publications Most Trusted. Most Cited. Most Read.

Title: Antibacterial and Biofilm-Disrupting Coatings from Resin Acid-Derived Materials

Author: Mitra S. Ganewatta, Kristen P. Miller, S. Parker Singleton, et al

Publication: Biomacromolecules

Publisher: American Chemical Society

Date: Oct 1, 2015

Logged in as:
Mitra Ganewatta
Account #:
3000859345

LOGOUT

PERMISSION/LICENSE IS GRANTED FOR YOUR ORDER AT NO CHARGE

This type of permission/license, instead of the standard Terms & Conditions, is sent to you because no fee is being charged for your order. Please note the following:

- Permission is granted for your request in both print and electronic formats, and translations.
- If figures and/or tables were requested, they may be adapted or used in part.
- Please print this page for your records and send a copy of it to your publisher/graduate school.
- Appropriate credit for the requested material should be given as follows: "Reprinted (adapted) with permission from (COMPLETE REFERENCE CITATION). Copyright (YEAR) American Chemical Society." Insert appropriate information in place of the capitalized words.
- One-time permission is granted only for the use specified in your request. No additional uses are granted (such as derivative works or other editions). For any other uses, please submit a new request.

BACK | CLOSE WINDOW

Copyright Clearance Center RightsLink®

Home | Account Info | Help

ACS Publications
Most Trusted. Most Cited. Most Read.

Title: Biobased Plastics and Elastomers from Renewable Rosin via "Living" Ring-Opening Metathesis Polymerization

Author: Mitra S. Ganewatta, Wenyue Ding, Md Anisur Rahman, et al

Publication: Macromolecules

Publisher: American Chemical Society

Date: Oct 1, 2016

Logged in as:
Mitra Ganewatta
Account #:
3000859345

LOGOUT

PERMISSION/LICENSE IS GRANTED FOR YOUR ORDER AT NO CHARGE

This type of permission/license, instead of the standard Terms & Conditions, is sent to you because no fee is being charged for your order. Please note the following:

- Permission is granted for your request in both print and electronic formats, and translations.
- If figures and/or tables were requested, they may be adapted or used in part.
- Please print this page for your records and send a copy of it to your publisher/graduate school.
- Appropriate credit for the requested material should be given as follows: "Reprinted (adapted) with permission from (COMPLETE REFERENCE CITATION). Copyright (YEAR) American Chemical Society." Insert appropriate information in place of the capitalized words.
- One-time permission is granted only for the use specified in your request. No additional uses are granted (such as derivative works or other editions). For any other uses, please submit a new request.

BACK | CLOSE WINDOW